2013

Regulation of Antigenic Variation in Trypanosoma Brucei

Imaan A. Benmerzouga
Cleveland State University

REGULATION OF ANTIGENIC VARIATION IN *TRYPANOSOMA BRUCEI*

IMAAN A. BENMERZOUGA

Bachelors of Science in Biology
Bachelors of Science in Honors Chemistry

Cleveland State University

May, 2008

Submitted in partial fulfillment of requirements for the degree

DOCTOR OF PHILOSOPHY IN REGULATORY BIOLOGY

at the

CLEVELAND STATE UNIVERSITY

June, 2013

This thesis/dissertation has been approved for

the Department of Biological, Geological,

and Environmental Sciences and for the

College of Graduate Studies of

Cleveland State University

By

_____ Date:_____
Advisor, Ph.D. BGES/CSU

_____ Date:_____
Valentin Boerner, Ph.D. BGES/CSU
Advisory Committee Member

_____ Date:_____
Roman Kondratov, Ph.D. BGES/CSU
Advisory Committee Member

_____ Date:_____
Alexandru Almasan, Ph.D. CCF/CSU
Advisory Committee Member

_____ Date:_____
Aaron Severson, Ph.D. BGES/CSU
Internal Examiner

_____ Date:_____
Kurt Runge, Ph.D. Lerner Research Institue
External Examiner

DEDICATION

To my dear father and mother, my lovely family, my beautiful niece Fatima and whoever made this possible.

ACKNOWLEDGMENTS

All praise to **ALLAH** the almighty for giving me the strength and health to earn my Ph.D. I would like to thank my father Dr. Ali Benmerzouga for his moral support and endless encouragement, my mother Mrs. Aouaouche Kaddou Benmerzouga for her support and care, my sisters: Asmaae, Khadidja, Haadjer, Safiya, Amina and my brother Zakaria for having faith in me and supporting me during this journey, Dr. Rachida Bouhenni for her constant contribution to my progress, Dr. Girish Shukla for showing me what I was gifted at: teaching, and also for his moral support, without his constant moral support, I would not have made it this far. Also, I would like to thank Dr. Tobili Sam-Yellowe, for giving me the opportunity to develop my teaching skills substantially and challenged me to continuously improve, Dr. Jeffery Dean for giving me the opportunity to grow as a graduate student and attend various conferences, Dr. Valentine Boerner for his inputs throughout my journey, Dr. Crystal Weyman for her advice and endless support, Dr. Aaron Severson for all his inputs and help throughout my thesis editing process, Dr. Alexandru Almasan and Dr. Roman Kondratov for their great support, Dr. XiaFeng Yang, who was an extraordinary person with her support and training, Dr. Ali Abulattif for all his help, the departments secretary: Monica Warner, for her generous help, my graduate lab mates for their continuous discussion and suggestions: Unnati Pandya, Ranjodh Sandhu and Vishal Nanavaty. In addition, I want to thank every person who was part of my life during this journey: Sujata Jha, Hanadi Rahwanji, Haifa Aljabreen, Soraya Oumaid and Sabrina Chougi. Finally, I want to deeply thank Bandar Al-Shammari, who constantly encouraged me and never allowed an obstacle to come my way, his support will not be forgotten.

REGULATION OF ANTIGENIC VARIATION IN *TRYPANOSOMA BRUCEI*

IMAAN A. BENMERZOUGA

ABSTRACT

Trypanosoma brucei is a protozoan parasite that causes sleeping sickness in humans and nagana in cattle. When inside the mammalian host, *T. brucei* cells stay in extracellular spaces and regularly switch their surface antigen, Variant Surface Glycoprotein (VSG), to escape the host's immune responses. To ensure the effectiveness of *VSG* switching, *T. brucei* expresses a single type of VSG at any time exclusively from one of 20 identical *VSG* expression sites located next to the telomere. Monoallelic expression of *VSG* and *VSG* switching are important for *T. brucei's* pathogenesis. Our major goal is to understand the mechanisms of antigenic variation regulation.

Binding of the Origin Recognition Complex (ORC) to replication origins is essential for initiation of DNA replication, but ORC has non-essential functions outside of DNA replication including gene silencing and telomere maintenance. An Orc1/Cdc6 homolog has been identified in *T. brucei,* but its function in gene silencing has not been investigated. In this study, we show that depletion of TbORC1 resulted in derepression of ES-linked silent *VSG*s in both mammalian-infectious bloodstream and insect procyclic forms. In addition, TbORC1 associates with telomere repeats but independently of known *T. brucei* telomere proteins, TbRAP1 and TbTRF. We conclude that TbORC1 is required to control telomere linked *VSG* gene silencing (*Mol. Microbiol.* 87(1): 196-210).

Telomeres are nucleoprotein complexes located at ends of linear chromosomes and are essential for maintaining genome integrity. We have identified *T. brucei* TRF as a duplex telomere DNA binding factor. Nevertheless, the function of TbTRF in antigenic

variation has not been studied. In this study, we solve the NMR structure of the TbTRF MYB domain and we determined point mutations that weaken or abolish the DNA binding activity of TbTRF *in vitro*. We successfully targeted these point mutations *in vivo* and studied the role of TbTRF DNA binding mutants in antigenic variation. Finally, we found that the modified J residue (beta-D-glucosyl-hydroxymethyluracil) found in telomeres does not influence the association of TbTRF with the telomere *in-vitro*.

Tel2 was first identified in yeast and has been shown to be essential for telomere length maintenance. Subsequently, Tel2 homologues have been identified in different organisms including worm, human, and *T. brucei*. Recent studies report that mammalian Tel2 regulates the stability of PI3-K related kinases (PIKK). TbTEL2 was identified through an *in silico* approach. Our preliminary data suggest that TbTEL2 is important for telomere end-protection, possibly regulates PI3K-Related protein kinases stability, and appears to affect *VSG* switching.

These studies will provide additional insights into *T. brucei's* pathogenesis, and possibly lead to the identification of putative targets for anti-parasitic therapies, not only against *T. brucei* but also other parasites that utilize antigenic variation to evade the host immune responses.

TABLE OF CONTENTS

ABSTRACT vi

LIST OF FIGURES xi

CHAPTER

I. INTRODUCTION.....1

Trypanosoma brucei ….....2

Trypanosoma brucei Life Cycle….....3

Class Kinetoplastida ....…….....5

African Sleeping Sickness……..….....6

Genome *of T. brucei* …...…….....9

Variant Surface Glycoprotein (VSG).....10

Architecture of *VSG* ES…….....11

Antigenic Variation …….....12

VSG Regulation…….....14

J-base modification in *T. brucei* 17

Telomeres and telomere complex….....18

II. MATERIAL AND METHODS.....21

Plasmids.....21

T. brucei strains…….....23

Generation of Anti-J-base Serum.…….....25

Chromatin IP…….....…….....26

RNA isolation and reverse transcription…….....26

Quantitative RT-PCR ….....27

Western Blot.....27
Pulse field Gel Electrophoresis and In-gel Hybridization.....28
VSG Switching Assays.....29
Dot Blots 31
Immunofluorescence Analysis.....31
Immunoprecipitation.....32
Southern Blotting.....33
Flow Cytometry.....33
Yeast-two-hybrid Analysis.....34
Isothermal Titration Calorimetry (ITC).....34
III. TRYPANOSOMA BRUCEI ORC1 IS ESSENTIAL FOR CELL CYCLE PROGRESSION AND *VSG* SILENCING.....35
ABSTRACT.....35
INTRODUCTION..... 36
MATERIALS AND METHODS 40
RESULTS.....40
DISCUSSION.....54
IV. CHARACTERIZE THE FUNCTIONS OF TTAGGG REPEAT BINDING FACTOR IN TRYPANOSOMA BRUCEI.....60
ABSTRACT.....60
INTRODUCTION 61
MATERIALS AND METHODS.....64
RESULTS.....64
DISCUSSION.....82

V. CHARACTERIZATION OF TRYPANOSOMA BRUCEI TEL2 87

ABSTRACT 87

INTRODUCTION 88

MATERIALS AND METHODS 88

RESULTS 90

DISCUSSION…….....90

VI. PRELIMINARY DATA FOR FUTURE STUDIES…...101

BIBLIOGRAPHY.....119

APPENDICES

A. EQUATIONS USED IN THESE STUDIES.....137

B. PRIMERS USED IN THESE STUDIES…….139

C. PLASMIDS GENERATED FROM THESE STUDIES……..141

D. ANTIBODIES USED IN THESE STUDIES……...143

E. T. BRUCEI STRAINS GENERATED FROM THESE STUDIES……..…144

F. ABBREVIATIONS……..145

LIST OF FIGURES

Figure Page

1-1. An introduction to *Trypanosoma brucei*……11

1-2. Antigenic variation.....13

1-3. *T. brucei's* telomere complex.....20

2-1. The switching assay.....30

3-1. Growth analysis for TbORC1 depleted cells.....41

3-2. Cell cycle analysis of BF cells upon the depletion of TbORC1…….....42

3-3. Q-RT PCR analysis of various ES-linked subtelomeric *VSG*s in both PF and BF cells upon the depletion of TbORC1……...…….....……..44

3-4. Depletion of TbORC1 resulted in derepression of ES-linked VSG expression.....45

3-5. Silent VSG derepression in TbORC1 depleted cells.…….....46

3-6. Silent VSGs are expressed in TbORC1 depleted cells.....…..….....47

3-7. TbORC1 cells originally express VSG2.…….....…….....48

3-8. TbORC1 associates with telomeres in BF and PF cells.…….....50

3-9. Yeast-two-hybrid analysis of the interaction of TbORC1 with TbTRF or TbRAP1.51

3-10. TbORC1 does not interact with TbTRF or TbRAP1 *in vivo*.…….....52

3-11. Association of TbTRF or TbRAP1 with telomeres in the presence or absence of TbORC1…….....…….....…….....…….....53

3-12. Depletion of TbORC1 did not affect TbTRF or TbRAP1 protein levels……54

4-1. TbTRF domains….....…….....….....…….....63

4-2. Growth curve analysis for all TbTRF-RNAi clones..….....…….....65

4-3. Western analysis for TbTRF in all TbTRF-RNAi clones to confirm the transient

depletion of TbTRF.…….....…….....…….....…….....66

4-4. TbTRF amino acid sequence…….....…….....…….....68

4-5. NMR structure of TbTRF MYB domain.…….....…….....68

4-6. *In vitro* DNA binding activity of TbTRF mutants using Isothermal Titration Calorimetry (ITC).…….....…….....…….....…….....70

4-7. TbTRF MYB domain mutants with abolished DNA binding activity *in vitro*……...71

4-8. TbTRF MYB domain mutants with weakened DNA binding activity *in vitro*……..72

4-9. Generation of TbTRF MYB domain mutants *in vivo*..…….....……..73

4-10. Representative sequencing data of TbTRF MYB domain mutations in *T. brucei* cells.…….....…….....…….....…….....74

4-11. Western confirmation of *T. brucei* cells harboring indicated point mutation in the MYB domain…….....…….....…….....…….....75

4-12. Growth Curve analysis of TbTRF MYB domain mutants…….....76

4-13. Analysis of *VSG* silencing in TbTRF DNA binding mutants….……..….....77

4-14. Strategy to target TbTRF MYB domain mutants in the starter strain HSTB261….78

4-15. J modification does not affect the telomere DNA binding activity of TbTRF *in vitro*.…….....…….....…….....…….....79

4-16. Growth curve analysis upon the addition of J-synthesis inhibitor (DMOG)……80

4-17. Confirmation of the depletion of J *in vivo* upon addition of the J- synthesis inhibitor DMOG.…….....…….....…….....…….....82

5-1. Growth curve analysis upon the depletion of TbTEL2…….....92

5-2. Depletion of TbTEL2 led to decrease of G-overhang signal…. …….....94

5-3. Western blot analysis of TbTOR1 and TbTRF protein levels upon the depletion of

TbTEL2.…….....…….....…….....…….....95

5-4. Depletion of TbTEL2 led to increase in *VSG* switching frequency...…….....97

6-1. No changes in the transcription of *PURO* reporter gene upon the depletion of TbORC1.....103

6-2. G-overhang analysis in TbTRF mutants.....106

6-3. Yeast-two hybrid analysis of the interaction of TbTRF-R348K or TbTRF-Q320S with TbRAP1……...108

6-4. Yeast-two hybrid analysis of the interaction of TbTRF-R298K or TbTRF H346R with TbRAP1…….....109

6-5. ChIP analysis of TbRAP1 at telomeres.....110

6-6. Diagram of TbTRF-RNAi method in preparation for the switching assay…….111

6-7. *VSG* switching frequency upon the transient depletion of TbTRF……...112

6-8. *VSG* switching frequency in TbTRF mutants……...114

6-9: ChIP of TbTRF in the presence or absence of J-base……..116

CHAPTER I

INTRODUCTION

Summary

Trypanosoma brucei is the causative agent of African sleeping sickness or Human African Trypanomoasis (HAT), which is fatal if left untreated. Many drugs have been developed to treat HAT, but most of the drugs are toxic to patients. This makes the understanding of the molecular pathogenesis of *T. brucei* indispensable for the development of safer treatments. *T. brucei* manages to escape host immune responses via antigenic variation. *T. brucei* replicates in the bloodstream of its mammalian host and is continuously exposed to the host immune system. Therefore, *T. brucei* expresses a protective surface coat. This surface coat is known as Variant Surface Glycoprotein (VSG). There are more than 1000 *VSG* genes and pseduogenes in *T. brucei's* genome. This allows *T. brucei* to maximize the efficiency of escaping the host immune responses. In order to achieve this, *T. brucei* expresses one *VSG* at a time, a phenomenon known as monoallelic *VSG* expression. In addition, *T. brucei* regularly switches its expressed *VSG* via transcription or recombination based pathways. It is important to note that the *VSG* gene is exclusively expressed from an expression site located at the sub-telomere. Many factors that regulate antigenic variation have been described including telomeric proteins. Nevertheless, antigenic variation is a complex process and not all factors that regulate

antigenic variation have been identified. My thesis goal was to study the regulation of antigenic variation by proteins that associate with telomeres. These studies will possibly lead to the identification of putative targets for trypanocidal therapies.

In this chapter, I will introduce you to *Trypanosoma brucei*, its life cycle, the class Kinetoplastida, African sleeping sickness and its current available therapies. I will also introduce you to the concept of antigenic variation and how *T. brucei* utilizes antigenic variation. Also, I will introduce you to the factors that regulate antigenic variation and the modified thymine residue known as J-base or base J found in kinetoplastids. Finally, I will introduce you to telomeres and *T. brucei's* telomere complex.

Trypanosoma brucei

Trypanosoma brucei is a unicellular protozoan parasite that belongs to the class Kinetooplastida and the order Trypanosomatida. *T. brucei* is a heteroxenous organism, meaning it needs more than one host to complete its life cycle. There are three sub-species of *Trypanosoma brucei*: *T. brucei. brucei, T. brucei. gambiense* and *T. brucei. rhodesiense*. All three sub-species are morphologically indistinguishable. Nevertheless, there are some variations among these sub-species including the host they infect, the severity of the infection and their epidemiology. Both *T. b. gambiense* and *T. b. rhodesiense* are the etiological agents of African sleeping sickness in humans, where *T. b. brucei* is the parasite of native antelopes, live stock and other African ruminants causing animal trypanosomiasis or nagana (Roberts et al. 2009). All three sub-species utilize an insect vector from *Glossina spp. T. b. gambiense* causes a chronic form of sleeping sickness while *T. b. rhodesiense* causes an acute form of the disease. Finally, *T. b.*

gambiense is a major problem in Central and West Africa and *T. b. rhodesiense* is a burden to Eastern and Southern Africa (Roberts et al. 2009).

T. b. brucei does not infect human because it is sensitive to the normal human serum, which contains the trypanosome lytic factor (TLF). There are two mechanisms whereby resistance evolved against TLF. In *T. b. rhodesiense* the expression of a serum resistance associated protein (SRA) neutralizes TLF by binding to it (De Greef C et al. 1989). However, *T. b. gambiense* lacks SRA and instead the TLF receptor in *T. b. gambiense* has a greatly reduced affinity to TLF (Kieft et al. 2010), but other mechanisms of resistance remain unknown, since there is a group in *T. b. gambiense* that lacks SRA, uptakes the TLF and yet is resistant to the normal human serum (De Jesus E et al. 2013). These differences illustrate the diversity of *T. brucei* sub-species (Roberts et al. 2009).

Trypanosoma brucei Life Cycle

T. brucei undergoes complex changes during its life cycle, as means of surviving in the two hosts: insect and human (Figure: 1-1). Throughout its life cycle, *T. brucei* expresses surface glycoproteins. It all starts from a blood meal, where *T. brucei* is carried to the midgut of the tsetse fly (*Glossina spp*). It resides in the posterior section of the midgut and rapidly multiplies for approximately 10 days (Roberts et al. 2009). While in the midgut of the tsetse fly, *T. brucei* expresses procyclin as a surface molecule. Procyclin is a protease resistant surface molecule. It protects *T. brucei* from hydrolytic enzymes that are present in the tsetse's gut (Gruszynski et al. 2006). When *T. brucei* is ready to be transmitted to the mammalian host, it migrates through the digestive and respiratory tract of the tsetse fly, eventually reaching the salivary glands of the tsetse fly.

In the salivary glands, *T. brucei* prepares for infection and differentiates into the metacyclic form (a non-dividing infectious form of *T. brucei*), which is small, stumpy and has no flagellum. At this stage, while still in the insect, *T. brucei* initiates the expression of Variant Surface Glycoprotein (VSG), while the abundant procyclins are no longer expressed (Graham and Barry 1995). Metacyclic *VSGs* (m*VSGs*) are different from bloodstream form *VSGs* (B-ES), as they only constitute 1-2% of the *VSG* repertoire (Graham and Barry 1995). They are also monocistronically transcribed (Alarcon et al. 1994). The expression site is structurally different than the bloodstream expression site and the promoter of m*VSG* is only activated during metacyclic stage (Graham and Barry 1995). Upon a blood meal, the tsetse fly inoculates the mammalian victim with infectious metacyclic trypanosomes.

Metacyclic trypanosomes transform to an infectious dividing form known as bloodstream form and reside in the bloodstream, lymph nodes, spleen and cerebrospinal fluid of its mammalian host. A single bite from a tsetse fly inoculates the host with up to several thousands of metacyclic trypanosomes (Roberts et al. 2009). Depending on the sub-species, *T. brucei* may or may not reach the central nervous system (CNS). In acute infections by *T. b. rhodesiense*, trypanosomes invade almost all organs, which results in a rapid course towards death. In chronic infections via *T. b. gambiense,* trypanosomes invade the central nervous system causing the symptoms of sleeping sickness disease. Regardless of the sub-species, during this stage, *T. brucei* expresses bloodstream *VSGs*, where only one *VSG* is expressed at any time. There are more than 1000 *VSGs* that have been identified in *T. brucei's* genome, providing *T. brucei* with a huge repertoire to exhaust the host immune responses. Bloodstream *VSGs* like m*VSGs* are expressed from

sub-telomeric loci. When *T. brucei* reaches its terminal non-dividing stage, a blood meal by the tsetse fly from the mammalian host, once again, recapitulates the whole life cycle (Figure: 1-1a).

Class Kinetoplastida

Class Kinetoplastida harbors single cell organisms that parasitize many eukaryotes. In this class, there are three major parasites of the human, *Leshmania spp* that cause Leshmaniasis, *Trypansoma cruzi* that causes American trypanosomiasis or Chagas disease and finally, *Trypanosoma brucei,* the causative agent of African sleeping sickness in human. The majority of species that are under this class requires an arthropod or an insect vector to infect its mammalian host. This class was named after the "Kinetoplast", a single mitochondrial DNA containing body in addition to the nucleus. The kinetoplast is utilized to determine the stage of the parasite. Typically a species belonging to the class kinetoplastida should have the following stages: amastigote, promastigote, epimastigote and finally trypomastigote. An amastigote is a round form of the species with very short flagellum. This stage is found in *Trypanosoma cruzi* and *Leshmania spp*. These parasites live in the intercellular spaces of the host. In the promastigote stage, the kinetoplast is found at the anterior of the parasite's body. The epimastigote stage is similar to the promastigote stage in terms of the location of the kinetoplast, but during this stage a prominent undulating membrane appears. Upon full maturation, the parasite is in a trypomastigoe stage where the kinetoplast is found posterior to the nucleus (Roberts et al. 2009). In addition, the kinetoplast is used to determine the phase of the cell cycle. In *T. brucei* replication of the kinetoplast and the division of the kinetoplast precedes the

nuclear division. Therefore G1, S and G2 phases can be determined through cytological analysis for the location of the nucleus and kinetoplast as well as the DNA content (Sherwin and Gull 1989).

African Sleeping Sickness

Human African Trypanosomoasis (HAT) or African sleeping sickness is considered one of the most neglected tropical diseases (Stephens et al. 2012). Sub-Saharan Africa harbors the main habitat for tsetse flies, reporting the majority of the cases to the World Health Organization (WHO). Recent epidemiological studies have revealed a substantial decrease in the number of declared cases to WHO to approximately 10,000 cases a year or less (Bisser and Courtioux 2012). However, this number is largely an underestimation due to the lack of advanced molecular tools to diagnose trypanosomoasis at its early stages (Welburn and Maudlin 2012). In addition, during the early 1960s, the HAT disease was no longer considered a public health problem (Garcia et al. 2006). However, it returned to alarming levels in the 1990s (Garcia et al. 2006). Moreover, there are reportedly non-endemic cases that are a result from military assignments, tourists or immigrants that resided in sub-Saharan Africa. The non-endemic cases may not show the exact symptoms shown by the endemic cases due to their genetic differences, retarding their diagnosis and treatments (Blum et al. 2012).

Depending on the *T. brucei* sub-species, the average survival can range from 3 years to several weeks. The disease course is divided into two stages. The first stage is exemplified by fever, headache, swollen lymphnodes (lymphadenopathy), enlargement of the spleen and liver (hepato-splenomegaly). During the second stage, where *T. brucei* has

infiltrated the CNS and crossed the blood brain barrier (BBB), neuro-psychological disorders are prominent such as Parkinson like movements, paralysis of the extremities and speech disorders, in addition to disruption of the circadian rhythm or "sleeping disorder" hence the name "sleeping sickness" (Blum et al. 2012). Not all clinical presentations of HAT are comparable, making early diagnosis a great challenge. Host genetics, co-infections genetic background of the parasite and host-parasite interactions are major attributions to this diversity (Morrison 2011).

Treatment of HAT varies with the stage of the disease, where the later stage utilizes drugs with greater toxicity. The first stage drugs are Pentamidine for *gambiense* or Suramin for *rhodesiense* (Simarro et al. 2008). The Pentamidine mechanism of action is not completely clear. It is hypothesized that it interferes with *T. brucei's* nucleic acid metabolism. Pentamidine is an aromatic diamidine having various toxic side effects. In addition, it is not effective against the second stage of the Gambian HAT, making it the least effective chemotherapeutic treatment available (Bacchi 2009). On the other hand, Suramin is a sulfonated naphthylamine (Bacchi 2009). It has been shown to inhibit several enzymes including thymidine kinase and enzymes in the glycolytic pathway. However, Suramin does not cross the BBB, making it a less effective drug against HAT (Wang 1995).

The second stage disease drugs are Eflornithine or Melarsoprol. Eflornithine or difluoromethylornithine (DFMO) is less toxic and only effective in the Gambian HAT. DFMO is an irreversible inhibitor of ornithine decarboxylase (ODC). ODC is the rate-limiting and the initial enzyme in the polyamine synthetic pathway (Bacchi 2009). However, DFMO is not trypanocidal and depends on the immune system to eliminate

non-dividing trypanosomes. Melarsoprol is the most toxic drug available to treat HAT. It is arsenical and targets the S-H group found in many enzymes. It also, interferes with ATP production. Death of trypanosomes occurs as a result of diminished energy (Bacchi 2009). Melarsoprol is insoluble in water and only soluble in organic solutions such as propylene glycol. In addition, it must be administered intravenously causing damage to the veins. Death occurs within 48 hours of melarsoprol treatment due to its adverse side effects such as pulmonary edema and encephalopathy (Bacchi 2009). The high failure rate of melarsoprol treatment makes it a less effective treatment available for HAT (Chappuis 2007).

Finally, most recently a combination of Nifurtimox and Eflornithine has been introduced in the clinics as a cost-effective treatment for HAT (Simarro et al. 2008). Nifurtimox is a registered drug to treat American sleeping sickness disease. Clinical trials for this combination showed >94% cure rate (Chappuis 2007). Currently, this combination therapy is the best treatment option available for Gambian HAT (Alirol et al. 2013). Careful follow up of all cases will deduce whether this combination therapy results in any relapse, since resistance to mono-therapy has emerged (Alirol et al. 2013).

All drugs require special administration and special training. Many of the drugs are toxic and are not effective for both stages. In addition, resistance has emerged against several available drugs (Alirol et al. 2013). Moreover, recent reports have shown that *T. b. gambinese* crosses the BBB five hours post infection complicating the available courses of treatment (Frever et al. 2012). Therefore, it is crucial to discover trypanocidal drugs that will be effective to kill the trypanosome regardless of disease stage. In addition, vector control must be used against *Glossina spp* that causes HAT (Simarro et

al. 2008). Active research is on going to find bait-based traps that will help control the *Glossina spp* causing HAT. In addition finding safer and more effective remedies for HAT is urgently needed. This requires the identification of improved drug targets by the identification of essential genes in *T. brucei*, that if targeted will not affect the host.

Genome of T. brucei

The genome of *Trypanosoma brucei* is 26 megabase in size predicting 9068 genes (Berriman et al. 2005). The 26 Mb genome consists of 11 diploid large chromosomes known as Mega Base Chromosomes (MBCs) ranging in size from 1-5.2 Mb (Melville et al. 1998), several Intermediate Chromosomes (ICs) ranging in size 200-900 Mb, and finally minichromosomes (MCs) that range in size between 50- 150 kb (El-Sayed et al. 2000). The terminal repeats of MBCs, ICs and MCs are of TTAGGG sequence. Some of the telomeres of MBCs and ICs are linked to expression sites for genes encoding Variant Surface Glycoprotien (*VSG*) (El-Sayed et al. 2000). MCs carry silent *VSG* gene copies and are mainly thought to contribute to the *T. brucei* genome as a reservoir of additional *VSGs* (Alsford et al. 2001). Unlike MBCs and ICs, none of the MCs are linked to expression sites (El-Sayed et al. 2000). MCs replicate and segregate faithfully over several years of growth (Alsford et al. 2001). There are 1700 *T. brucei* specific genes and ~ 900 pseudogenes (Berriman et al. 2005), most *VSG* genes in the genome are pseudogenes (Berriman et al. 2005; Rudenko 2011,), and little is known to how pseudogenes are recombined to produce functional *VSGs* (Rudenko 2011).

Variant Surface Glycoprotein (VSG)

VSG is a dense layer of a single species of glycoprotein (Borst and Rudenko

1994). There are approximately 10^7 identical molecules of VSG on the surface of the *T. brucei*. These VSGs are relatively 60 kDa in molecular mass (Metcalf et al. 1987). The N-terminus of VSG is hydrophilic, where the C-terminus is hydrophobic (Carrington et al. 1991). The N-terminus of VSG extends outwards facing the extracellular space, where the hydrophobic pocket is tethered to the plasma membrane through a GPI (glycosylphosphatidylinositol) anchor (Dubois et al. 2005). This rod-like architecture allows the VSGs to be tightly packed creating a dense layer on the surface of the trypanosome (Figure: 1-1b).

At the sequence level, the N-terminus of *VSG* is variable among all VSGs, while the C-terminus is quite conserved (Carrington et al. 1991). Despite the differences at the sequence level for different *VSGs*, high-resolution X-ray crystallography structures revealed a conserved secondary and tertiary structure (Metcalf et al. 1987), possibly to pack all *VSGs* in a similar manner prior to becoming a surface coat (Dubois et al. 2005). VSGs are susceptible to cleavage via proteases such as a zinc metalloprotease activity (MSP-B) and GPI-specific phospholipase (GPI-PLC) to shed a pre-existing VSG (Gruszynski et al. 2006). It takes approximately 48 hours for a pre-existing *VSG* to be completely eliminated and replaced with a new VSG coat (Dubois et al. 2005).

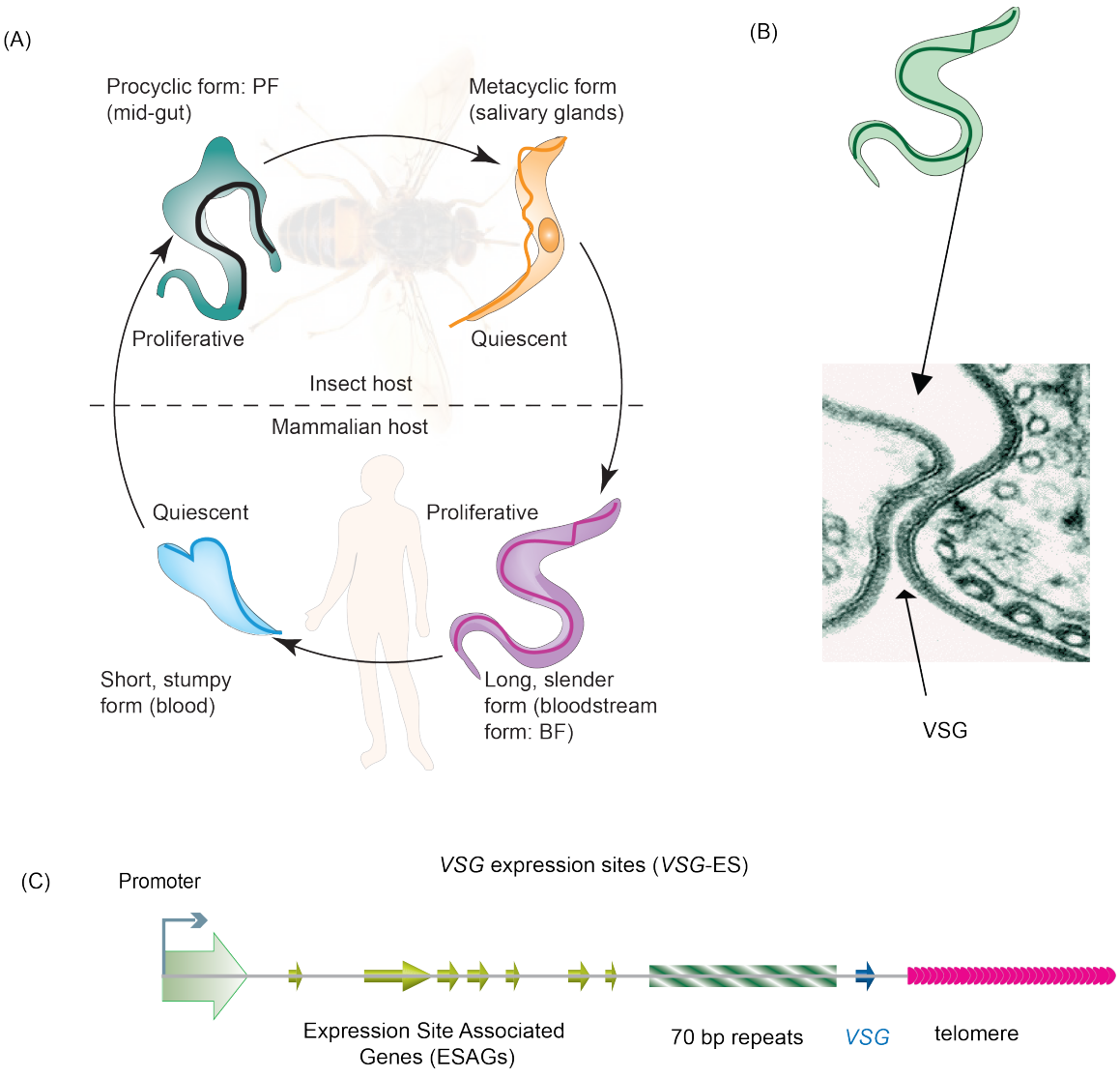

Figure 1-1: An introduction to *Trypanosoma brucei* . (A) Life cycle of *T. brucei* (Lee et al. 2007). (B) EM of a cross section of *T. brucei* cell showing VSG molecules. Image was obtained from tryps.rockefeller.edu. (C) Architecture of a *VSG* expression site.

Architecture of VSG-ES

T. brucei's VSG-ES is composed of the *VSG* at a sub-telomeric position, a 70 bp upstream repeat sequence and several expression site associated genes or (ESAGs), which are located several kbs upstream of *VSG* gene (Alexandre et al. 1988). ESAGs are believed to provide genomic redundancy or polymorphism to facilitate homologous

recombination necessary for host adaptation (Berriman et al. 2002). The promoter is located 40-60 kb upstream of the *VSG* gene (Pays et al. 1989). Transcription of *VSG*-ES is carried out by RNA Pol-I; the polymerase resistant to alpha amanitin (Pays et al. 1989).

Antigenic Variation

Many parasites and microbial pathogens evade the immune responses via antigenic variation, a phenomenon that is common among parasites or microbes that express a surface molecule (Li 2012). In antigenic variation, *T. brucei* expresses a single surface molecule at anytime, and regularly switches the expressed surface molecule (Figure 1-2a) to escape the host immune responses (Namangala 2011). In order to achieve antigenic variation, *T. brucei* must meet three criteria: First, it must harbor antigenically distinct surface antigens that are encoded from the same gene family. Second, a mechanism whereby *T. brucei* cells express one surface molecule at a time and finally, a mechanism that enables *T. brucei* to regularly switch its surface antigen (Stockdale et al. 2008). *VSG* genes and psudeogenes serve as a huge repertoire for *T. brucei*, conferring to the first requirement. *VSG* array can be found at subtelomeric loci of MBCs, linked to expression sites of MBCs or ICs and at subtelomeres of MCs (Figure: 1-2b). In addition, *T. brucei* expresses one *VSG* at anytime through monoallelic expression, where all the expression sites are silent except for the expression site of the active *VSG* (Figure: 1-2c). Finally, *T. brucei* switches its expressed surface antigen through transcription or recombination based pathways as illustrated in (Figure: 1-2d). During *VSG* switching, *T. brucei* can undergo an *in-situ* switch by turning off the promoter of the originally active ES and turning on the promoter of the originally silent ES.

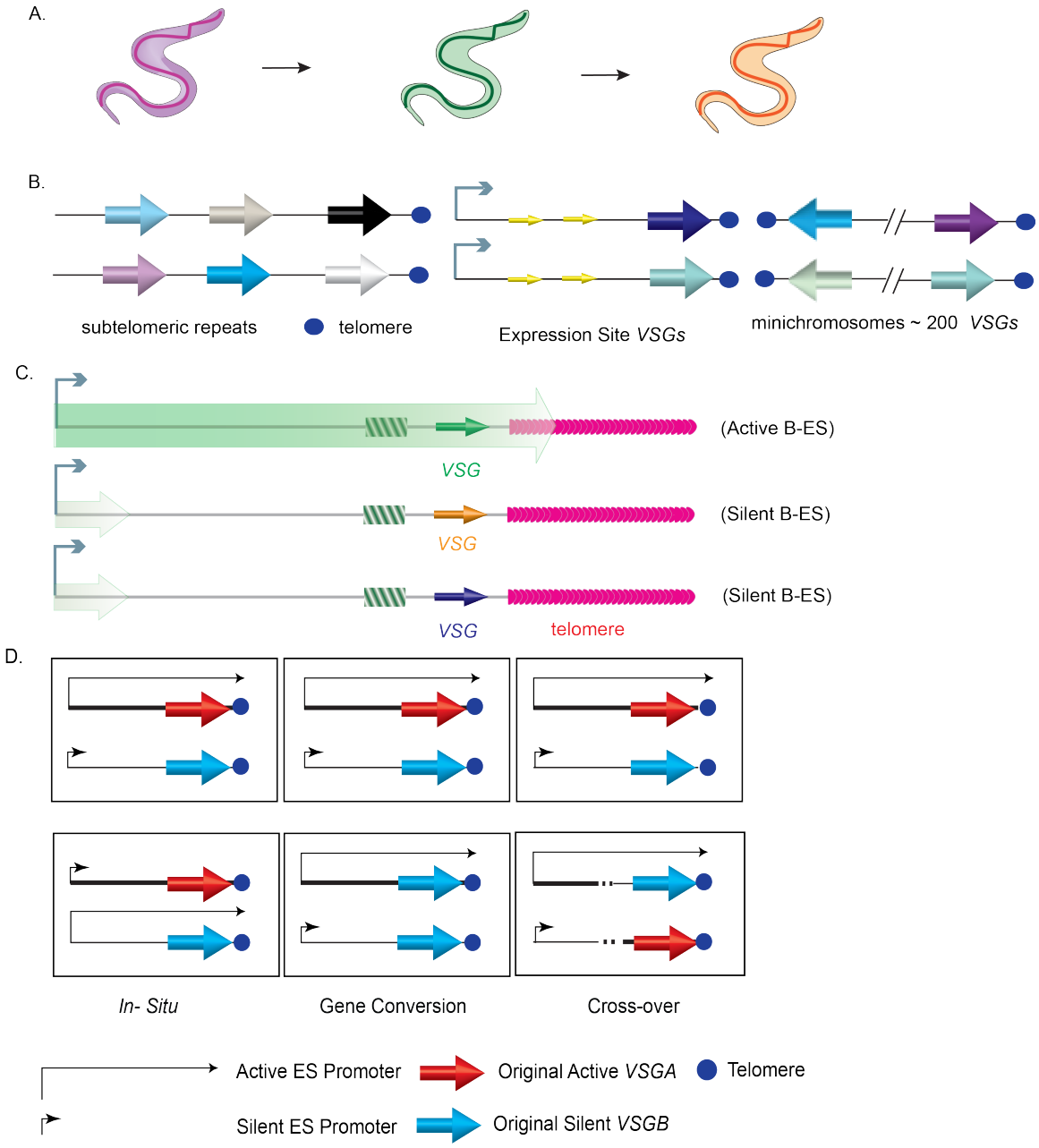

Figure 1-2: Antigenic Variation**.** (A) Antigenic variation in *Trypanosoma brucei*. (B) *VSG* genes repertoire. (C) Monoallelic expression. (D) *VSG* switching: Possible mechanisms.

It can also undergo a Gene Conversion event or a Telomere Exchange. In Gene Conversion, the original *VSG* is lost in the genome. In addition, either a whole expression site is duplicated and inserted into the originally active ES or only the *VSG* is duplicated

and inserted into the originally active ES. Finally, in a Telomere Exchange, the *VSG* in the originally silent ES is crossed-over with the *VSG* in the originally active ES. *VSG* switching and monoallelic expression are tightly regulated in *T. brucei*, making antigenic variation one of the most sophisticated methods developed by this unicellular parasite to evade the host immune system (Taylor and Rudenko 2006).

VSG Regulation.

Several factors have been reported to regulate *VSG* switching or monoallelic expression or both (reviewed by Li 2012). Recent studies have shown that *VSG* can be regulated by 1) Chromatin remodeling factors (Janzen et al. 2006; Hughes et al. 2007, Wang et al. 2010; Denninger et al. 2010; Povelones et al. 2012) and nucleosome packaging (Rudenko 2010; Stanne and Rudenko 2010; Figueiredo and Cross 2010), 2) Transcription elongation and transcription factors (Vanhamme et al. 2000; Narayanan et al. 2011), 3) Telomere proteins (Yang et al. 2009) and telomere length (Hovel-Miner et al. 2012), 4) DNA recombination (McCulloch and Barry 1999; Proudfoot and McCulloch 2005; Hartley and McCulloch 2008; Kim and Cross 2010; Kim and Cross 2011) and 5) DNA replication (Tiengwe et al. 2012a; Benmerzouga et al. 2013).

Chromatin remodeling was shown to play a crucial role in the regulation of *VSG* expression at the promoter level. Several studies reported chromatin-remodeling factors influencing the expression of silent *VSGs* at the promoter, where transcription at the promoter increases upon the depletion of this factor but does not reach the *VSG* and hence no increase in *VSG* expression is observed. TbDot1b, a histone 3 lysine 76 methyltransferase in *T. brucei*, regulates the expression of silent *VSGs*. The deletion of

TbDot1b resulted in a 10-fold increase in transcription of silent B-ES (Janzen et al. 2006). ISWI, a novel member of the chromatin remodeling family SWI/SNF2-related was reported in *T. brucei*. Depletion of TbISWI led to the derepression at the ES promoter by 30-60 fold in BF cells and 10-17 fold in PF cells (Hughes et al. 2007). Another study by (Denninger et al. 2010) reported that the chromatin remodeling complex, FACT subunit- TbSpt16- was important for the silencing at the ES promoter in both life stages. Finally, the depletion of the histone deacetylase (DAC3) showed derepression at the promoter, a similar observation that was observed for TbISWI (Wang et al. 2010). Although there are Sir2 related proteins in *T. brucei*, which are NAD-dependent histone deacetylases, none of the TbSir2rps influence *VSG* silencing or switching (Alsford et al. 2007). It is evident from these studies that chromatin remodeling plays a regulatory role in *VSG* silencing and not all known chromatin remodeling factors influence *VSG* silencing. Finally, depletion of Histone 1 (H1) resulted in 6-8 fold of derepression at the promoter of a silent *VSG* in BF cells and a 3 fold derepression in PF cells (Povelones et al. 2012). In addition to chromatin remodeling factors, nucleosome packaging was shown to be different between active and silent B-ES (Stanne and Rudenko 2010), where the active ES is depleted of nucleosomes.

A second factor regulating *VSG* expression is transcription. Early studies showed that the silent B-ESs are transcribed; however transcription is rapidly attenuated (Vanhamme et al. 2000). In addition, a recent study showed that a novel transcription regulator NLP (NucleoplasminLike-Protein) regulates the expression of silent ES. The depletion of NLP resulted in a 45-60 fold increase in the expression of the originally silent ES (Narayanan et al. 2011).

Telomere Position Effect (TPE) was proposed to play a critical role in the regulation of *VSG* (Dreesen et al. 2007), ever since the discovery that *VSGs* are exclusively expressed from sub-telomeric loci (De Lange and Borst 1982). Glover and Horn (2006) showed that an artificial seeding of telomeres affected the expression of Pol-I reporter gene transcription in both life stages BF and PF. However, not until recently it was shown that the depletion of the telomeric protein TbRAP1 caused the derepression of all silent B-ES linked genes (Yang et al. 2009). In addition, telomere length was shown to affect the rate of *VSG* switching, where cells with extremely short telomeres in telomerase null background had higher frequency of *VSG* switching as opposed to the cells that had longer telomeres (Hovel-Miner et al. 2012). These findings clearly support the hypothesis that telomeres influence the regulation of *VSG*.

Homologous recombination is the major pathway for *VSG* switching (McCulloch and Barry 1999). In *T. brucei*, six TbRAD51 related proteins were identified (Proudfoot and McCulloch 2005) and among the six proteins, TbRAD51 and TbRAD51-3 deletion led to a decrease in *VSG* switching. In addition, a conserved key regulator of homologous recombination BRCA2, which binds to RAD51, was found in *T. brucei*. Deletion of TbBRCA2 led to decrease in the *VSG* switching frequency (Hartley and McCulloch 2008). Deletion of TbTOPO3-α resulted in a significant increase in *VSG* switching frequency (Kim and Cross 2010). Finally, TbRMI-1, a homologue belonging to the RTR complex (REQ-helicase-toposisomerase III α and RMI1/2), which suppresses inappropriate homologous recombination, resulted in a significant increase in *VSG* switching frequency (Kim and Cross 2011).

Finally, DNA replication, one of the most critical processes for the survival of an

organism was carefully characterized lately by multiple groups and showed that the depletion of TbORC1 affected *VSG* silencing (Tiengwe et al. 2012a, Benmerzouga et al. 2013). In the first study, Tiengwe et al. (2012) showed that the depletion of TbOrc1 resulted in the derepression of metacyclic *VSGs* (m*VSGs*). Moreover, Benmerzouga et al. (2013) illustrated that depletion of TbORC1 affected *VSG* silencing in PF cells and BF cells as well as a significant increase in *VSG* switching frequency. Taken all of these studies together, it is evident that *VSG* regulation is a complex process involving multiple factors and multiple mechanisms. Therefore, it is possible that more factors will be identified in the near future.

J-base Modification in T. brucei

A novel modification found in kinetoplastids was first recognized by Bernards et al. (1984), where the digestion pattern of the two enzymes *PstI* and *PvuII* changed depending on whether the telomere was associated with an active or silent ES. *PstI* or *PvuII* were partially cleaved at a silent ES but fully digested at the same ES when it was active. However, this modification was completely absent in the procyclic form (Bernards et al. 1984). The first attempt to identify this putative nucleotide was done by Gommers-Ampt et al. (1991), where they found two unusual nucleotides pdJ and pdV. The pdV nucleotide was present in both life-stages but the pdJ nucleotide was exclusively expressed in BF cells and enriched at telomeric repeats. In addition, pdJ was found to be different than usual eukaryotic DNA modifications and exclusively expressed in kinetoplastids (Gommers-Ampt et al. 1993). The nucleotide pdJ, now known as base J (beta-D-glucosyl-hydroxymethyluracil), was physically shown to associate with silent but

not active *VSG* ESs by immunoprecipitating J (van Leeuwen et al. 1997). In addition, J was quite abundant at telomeres (van Leeuwen et al. 1998b), not found in insect stage form (van Leeuwen et al. 1998a) and targets not only telomeres but tandem repeats as well (van Leeuwen et al. 2000). J base is synthesized in two steps, first the thymidine is hydroxylated by two thymidine hydroxlyases JBP1 and JBP2 and then glycosylated by yet un-identified enzymes (Cliffe et al. 2009). Nevertheless, J is not a target for DNA glycosylases (Ulbert et al. 2004). Deletion of either JBP1 or JBP2 resulted in the decrease of the levels of J and J was completely abolished when both JBP1 and JBP2 were deleted (Cliffe et al. 2009). JBP1 and JBP2 null cells exhibited normal cell growth indicating that base J is not essential in *T. brucei* (Cliffe et al. 2009). Studies are on-going to deduce the functional relevance of base J in *T. brucei*. Moreover, base J showed functional relevance in other Kinetoplastida related organisms, *Leishmania spp* (van Luenen et al. 2012) and *Trypanosoma cruzi* (Ekanayake et al. 2011), where depletion of J resulted in increase of transcription of Pol-II transcribed genes. It remains to be determined whether presence of J in *T. brucei* is of any functional relevance (Borst and Sabatini 2008).

Telomeres and telomere complex

Telomeres are nucleoprotein complexes located at ends of linear chromosomes (Blackburn 1991). Telomere DNA usually consists of simple repetitive TG-rich sequences, and there is often a single-stranded 3' G-rich overhang at the very end of the telomere (de Lange 2005). Telomeres are important for cellular homeostasis (Diotti and Loayza, 2011). Telomeres shorten with each round of cellular proliferation. This

phenomenon is known as cellular senescence (Blackburn 2001). Thus telomeres deduce the life span of a cell. The shelterin complex protects telomeres and mediates both telomere length and telomere protection (de Lange 2005). In humans, the telomere DNA is bound by two TTAGGG repeat binding factors: hTRF1 (Zhong et al. 1992,) and hTRF2 (Broccoli et al. 1997). These factors recruit the other telomeric factors, hRAP1, hTin2, hTPP1 and hPOT1 (de Lange 2005), which are all essential for cellular homeostasis (Diotti and Loayza 2011).

In *T. brucei,* several essential telomeric proteins were identified (Li et al. 2005; Yang et al. 2009): TbTRF and TbRAP1 (Figure 1-3). TbTRF is the duplex telomere DNA binding factor. It plays an essential role in maintaining the telomere G-overhang structure (Li et al. 2005). TbRAP1 is the TRF-interacting factor and is essential for silencing ES-linked *VSG* genes through a TPE-like mechanism (Yang et al. 2009). Additional factors are being characterized such as TbTIF (TbTRF-interacting factor) and has been show to be important for *VSG* switching regulation (Jehi and Li, unpublished data). All *T. brucei* telomeric proteins are essential genes, making them an attractive therapeutic target against *T. brucei* (Li 2012). Nevertheless, the consequences of dysfunctional antigenic variation as a result of targeting these genes must be carefully characterized. *T. brucei* tightly regulates antigenic variation to prolong its survival in its mammalian host (Rudenko et al. 1998). It is possible that dysfunctional antigenic variation not only makes *T. brucei* vulnerable to complete elimination by host immune responses, but also, it makes it capable of escaping early immune detection (Dubois et al. 2005). Therefore, it is essential to dissect the consequences of deletion or depletion of essential genes to elucidate the most effective drug targets.

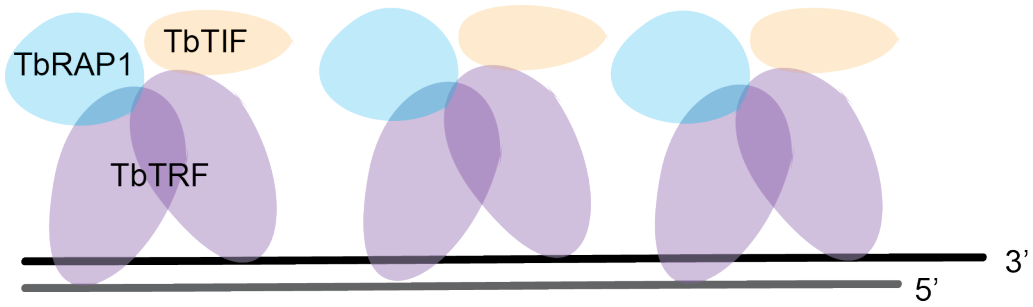

Figure 1-3: *T. brucei’s* telomere complex. TbTRF is the duplex telomere DNA binding factor (Li et al. 2005). TbRAP1 interacts with TbTRF and is essential for *VSG* silencing (Yang et al. 2009). TbTIF is also a TbTRF interacting factor and is important for *VSG* switching (Jehi and Li, unpublished data).

CHAPTER II

MATERIALS AND METHODS

Plasmids

For a full list of primer sequences refer to Appendix B. To generate psk-hygro-ko-TbORC1, the 5`-UTR of TbORC1 was PCR amplified from *T. brucei* 927 genomic DNA using primers 1 and 2. The 3`-UTR of TbORC1 was PCR amplified using primers 3 and 4. The UTR's were digested and ligated into a pBlueScript vector. To generate pFLAG-HA-HA (F2H)-ORC1, the TbORC1 N-terminal F2H-tagging construct, full-length TbORC1 (Tb11.02.5110) was PCR amplified using primers 5 and 6. The 5' UTR region (~ 500 bp) was PCR amplified using primers 1 and 2. PCR products were inserted into pBlueScript to flank a cassette including the puromycin resistance gene (*PURO*), the alpha/beta tubulin intergenic sequence, and the F2H tag.

For yeast 2-hybrid analysis, the pACT2-TbORC1 construct was generated by amplifying TbORC1 using primers 5 and 7. The amplified TbORC1 was digested with *BamHI* and *EcoRI*. Finally, the amplified TbORC1 ORF was inserted into the *BamHI* and *EcoRI* sites of pACT2. The pBTM116-TbORC1 construct was generated by amplifying TbORC1 using primers 8 and 9. The amplified TbORC1 was digested with *EcoRI* and *BamHI*. Finally, the amplified TbORC1 ORF was inserted into *EcoRI* and *BamHI* sites of pBTM116.

To generate various TbTRF DNA binding mutant constructs, the N- terminus (NT) of TbTRF was amplified using primers 10 and 11. The C-terminus (CT) of TbTRF was amplified from TbTRF constructs harboring specific point mutations (made by Li, X) using primers 12 and 13. Two-step PCR was used to combine the two fragments. The first step used the overlapping fragments for extension at 53°C followed by a second step PCR that amplified TbTRF using primers 10 and 13. The TbTRF products harboring particular point mutations were ligated with a construct containing a Ty1 tag, *BLE* and *PURO* genes.

To target TbTRF DNA binding mutants in the HSTB261 reporter strain, TbTRF mutants were amplified using primers 10 and 13 and inserted into a Ty1 and *BLE* containing construct. For TbTRF MYB domain yeast-2-hybrid analysis, the full-length TbTRF harboring the following MYB domain mutations R348K, R298K, H346R and Q320S were fused to LexA binding domain and inserted into *PstI* and *BamHI* sites of pBTM116. Full-length TbTRF was amplified from plasmids harboring individual point mutations using primers 14 and 16. The TbTRF MYB domain was amplified using primers 15 and 16.

To generate pFLAG-HA-HA (F2H)-TbTOR1, the TbTOR1 N-terminal F2H-tagging construct, the NT of TbTOR1 was PCR amplified using primers 26 and 27. The 5' UTR region (~ 500 bp) was PCR amplified using primers 23 and 24. PCR products were inserted into similar construct described in generating the F2H-TbORC1 construct.

T. brucei strains

Bloodstream antigenic type MITat 1.2 clone 221a *T. brucei* (VSG2-expressor) was used. Cells harboring the T7 polymerase and the tetracycline (Tet) repressor, single marker (SM, bloodstream) was used for conditional expression of the TbTRF double-stranded RNA (dsRNA) or TbORC1 (dsRNA). All bloodstream (BF) cells were cultured in HMI-9 with appropriate drug selection. Lister 427 procyclic cells (PF) were used for procyclic form experiments. The 29-13 PF cells harboring T7 polymerase and the tetracycline (Tet) repressor were used for conditional expression of TbORC1 dsRNA.

Cells carrying one endogenous allele of the N-terminus F2H tagged TbORC1 in BF form was generated by transfecting *Kpn*I/*Sac*II-digested pF2H-TbORC1. The C-terminus of TbORC1 in PF cells was PTP tagged by transfecting *SalI*-digested pORC1-PTP-NEO (Cells obtained from Concepción-Acevedo, J).

TbORC1 RNAi cells were established by transfecting *SacII*-linearized pStLBFORC1 construct (obtained from Concepción-Acevedo, J) into SM cells. Transfections were performed using an AMAXA Nucleofactor (Lonza, Inc.) according to manufacture protocol.

TbORC1 single knockout cells were generated by replacing the TbORC1 allele with a *HYG* gene using a targeting construct (See plasmids section). The TbORC1 knockout targeting construct was linearized with *XhoI* and *NotI,* and transfected into TbORC1 RNAi cells. Correctly targeted clones were confirmed by Southern Blot analysis.

For the TbTRF single knockout cells, TbTRF allele was replaced with a *HYG* gene by transfecting SM cells with a construct containing *HYG* gene (Li et al. 2005). The

construct was linearized with *NotI* and *ApaI*. Upon Southern confirmation, cells were transfected with targeting constructs harboring the following point mutations in the MYB domain: R298K, Q320S, Q321S, H346R, R348K and R352K that were generated as described (See plasmid section). Constructs were linearized with *SacII* and targeted into the SM-TbTRF +/- strain. Surviving clones were selected and confirmed via Southern, Western and sequencing. Sequencing data were analyzed using SeqMan by aligning the wild-type TbTRF MYB domain with the sequenced results of the mutants. Only correctly incorporated point mutations in the MYB domain of TbTRF genomic DNA were used for further studies.

Cells for the switching assays were established as described in (Kim and Cross 2010) with minor modifications. First a single knockout of TbTRF was generated in HSTB261 strain. HSTB261 contains a blasticidin gene (*BSD*) at the active ES promoter and a puromycin gene (*PURO*) fused with *Herpes simplex* virus thymidine kinase (*PURO-TK)*. Constructs were linearized with *SacII* and targeted into HSTB261-TbTRF +/- cells; surviving clones were selected and confirmed via Southern, Western followed by sequencing; only correctly incorporated point mutations in the MYB domain of TbTRF were used for the switching assays studies. At least two independent cell lines per mutant were characterized.

The TbTRF-RNAi cells in HSTB261 strain were generated by targeting a *NotI* linearized PZJMβ-TbTRF construct (Li et al. 2005). Surviving clones were screened for doxycycline sensitivity; only clones exhibiting strong depletion of TbTRF were used for *VSG* switching studies.

TbTEL2 RNAi cells in SM and in HSTB261 strain were generated by targeting a

NotI linearized PZJMβ-TbTEL2 construct (made by Li, B). Clones were tested for doxycycline sensitivity; only clones exhibiting depletion of TbTEL2 were used for further studies. TbTEL2 RNAi was also introduced into a TbTEL2 +/- strain. One of the TbTEL2 alleles was replaced with a *BSD* gene. In addition, the other allele of TbTEL2 was F2H-tagged using a F2H-targeting construct (made by Li, B). Finally, the F2H-TbTOR1 cells were generated by targeting the NT tagging construct of TbTOR1 in the TbTEL2 -/RNAi cells.

Generation of Anti-J-base serum

Base J was conjugated to BSA or mKLH according to manufacture's guidelines (*Thermo Fisher Scientific)*. Briefly, the pH of EDC conjugation solution was adjusted to pH 6.0 with 0.1 M NaOH and 250 μl of 1 M imidazole. After adjusting the pH of the solution, J-base powder (obtained from Dr. Zhao) was mixed with EDC conjugation buffer. The mixture was incubated at 37 °C for 10 minutes. BSA and mKLH were prepared by adding 200 μl of ddH2O to each vial to make 10 mg/ml of BSA and 10 mg/ml of mKLH. Dissolved J-base was added to the conjugating protein (BSA or mKLH) and rotated at room temperature (RT) for 2 hours. The conjugated hapten was purified by desalting. The concentration of J-base and conjugated-J-base was measured using Nanodrop (*Thermo Scientific*). For each individual conjugation, BSA or mKLH conjugated J-base was sent to *ProSci* for antibody generation. Bleeds were collected over 8 weeks.

For antibody (Ab) characterization, 1 μg of DNA from SM was blotted on to a N+ hybond membrane using a slot blot apparatus. The membrane was blocked for 1 hour in

PBST (10 mM Tris-HCl, pH 7.4 0.02% Tween-20) with 5% milk powder, washed 3 times with PBST, and incubated with J serum diluted in PBST + 2% milk for 2 hours. The blot was washed 3 times with PBST, incubated with secondary Ab diluted in PBST + 2% milk for 1 hour, washed 3 times with PBST and developed with ECL.

Chromatin IP (ChIP)

~$1x10^8$ cells were harvested and fixed with 1% formaldehyde for 20 minutes at room temperature. *T. brucei* BF cells were lysed and sonicated using a Bioruptor®300 for 4 cycles with high output 30s on/off per cycle. Lysates were incubated using Dynabeads® with or without specific antibodies to immunoprecipitate protein-DNA complexes. For PF of *T. brucei*, cells were lysed and sonicated using a Bioruptor®300 for 10 cycles with medium output 30s on/off per cycle. Lysate was subjected to immunoprecipitation using IgG Sepharose 6 Fast Flow. Prior to IP, beads were washed and equilibrated following manufacture's protocol. Immunoprecipitated DNA was purified using the Qiaquick spin PCR purification Kit (*Qiagen*) and analyzed by Southern hybridization using a telomere specific probe: TTAGGG. As a control for pull-down specificity, blots were hybridized with 50 bp repeats probe.

RNA Isolation and Reverse Transcription

Total RNA was extracted from cells using RNAstat (*TEL-TEST, Inc*) and purified with Qiagen RNeasy kit and treated with DNase (*Qiagen*). Reverse transcription was carried out using M-MLV (*Promega*) according to the manufacturer's protocol.

Quantitative RT-PCR

Quantitative real-time RT-PCR was performed using BioRad iTaq SYBR Green Supermix with ROX according to the manufacturer's protocol. The amount of DNA was quantified by DNA Engine Opticon 2 (*BioRad*). Only primers giving specific PCR products were used. The normalized fold change in mRNA level was calculated according to the formula in appendix A. The Sequence of RT-PCR primers used in these studies can be found in Table S1 in (Yang et al. 2009).

Western Blot

For details regarding each antibody, refer to appendix D. In TbORC1-RNAi cells, F2H-TbORC1 was detected using 12CA5, monoclonal antibodies against HA. In TbORC1-PTP-NEO cell line, TbORC1-PTP was detected using protein A antibody. Rabbit antibodies specifically against VSG2, VSG13 and VSG9 were used to detect expression of these VSGs. Expression of LexA Binding Domain- and Gal4 Activation Domain-fusion proteins were detected using monoclonal antibody against LexA and monoclonal antibody against GAL4.

For Western analysis in TbTRF mutants, TbTRF was detected using a lab antibody against TbTRF: 1260 or 1261 (Li et al. 2005). For Ty1-TbTRF we used the commercially available BB2 antibody. As a loading control we used anti-beta tubulin TAT-1 (Yang et al. 2009). In TbTRF RNAi cells, TbTRF was detected using the same antibody 1260, and as a loading control we utilized EF-2 antibody or antibody against H3.

Pulse field Gel Electrophoresis and In-gel Hybridization

Undigested chromosome DNA was prepared in the form of plugs. Approximately, 120 million cells were harvested and washed with 1xTDB (5 mM KCl, 80 mM NaCl, 1 mM MgSO4, 20 mM Na2HPO4, 2 mM NaH2PO4, 20 mM glucose [pH 7.4]). Cells were re-suspended in L-buffer (0.01 M Tris-HCl pH 7.6, 0.02 M NaCl, 0.1 M EDTA pH 8.0) to a final concentration of 4 x 10^8 cells/ml. Cells were incubated at 42-50 °C for 10 minutes. An equal amount of 50 °C low melting agarose was added to cells and ~ 1x10^7 cells were loaded in the plug preparing chambers. The DNA plugs were allowed to solidify at RT for 10 minutes. The plugs were put in L-buffer with 1% N-L sarcosyl and Proteinase K (100 μg/ml) for 48 hours. After 48 hours, plugs were washed with L-buffer twice for 10 minutes each. The incubation step, as mentioned above, was done for another 48 hours. After 48 hours, the plugs were washed with L-buffer twice for 10 minutes each at 50 °C and then, the plugs were allowed to cool to 4 °C prior to running.

In order to run PFGE, 3 liters of 0.5 x TBE (40 mM Tris-Cl pH 8.3, 4 mM boric acid, 1 mM EDTA) were prepared. Out of the 3 liters of 0.5 x TBE, 200 mls were used to prepare 1.2% agarose gel. The plugs were loaded and PFGE conditions were set as follows: initial pulse for 1500s, ending pulse for 700s, voltage at 2.5 V/cm for 120 hours at 14°C. After 120 hours, the gel was stained for 1 hour in 0.5 x TBE containing 1 µg/ml EtBr and washed for 30 minutes with ddH2O prior to scanning. After scanning, the gel was dried overnight using a gel dryer with frequent changes of whatman paper in the first 2 hours.

For in-gel hybridization, the gel was pre-hybridized at 50 °C in Church Mix (0.5 M NaPi pH 7.2, 4 mM EDTA pH 8.0, 7% SDS, 1% BSA) for at least 30 minutes.

Meanwhile, oligonucleotides were labeled with ATP (γ-32 P) using T4 polynucleotide kinase. A TelC4 oligonucleotide was used to detect the G-strand and a TelG4 oligonucleotide was used to detect the C-strand. The latter serves as a loading control. The gel was hybridized with the radioactive probes at 50 °C in 25 ml Church Mix overnight, washed in 4 x SCC at 55 °C three times, each for 30 minutes. The final wash was done once in 4 x SCC with 0.1% SDS at 55 °C for 30 minutes. The radioactive gel was wrapped and exposed for both TelC4 and TelG4 hybridization (refer to Appendix A for formula).

VSG Switching Assays

VSG switching phenotypes were determined by transiently knocking down TbTRF transcripts. HSTB261-TbTRF-RNAi cells were maintained in the presence of blasticidin and puromycin to homogenize the cell population (VSG2-expressors). Cells were then allowed to switch in the absence of drug selection for 24 hours, with or without induction (200 ng/ml doxycycline). Plating efficiency was assessed to determine cell viability after TbTRF knockdown and this was taken into account to calculate the *VSG* switching frequency. Doxycycline was washed off TbTRF RNAi induced cells after 24 hours, and the cells were allowed to recover. When the cells reached the same population doubling as without induction, ~ 0.5 million cells were added to a medium containing 4 μg/ml Ganciclovir (GCV) and distributed into 3 x 96-well plates. Switchers were verified using a dot blot for VSG2 prior to deducing the switching frequency. In addition, switchers were verified for potential spontaneous mutations that result in false switchers by the analysis of puromycin sensitivity at 2 μg/ml. The switchers were collected and a

Raw Frequency (RF) was calculated, which is the number of switchers collected divided by the total number of cells plated. To determine cell growth, cells are plated in the absence of GCV and a plating efficiency (PE) was calculated, which is the number of wells exhibiting growth divided by the number of wells plated. Switching frequency was reported as the RF normalized with PE (Figure 2-1).

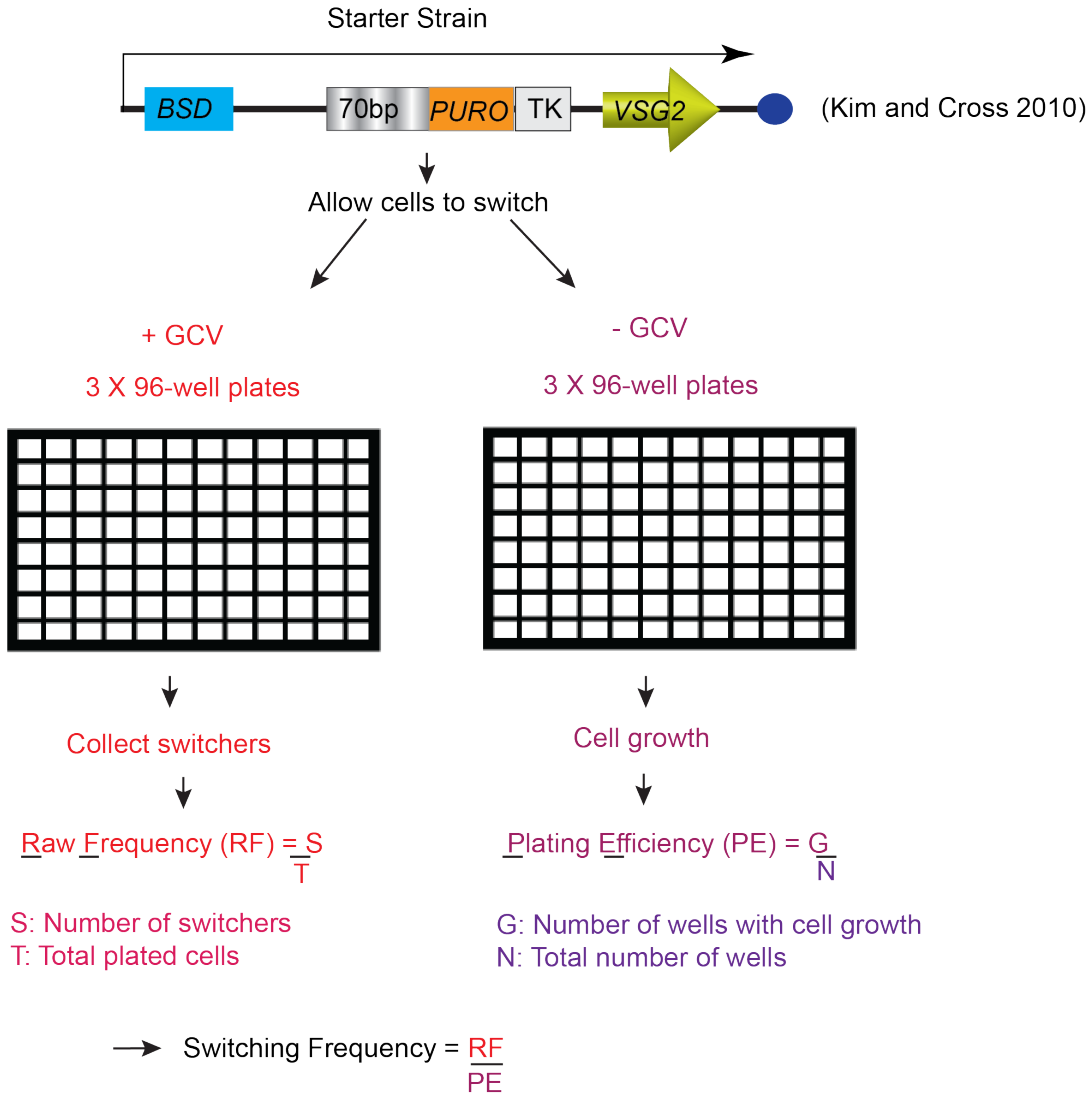

Figure 2-1: The Switching Assay. Cells were maintained under the selection of blasticidin and puromycin until the initiation of the switching assay. To initiate the switching assay, selective drugs were removed and cells were allowed to switch. Cells were platted in the presence or absence of GCV (see text for details). The RF was determined from the cells platted with GCV. The PE was determined from the cells

platted in the absence of GCV. The RF was normalized with PE for the reported switching frequency.

For TbTRF MYB domain mutants, single knockout and wild-type HSTB261 cells were maintained in the presence of blasticidin and puromycin to homogenize the cell population (VSG2-expressors). Cells were then allowed to switch in the absence of drug selection for 3 days. When cells reached comparable population doubling, the same switching assay as described above was carried out.

Finally, for TbTEL2 switching assay, TbTEL2 transcripts were depleted for 72 hours, when cells reached comparable population doublings as without induction the same switching assay as described above was carried out.

Dot Blot

Approximately 1-2 million cells were harvested at 2000 rpm at RT for 10 minutes. Approximately 20 µl of medium was left behind. The pellet was re-suspended in the remaining medium. A Nitrocellulose membrane was pre-wet with ddH2O for 1 minute and 1 x PBS for 5 minutes. Approximately 5 µl of cells were loaded as a dot on the membrane. The dots were allowed to dry for 5 minutes on the membrane before blocking. The membrane was blocked with 1 x PBST + 10% milk for 30 minutes. The hybridization was done with VSG2 antibody diluted in 1 x PBST + 5% milk for one hour. The membrane was washed 3 x with 1 x PBST, hybridized with secondary antibody ECL-IgG-anti-rabbit for one hour, and then washed 3 x with 1 x PBST.

Immunofluorescence Analysis

Immunofluorescence was carried out as described previously (Lowell and Cross

2004) with minor modifications. Briefly, induced (Day 0) and un-induced (Day 4) TbORC1 RNAi cells were harvested and fixed with 2% formaldehyde and permeabilized with 0.2% NP40 in PBS. After blocking with PBS/Gelatin, cells were incubated with Alexa-488 conjugated anti-VSG3 and Alexa-647 conjugated anti-VSG13. Cell images were captured using a DeltaVision image restoration microscope (Applied Precision/Olympus), deconvoluted by using measured point spread functions, and edited with Adobe Photoshop.

Immunoprecipitation

Approximately $1x10^8$ cells harboring an endogenous TbORC1-PTP or WT427 (no tag control) were lysed by vortexing the lysate with acid washed glass beads for 40 seconds ON/OFF intervals, repeated for 3 times. Protein extract was pre-cleared with pre-washed protein G beads (*Sigma*). The pre-cleared lysate was immunoprecipitated using IgG Sepharose 6 Fast Flow (*GE Healthcare*). Prior to IP, IgG beads were washed, equilibrated following the manufacture protocol. The IP product was washed five times with TST buffer (50 mM Tris-buffer pH 7.6, 150 mM NaCl and 0.05 % Tween 20) and once with 5 mM NH4Ac (pH 5.0). The IP product was eluted with 2 M glycine pH 2.2. All buffers were supplemented with 1 mM PMSF, protease inhibitor cocktail for mammalian cells (*Sigma*), 4 μg/ml pepstatin A, and 0.5 mg/ml TLCK immediately before use. Samples were analyzed by Western blot.

Southern Blotting

Genomic DNA was prepared using DNAzol. Briefly, 100 million cells were harvested, washed with 1 x TDB and re-suspended in 1 ml DNAzol. After 30 minutes, the samples were spun at full speed for 10 minutes, only the supernatant was transferred to a new tube and DNA was precipitated with 100% ethanol. The DNA was washed with 70% ethanol and allowed to air-dry. The DNA pellet was re-suspended in 30 µl of TE buffer. DNA concentration was measured using NanoDrop 2000 (*Thermo Scientific*). Approximately 5 μg of digested DNA were loaded into a 0.7% agarose gel in 0.5 X TAE and ran at 100V until the orange dye reached the end of the gel. The gel was depurinated, denatured and then neutralized before blotting. DNA was blotted on hybond Nylon membrane, cross-linked prior to hybridization, pre-hybridized with Church Mix and hybridized with the specific probe at 65 °C. The blot was washed three times in 15 minute washing intervals with Church Wash at 65 °C, wrapped and exposed.

Flow Cytometry

For each analysis ~ 20 million cells were harvested by centrifugation at 1500 rpm for 10 minutes at 4 °C. Cells were washed twice with 1 x TDB + 2 mM EDTA solution then re-suspended in 200 μl of the same buffer. Cells were fixed by adding 2 ml of 70% ice-cold ethanol drop-wise while vortexing. Cells were stored at 4 °C for at least 12 hours. Prior to FACS analysis, cells were harvested by spinning for 10 minutes at 1500 rpm at 4 °C. Pelleted cells were re-suspended in 0.5 ml staining solution (1 x PBS + 2mM EDTA, 200 μg/ml RNAseA, 50 μg/ml Propidium Iodide). Cells were incubated at 37 °C

for 30 minutes in staining solution and then we proceeded with FACS (cell cycle analysis). Data was analyzed using FlowJo software.

Yeast-two-hybrid Analysis

Proteins were fused to either a LexABD or a GAL4AD. Interaction was measured as an output of β-galactosidase activity, where transcription of β-galactosidase was a result of protein interaction. β-galactosidase cleaves β- O-nitro-phenyl-β-D-galactopyranoside (ONPG), which serves as a readout for the assay. For each strain, at least three independent clones were tested in each assay. The average values and SD was calculated from the combined results.

Isothermal Titration Calorimetry (ITC)

ITC was performed and analyzed by our collaborator (Li, X) using an iTC200 microcalorimeter (MicroCal). To measure the TbTRF MYB-DNA interaction, the injection syringe was loaded with 40 μl of TbTRF MYB sample and the cell was loaded with 200 μl of telomere DNA in the form of oligonucleotides. As a control to TbTRF and telomere DNA interaction, the cell was loaded with 200 μl non-telomeric DNA (5' GAA TCT GGT GAG AGC GAC CCC GAT GAC GG 3'). Typically titrations consisted of 20 injections of 2 μl with the duration of each injection being 4 seconds. Between two injections, approximately 200 seconds were allowed to elapse so that samples reach equilibrium before re-injection. The data were analyzed using Origin 7.0 in order to determine the dissociation constant (Kd), as long as the heat curve could be fit to some mode. In the cases where there was no heat curve generated, Kd could not be determined.

CHAPTER III

TRYPANOSOMA BRUCEI ORC1 IS ESENTIAL FOR CELL CYCLE PROGRESSION AND VSG SILENCING[1]

Imaan Benmerzouga et al.

ABSTRACT

Binding of the Origin Recognition Complex (ORC) to replication origins is essential for initiation of DNA replication, but ORC has non-essential functions outside of DNA replication, including heterochromatic gene silencing and telomere maintenance. *Trypanosoma brucei,* a protozoan parasite that causes human African trypanosomiasis, uses antigenic variation as a major virulence mechanism to evade the host's immune attack by expressing its major surface antigen the Variant Surface Glycoprotein (VSG), in a monoallelic manner. An Orc1/Cdc6 homologue has been identified in *T. brucei*, but its potential involvement in *VSG* repression has not been thoroughly investigated. In this study, we show that TbORC1 is essential for cell cycle progression in mammalian-infectious bloodstream form (BF). Depletion of TbORC1 resulted in derepression of telomere-linked silent *VSGs* in both BF and PF, cells. TbORC1 associates with telomere

---

[1] As it appears in the Journal of *Molecular Microbiology*, 87(1): 196-210

repeats but appears to do so independently of two known *T. brucei* telomere proteins, TbRAP1 and TbTRF. We conclude that TbORC1 has conserved functions in cell cycle progression and is also required to control telomere-linked *VSG* expression. This chapter presents the work done solely by the author.

INTRODUCTION

Faithful replication of DNA is critical for cell survival. DNA replication nucleates from sites known as replication origins (Gilbert 2001), where a pre-RC complex forms. The pre-RC complex is initiated by the binding of the ORC complex containing Orc1-Orc6 to DNA (Nasheuer et al. 2002). The pre-RC complex recruits cdc6 (cell division cycle-6), which also binds the replicating DNA. Cdc6 recruits cdt1, which acts as an adaptor to recruit the MiniChromosome Maintenance (MCM) complex (MCM2 to MCM7) (Diffley et al. 1994; Speck et al., 2005; Chen et al. 2007). Successful assembly of the pre-RC complex allows licensing of replication origins and DNA replication can initiate. DNA replication is carefully coordinated with cell-cycle progression. In eukaryotes, this is achieved by the binding of the pre-RC complex to replication origins only in G1 phase so that entry to S-phase is regulated (Diffley 2004; Blow and Dutta 2005).

The pre-RC complex is assembled upon the exit of mitosis and through G1 phase. In budding yeast, ORC proteins associate with the chromatin throughout the cell cycle (Stillman 2005), CDC6 is phosphorylated by cyclin-dependent kinases (CDK) and degraded at the G1/S transition (Elsasser et al. 1999; Drury et al. 2000). However, in

mammalian cells, the ORC1 protein level is regulated during the cell cycle. In S phase, mammalian ORC1 is polyubiquitinated by the SCF complex, followed by degradation by the 26S proteasome (Mendez et al. 2002), but CDC6 associates with the chromatin throughout the cell cycle (Blow and Dutta 2005).

ORC recognizes and binds to replication origins (Bell, 2002). ORC1 to ORC5 have one or two winged helix (WH) motifs that are involved in DNA binding (Gajiwala and Burley 2000). They also have a central AAA+ ATPase domain, which is important for specific DNA sequence recognition (Bell 2002). ORC has roles outside of DNA replication, such as the heterochromatin formation in yeast (Foss et al. 1993; Micklem et al. 1993; Bell et al. 1993), heterochromatin formation in Drosophila (Pak et al. 1997), gene silencing in *Plassmodium falciprium*, the causative agent of malaria (Mancio-Silva et al. 2008), chromatin remodeling in mammalian cells (Prasanth et al. 2004; Prasanth et al. 2010), association with centrosomes and centromeres in mammals (Prasanth et al. 2004; Hemerly et al. 2009) and centromere identity in yeast (Koren et al. 2010). Interestingly, the DNA replication initiation function of ORC does not necessary overlap with its other functions (Chakraborty et al. 2011).

In budding yeast, a mutation in ORC2 disrupted silencing at HMR and caused a cell-cycle arrest, in correlation with impaired DNA replication (Foss et al. 1993; Micklem et al. 1993). In Drosophila, ORC2 interacts with heterochromatin protein 1 (HP1) and mutant ORC2 caused a defect in HP1 localization (Pak et al. 1997). In *P. falciprium*, ORC1 is required for the silencing of the *var* genes, which are located at subtelomeres.

In mammalian cells, ORC2 is tightly bound to heterochromatin, HP1-alpha and HP1-beta and the depletion of ORC2 disrupted HP1 localization (Prasanth et al. 2004). In

addition, ORC1 and ORC3 tightly bind HP1-alpha and as ORC2, the depletion of ORC3 disrupted the localization of HP1-alpha (Prasanth et al. 2010). Moreover, the depletion of HP1 resulted in the loss of ORC2 binding to heterochromatin (Prasanth et al. 2010). Taking these studies together, the ORC complex is important for heterochromatin organization in mammalian cells.

Both ORC1 and ORC2 associate with centrosomes (Hemerly et al. 2009) but ORC2 mediates chromosome segregation and is important for centrosome copy number (Prasanth et al. 2004). ORC6 is important for cytokinesis and localizes to kinetochores (Prasanth et al. 2002). In pathogenic yeast *C. albicans*, centromere and neocentromere origins are associated with ORC and are the first to fire in early S-phase. The association of ORC to centromeres was disrupted when the levels of Histone 3 (H3) was altered at centromeres. This study illustrates that the identity of centromeres, at least in *C. albicans*, is depicted by its heterochromatin, allowing it to be the first to fire during replication (Koren et al. 2010). Mammalian ORC proteins interact with the telomere protein TRF2, and this interaction is important for assembly of the pre-RC at the telomere (Tatsumi et al. 2008; Deng et al., 2009). In addition, mammalian TRF2 interacts with ORC1 through its N-terminus (Atanasiu et al., 2006) and it is possible that this association is important for heterochromatin formation at telomeres (Deng et al. 2009). Taking all of these studies together, it is clear that ORC has functions outside of DNA replication.

Trypanosoma brucei is a protozoan parasite that causes African sleeping sickness in humans. *T. brucei* escapes the host immune system by regulatory switching its surface molecule, Variant Surface Glycoprotein (VSG). VSG expression is tightly regulated and many factors were reported to be involved in this regulation (see chapter I).

An Orc1/cdc6 homologue, hereafter known as TbORC1, was identified in *T. brucei* (Godoy et al. 2009). The primary sequence of TbORC1 contains a nuclear signal (NLS) in its N-terminal region. It also contains Walker A and B motifs (Godoy et al. 2009). It also contains sensor I and sensor II regions (Godoy et al. 2009). These features are typical of members of the pre-replication machinery having the AAA+ ATPase fold (Calderano et al. 2011). For sequence alignment analysis, refer to (Godoy et al. 2009). In addition, genome wide ChIP identified binding sties for TbORC1 along all megabase chromosomes. From these binding sites, ~ 20% appeared to be replicated in early S phase and are considered to be DNA replication origins. There are ~ 100 predicted origins of replication in *T. brucei* (Tiengwe et al. 2012a).

Additional ORC subunits have been described since the identification of TbORC1 such as Orc1-like or Orc1b and Orc4 (Dang and Li 2011; Tiengwe et al. 2012b). As expected, TbORC1 is required for nuclear DNA replication in both PF and BF cells. However, no functional studies have been done to study the function of TbORC1 in gene silencing in *T. brucei*.

In this study, we report that TbORC1 is critical for normal cell cycle progression and *VSG* regulation. We also report that TbORC1 associates with telomeres independent of two known *T. brucei* telomere factors. Our results show that depletion of TbORC1 impaired normal progression of the cell cycle, and it resulted in the derepression of ES-linked *VSGs* in both life stages BF and PF. Finally, TbORC1 associates with telomeres, a possible mechanism whereby TbORC1 regulates *VSG* expression. The author generated the following presented data.

MATERIALS AND METHODS

Plasmids and *T. brucei* strains generated and used for these studies are described in chapter II. Detailed procedures for flow cytometry, q-RT-PCR, immunofluorescence, chromatin IP, yeast-two-hybrid, Western analysis and IP can be found in chapter II.

RESULTS

TbORC1 is required for cell cycle progression

Previous studies have demonstrated that TbORC1 is essential for cell growth (Goody et al. 2009). In addition, a direct role of TbORC1 in DNA replication was demonstrated (Benmerzouga et al. 2013). Nevertheless, careful characterization of the functions of TbORC1 in antigenic variation was not performed. We established inducible TbORC1 RNAi in BF cells that produce a stem-loop dsRNA. We targeted a FLAG-HA-HA (F2H) tag to the N-terminus of one endogenous TbORC1 allele to monitor the expression level of the F2H-TbORC1 protein after induction of RNAi.

The induction of TbORC1 RNAi led to depletion of the F2H-TbORC1 protein in two independent clones and caused a growth defect (Figure: 3-1a). Particularly, when the same TbORC1 RNAi construct was introduced into TbORC1 single-allele knockout (SKO) cells, RNAi induction caused a more severe growth defect, arresting cell growth after only one day (Figure: 3-1a). The protein levels for TbORC1 were monitored using an antibody against F2H. Without any depletion, F2H-TbORC1 is detected (Day 0) and upon induction, F2H-TbORC1 is no longer detected using Western Blot analysis (Day 1 and Day 2; Figure: 3-1b).

In order to investigate the function of TbORC1 in cell cycle progression, we

looked at the cell cycle profiles upon the depletion of TbORC1 in BF cells by FACS analysis of Propidium Iodine stained cells. Looking at a normal cell cycle profile for BF cells, the first peak represents cells with 2C DNA content, where the second peak represents cells with 4C DNA content and the gate in-between 2C and 4C is the S-phase (Figure: 3-2a).

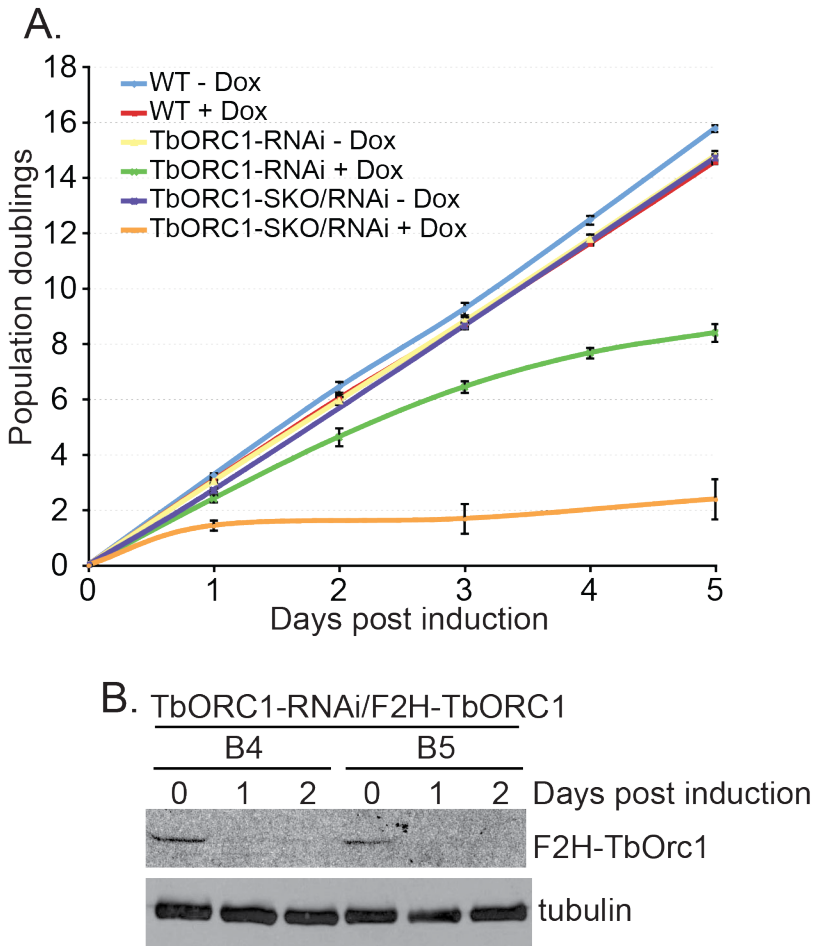

Figure 3-1: Growth analysis for TbORC1 depleted cells. (A) Depletion of TbORC1 in BF cells resulted in a growth defect. A more severe growth defect or an arrest was observed when dsRNA of TbORC1 was expressed in a background of a single allele of TbORC1. The arrest occurred within 24 hours. (B) Confirmation of the depletion of TbORC1 in two independent clones upon the induction of TbORC1 stem loop dsRNA; clones B4 and B5.

Analysis of the gating profiles generated from un-induced cells showed a normal distribution of cells with 2C (G1, ~ 56%), S (~ 8%) and 4C (G2/M, ~ 30%) DNA

contents. However, in TbORC1-depleted cells (at day 3), we observed a significant decrease in the number of 2C cells (~ 34%) and a significant increase in the number of 4C (~ 48%) and S cells (~ 12%) (Figure: 3-2 a, b). Our data suggests that TbORC1 is essential for cell growth in the BF stage and is absolutely required for normal cell-cycle progression.

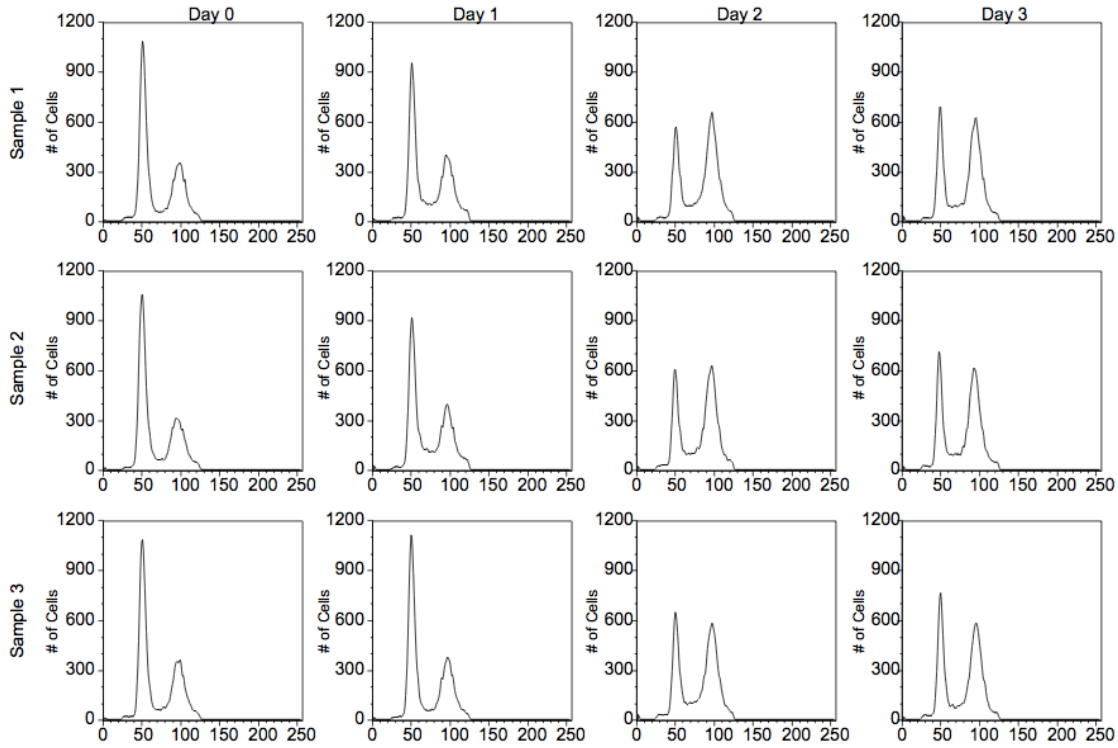

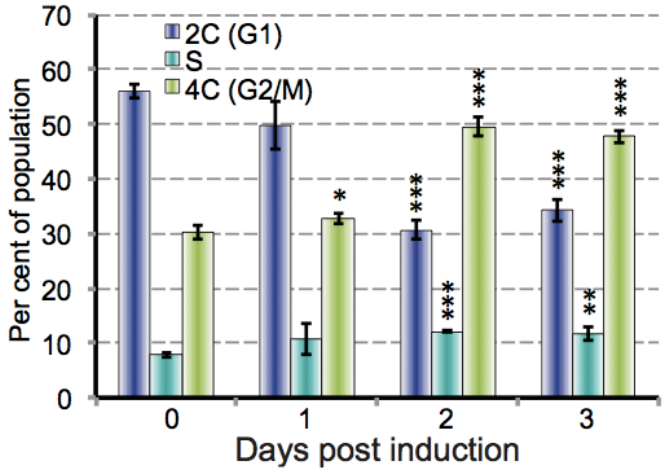

Figure 3-2: Cell cycle analysis of BF cells upon the depletion of TbORC1. (Top) Flow cytometry of BF TbORC1 RNAi cells. Three independent samples were analyzed and labeled as samples 1-3. (Bottom) Quantification of populations of cells at different cell cycle stages before (day 0) and after (days 1, 2 and 3) depletion of TbORC1. Unpaired *t*-tests were performed to compare day 1, 2 and 3 values with the day 0 value. One asterisk, $0.009 < P \leq 0.05$; two asterisks, $0.0001 < P \leq 0.009$; three asterisks, $P \leq 0.0001$.

TbORC1 is required for complete silencing of ES-linked subtelomeric VSGs

The ORC1 subunit has been documented to play pivotal roles in transcriptional silencing in yeast (Foss et al. 1993; Micklem et al. 1993; Bell et al. 1993), heterochromatin organization in mammals (Chakraborty et al. 2011), and the metacyclic form of *T. brucei* (Tiengwe et al. 2012a). We investigated whether the depletion of TbORC1 would affect sub-telomeric silent *VSGs*. To do so, we looked at the steady state mRNA levels of various ES linked *VSGs* upon the depletion of TbORC1 in both PF and BF cells. In both cases, depletion of TbORC1 was confirmed.

Quantitative real-time PCR (q-RT-PCR) measured the mRNA levels of several ES-linked silent *VSGs* before and after the TbORC1 RNAi induction. PF cells repress all *VSGs* and express procyclin as a surface molecule. We examined whether any derepression is taking place in PF TbORC1 depleted cells. TbORC1 depletion in PF caused a mild derepression of ES-linked *VSGs* (Figure: 3-3a), when compared with the derepression levels in BF cells. In BF cells, we observed a moderate derepression of the ES-linked subtelomeric *VSG*s (Figure: 3-3b).

The de-repression levels for different *VSG*s in BF cells were various, ranging from 3-fold (*VSG*9) to as high as 6-fold (*VSG*11) on day 2 and from 4-fold (*VSG*16) to 12-fold (*VSG*6) on day 4 of TbORC1 RNAi induction, respectively. As a control, several control genes located in the chromosome-internal loci, including rRNA, *TbTERT*

(telomerase protein component gene), *TbPGI* (Tb927.1.3830, which encodes glycosomal glucose-6-phosphate isomerase), *TbRPS15* (Tb927.7.2370, a putative ribosomal protein gene), and the originally active *VSG2* were analyzed for a potential global derepression phenomenon, however, we did not observe any significant changes in the mRNA levels of the control genes, further solidifying the conclusion that the depletion of TbORC1 resulted in an increase in ES linked sub-telomeric *VSG* expression.

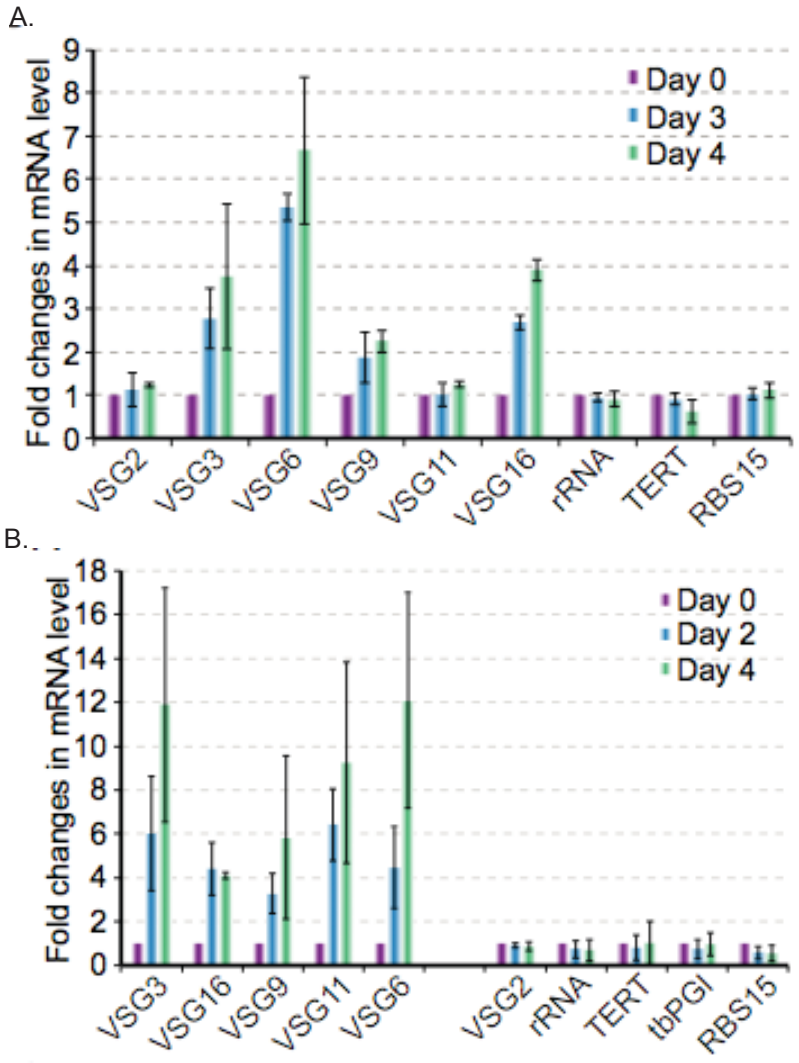

Figure 3-3: qRT PCR analysis of various ES-linked subtelomeric *VSGs* in both PF and BF cells upon the depletion of TbORC1. Steady-state mRNA levels of several silent *VSG*s, the active *VSG*2, and control genes were analyzed by qRT-PCR, using tubulin gene as an internal loading control. The fold changes in mRNA level after RNAi induction are plotted. Day 0 values were set to 1. rDNA, TbTERT, TbPGI and TbRPS15

genes were analyzed as controls. Fold changes were averaged from at least three independent experiments. Standard deviations are shown as error bars. (A) PF cells (B) BF cells.

In an attempt to confirm our data with protein expression of ES-linked VSGs, we tested the expression of VSG9 and VSG2 after depleting TbORC1. In agreement with the our qRT-PCR results, upon the depletion of TbORC1, originally silent VSG13 and VSG9 protein levels were expressed by day 4. (Figure: 3-4). These data suggest that TbORC1 plays a critical role in silencing ES-linked *VSGs*.

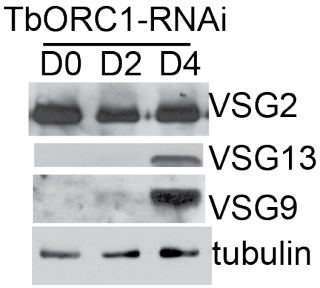

Figure 3-4: Depletion of TbORC1 resulted in derepression of ES-linked VSG expression. Western analysis of the following VSGs: VSG2, VSG13 and VSG9. The VSG2 is the original active VSG in these cells. The expression of any other VSG (VSG13 and VSG9) indicates a derepression phenotype. Upon the depletion of TbORC1, both VSG13 and VSG9 were expressed by day 4 of TbORC1 depletion, in addition to VSG2. Tubulin was used as a loading control.

To test whether the derepressed VSGs are expressed simultaneously within the same cells, we carried out IF analysis using antibodies specific to two silent VSGs, VSG3 and VSG13. As shown in Figure 3-5, no VSG3 or VSG13 expression was detectable before the induction of TbORC1 dsRNA. In contrast, by day 4, we can see a clear expression of both VSGs in the same cells, indicating that different silent ES-linked VSGs can be derepressed simultaneously in TbORC1 depleted cells.

In addition, we stained the cells with both anti-VSG2 antibody and another antibody specific to the silent VSG3 or VSG13. After TbORC1 RNAi induction, we observed that both VSG13 and VSG3 are derepressed while VSG2 remained active

(Figure: 3-6), which is consistent with our qRT-PCR data (Figure: 3-3).

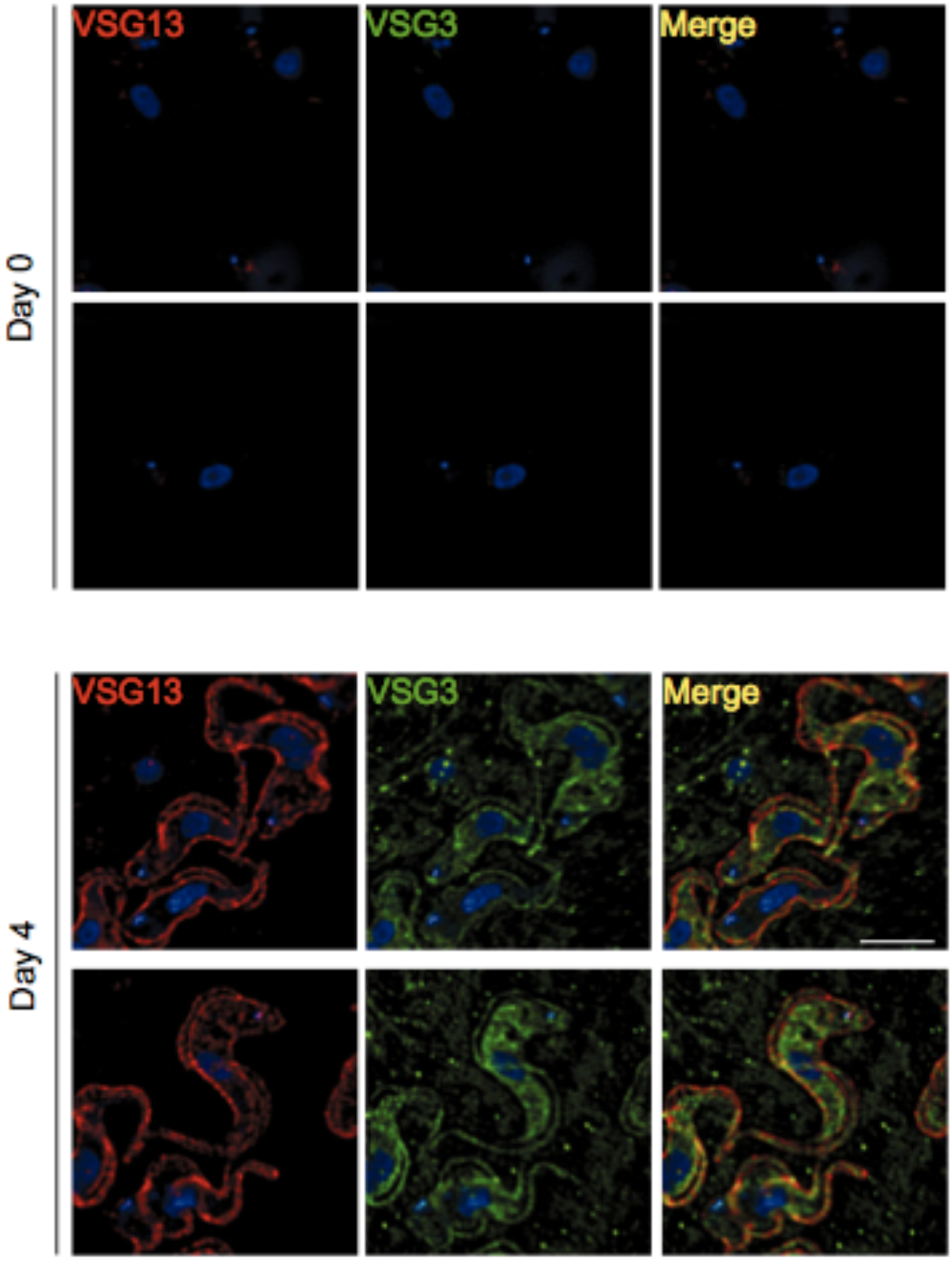

Figure 3-5: Silent VSG derepression in TbORC1 depleted cells. Two silent VSG proteins can be expressed simultaneously on the surface of a single TbORC1-depleted BF cell. VSG2-expressing BF cells were examined by immunofluorescence at indicated time points after TbORC1 RNAi induction. Cells co-expressing the silent VSG3 and VSG13 were visible 4 days post TbORC1 RNAi induction. A single layer of the z-stack images was shown for each time point to better illustrate the expression of derepressed VSGs and

their localization.

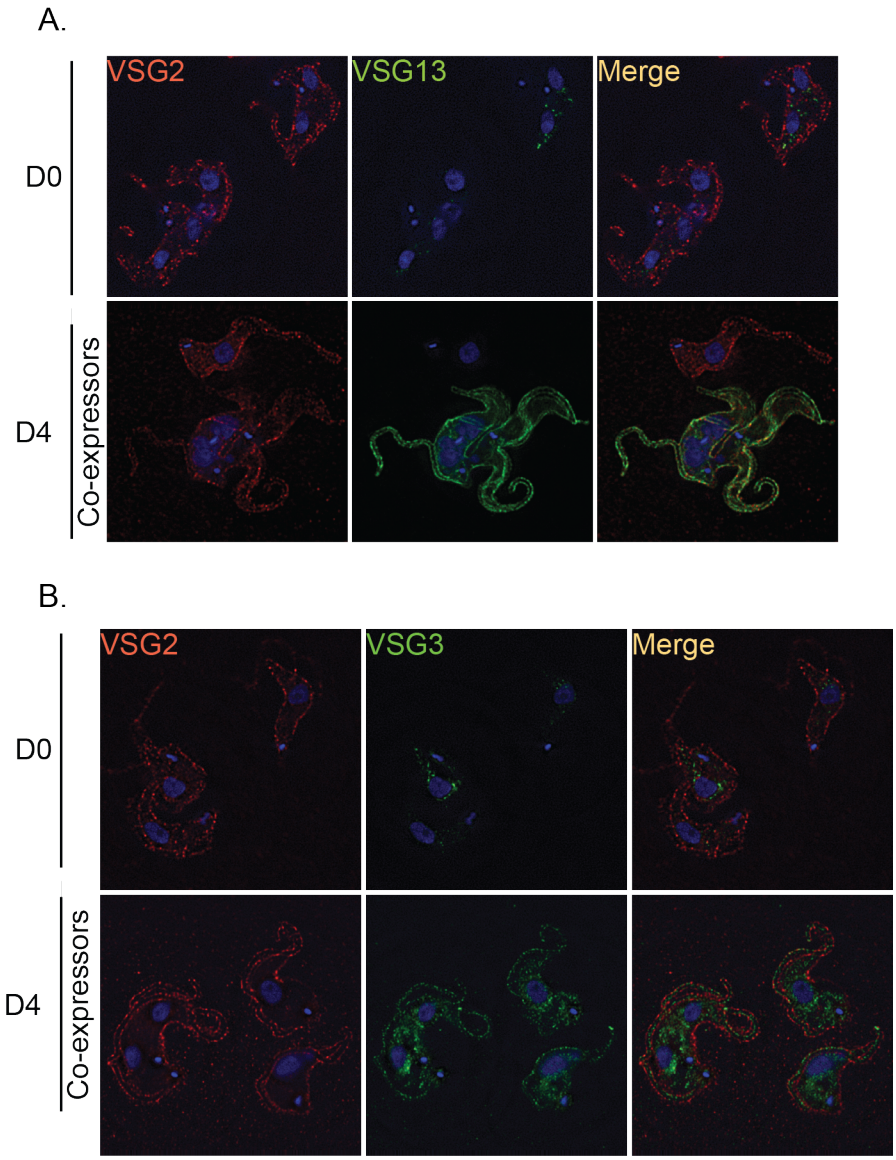

Figure 3-6: Silent VSGs are expressed in TbORC1 depleted cells. (A) The originally active VSG2 is co-expressed with VSG13 upon the depletion of TbORC1. (B) Similarly, the originally active VSG2 is co-expressed with VSG3 upon the depletion of TbORC1 (Note: The original population expresses VSG2 prior to the depletion of TbORC1).

Finally, VSG2 antibody (the active VSG) was so diluted that VSG2 appeared as a punctate stain on the surface of the cells (Figure: 3-6). To rule out the possibility that the starting populations were not VSG2 expressers, the same populations were stained with a

higher concentration of VSG2 antibody and indeed, the starting population were VSG2 expressers (Figure: 3-7).

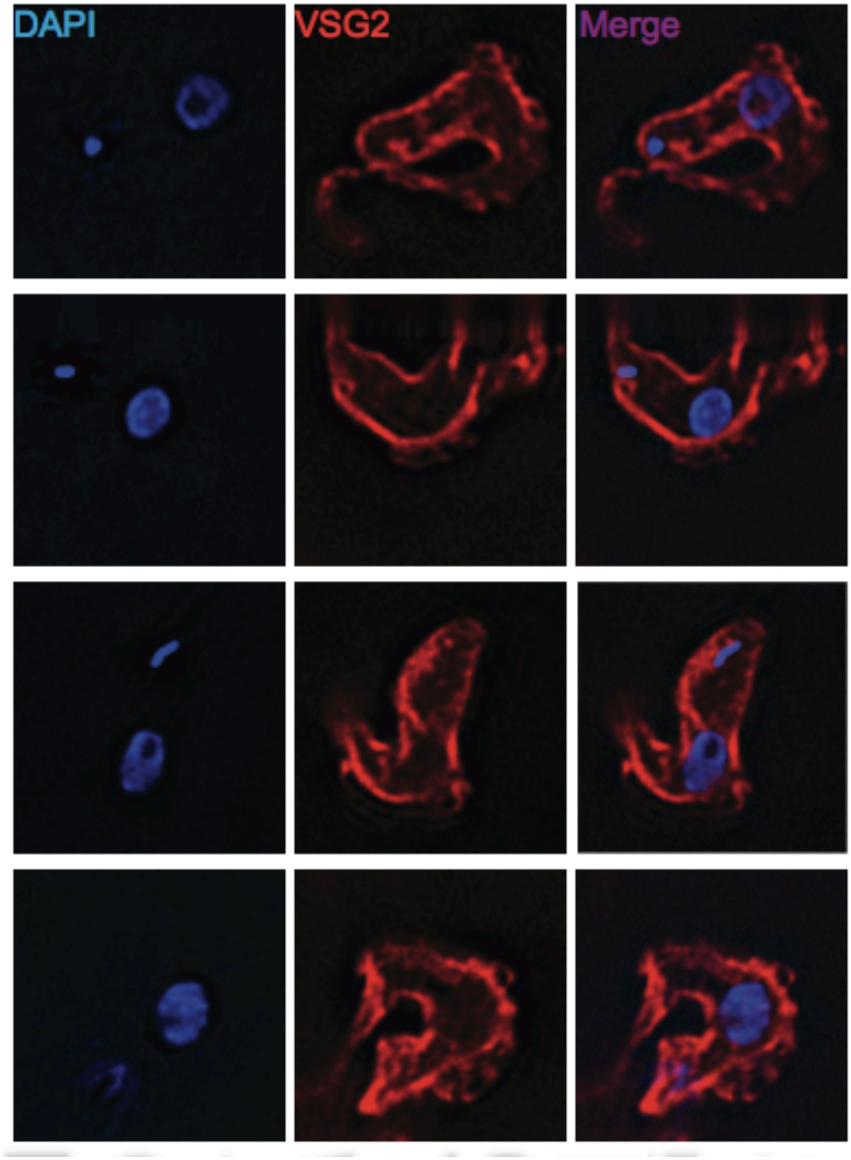

Figure 3-7: TbORC1 cells originally express VSG2. Cells were examined using rabbit antibody against VSG2. DAP1 was used to stain DNA (nucleus and kinetoplast). A stack of images was taken for each cell, but only one image is shown.

TbORC1 associates with telomeres

In mammals, Orc1 interacts with the telomeric protein TRF2 and TERRA, the RNA

transcripts of telomeres (Atanasiu et al. 2006 Tatsumi et al. 2008; Deng et al. 2009). TbORC1 is enriched at subtelomeric loci (Tiengwe et al. 2012a), hinting to the possible involvement of TbORC1 with telomeres; hence we asked whether TbORC1's effect on antigenic variation is due to its association with telomeres. To test this possibility, we performed chromatin IP (ChIP) in both BF cells expressing F2H-TbORC1 (Fig. 3-8, a & b) and in PF cells expressing TbORC1-PTP (Fig. 3-8, c & d). The PTP tag contains two protein A and one protein C peptide separated by a TEV cleavage site (Schimanski et al. 2005). TbORC1 proteins were immunoprecipitated using anti-HA antibodies (F2H-TbORC1) or IgG coupled sepharose beads (TbORC1-PTP). Precipitated DNA was analyzed by slot blot followed by hybridization with a telomeric probe and quantified as a percent of the input.

We found that telomere DNA was significantly enriched in precipitated fractions in both BF (Figure: 3-8 a, b) and PF cells (Figure: 3-8 c, d). As a negative control, wild-type cells without HA or PTP tag were precipitated with the respective antibodies (HA antibody in BF cells and IgG in PF cells). Negative controls did not precipitate down the telomere DNA, illustrating the specificity of the outcome of our ChIP. Therefore, TbORC1 appears to associate with the telomere DNA. However, TbORC1 association is not as much as TbTRF, when used as a positive control in ChIP. TbTRF appears to bind telomere DNA in a much higher amount (Figure: 3-8 a).

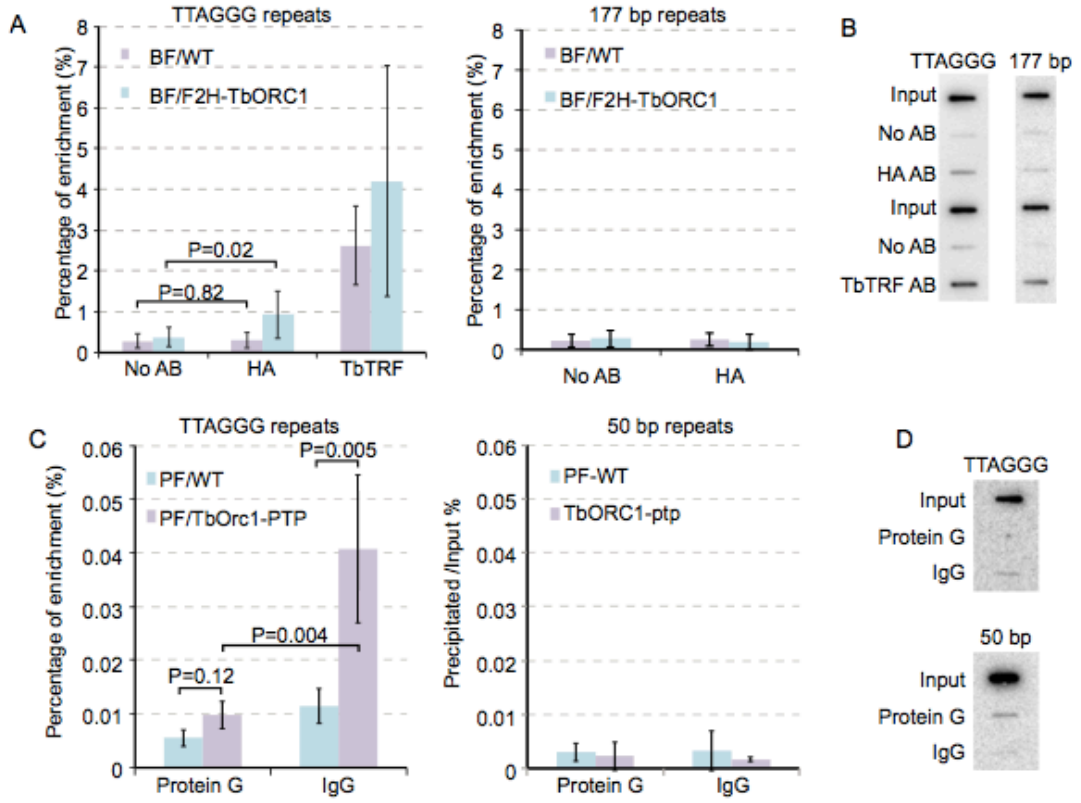

Figure 3-8: TbORC1 associates with telomeres in BF and PF cells. (A) ChIP of TbORC1 in BF cells, TbORC1 was F2H tagged and precipitated with an HA antibody to determine the specificity of the signal, a pull down with the HA antibody in an un-tagged cell line was performed. ChIP of TbTRF was carried as a positive control to telomere binding. Average enrichments were calculated from 15 independent experiments, and standard variations are shown as error bars. P values of unpaired t-tests are shown for indicated pairs of data. (B) Slot blot representation of TbORC1 binding to telomeres in BF cells. (C) ChIP of TbORC1 in PF cells, TbORC1 was PTP tagged and precipitated with IgG beads. To determine the specificity of the signal, a pull down with the IgG coupled beads was done in an un-tagged cell line. Average enrichments were calculated for 4 independent experiments, and standard variations are shown as error bars. (D) Slot blot representation of TbORC1 binding to telomeres in PF cells. Probes used are indicated on top.

TbORC1 associates with telomeres independent of known telomere factors TbTRF and TbRAP1

To study how TbORC1 is recruited to telomeres we investigated whether the association of TbORC1 to telomeres is a result of interaction with TbTRF or TbRAP1.

Yeast-two-hybrid analysis indicated that there was no interaction of TbTRF or TbRAP1 with TbORC1 *in vitro* (Figure: 3-9). In addition, we tested the interaction of TbORC1 with TbRAP1 and TbTRF in TbORC1-PTP tagged cell line, where immunoprecipitation was performed using IgG sepharsoe beads and any immunoprecipitated proteins were eluted after stripping. As indicated in figure: 3-10, when TbORC1 was pulled down, TbRAP1 or TbTRF was not present. However, they were present in the supernatant fraction, the fraction prior to immunoprecipitation, further confirming the lack of interaction *in vivo* between TbORC1 and TbTRF or TbORC1 and TbRAP1. These data are in agreement with our *in vitro* data.

A

LexA BD fusion protein	GAD fusion protein	β-galactosidase activity	
		average	STD
empty	empty	0.2	0.1
TbTRF	TbTRF	67.1	6.1
TbORC1	empty	0.1	0.03
TbORC1	TbTRF	0.1	0.02
empty	TbORC1	0.2	0.1
TbRAP1	TbORC1	0.2	0.1

B

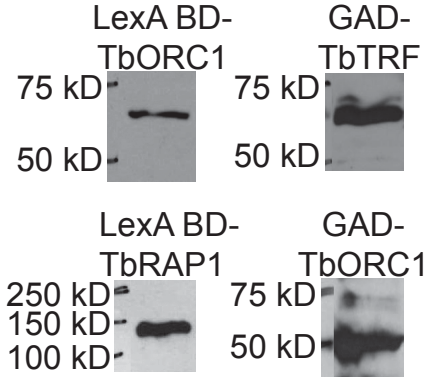

Figure 3-9: Yeast-two-hybrid analysis of the interaction of TbORC1 with TbTRF or TbRAP1. (A) β-galactosidase activity measurement of the *in vitro* interaction between TbORC1 and TbTRF or TbORC1 and TbRAP1. (B) Western analysis to confirm the expression of GAD-TbTRF, LexA-TbRAP1, GAD-TbORC1 and LexA-TbORC1.

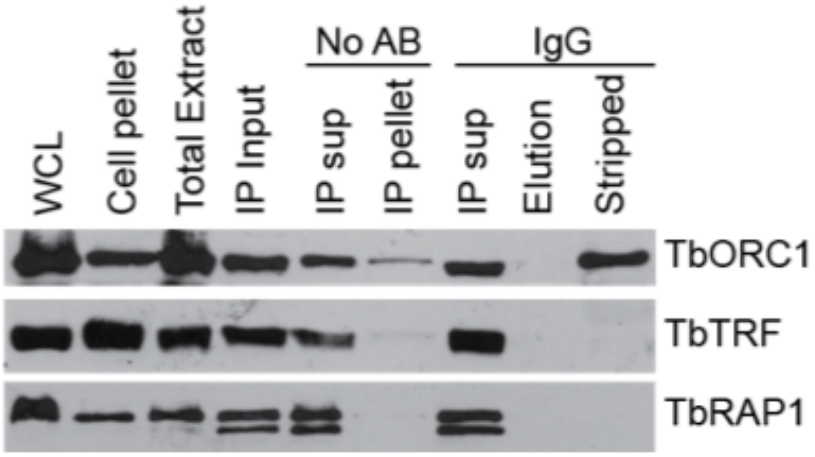

Figure 3-10: TbORC1 does not interact with TbTRF or TbRAP1 *in vivo*. Immuno-precipitation of TbORC1 in TbORC1-PTP expressing PF cells using IgG coupled beads or no antibody (No AB = non-coupled protein G beads). Cell lysate and precipitation products were analyzed by Western using antibodies against protein A, TbTRF or TbRAP1 as marked.

Since the interaction between known telomeric proteins and TbORC1 was negative, we expected that the protein levels of TbTRF or TbRAP1 would not significantly change upon the depletion of TbORC1. In addition, the association of TbTRF and TbRAP1 to telomeres will not be significantly affected upon the depletion of TbORC1. To test the latter, we performed ChIP of TbTRF or TbRAP1 in the presence or absence of TbORC1 and report no significant changes in the association of TbTRF or TbRAP1 to telomeres upon the depletion of TbORC1 (Figure: 3-11). As for the protein levels of TbTRF and TbRAP1, we do not report any significant changes in their protein levels upon depletion of TbORC1 (Figure 3-12).

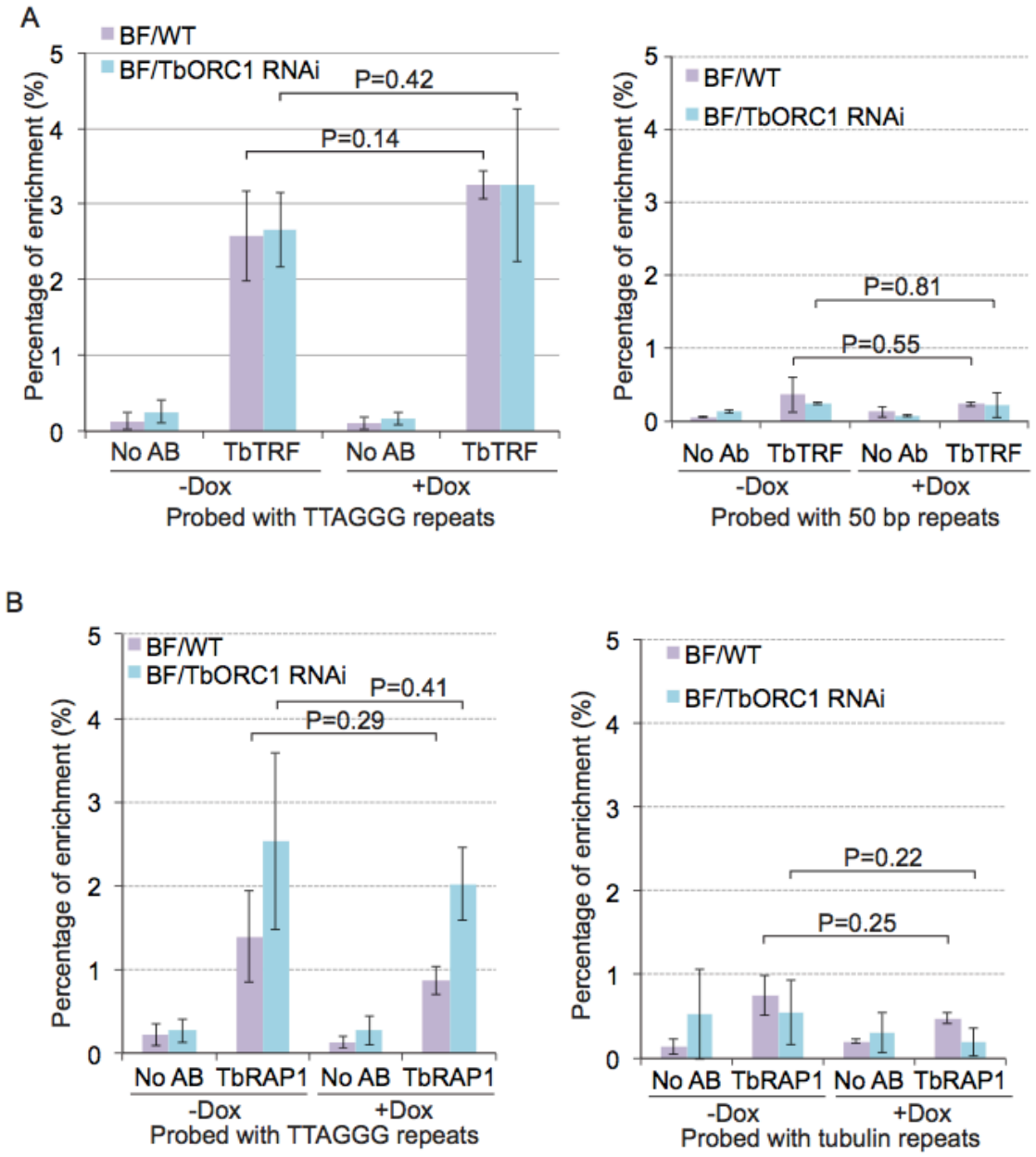

Figure 3-11: Association of TbTRF or TbRAP1 with telomeres in the presence or absence of TbORC1. (A) ChIP of TbTRF in presence or absence of TbORC1, no significant changes in the association of TbTRF with telomeres in the presence or absence of TbORC1. 50 bp repeats was used as binding specificity control, in that TbTRF specifically binds TTAGGG repeats. (B) ChIP of TbRAP1 in presence or absence of TbORC1; there were no significant changes in the association of TbTRF with telomeres in the presence or absence of TbORC1. Tubulin was used as binding specificity control for TbRAP1. In both ChIPs, wild-type cells were tested for the association of TbTRF and TbRAP1 with telomeres and no significant changes were observed with or without dox, validating our observations, that they are TbORC1 specific.

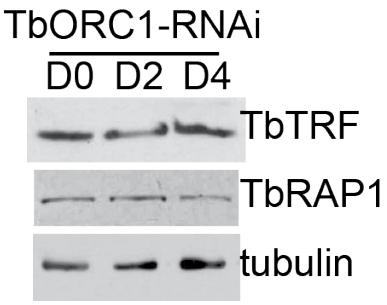

Figure 3-12: Depletion of TbORC1 did not affect TbTRF or TbRAP1 protein levels. Western analysis of TbTRF and TbRAP1 protein levels in the presence of TbORC1 (Day 0) and in the absence of TbORC1 (Days 2, 4). No significant changes in the protein levels were observed.

DISSCUSSION

TbORC1 and cell cycle progression

Our data collectively demonstrated that TbORC1 is critical for normal cell cycle progression. Upon the depletion of TbORC1, we observed a significant decrease in population in G1 phase, significant increase in the population in S phase and G2/M phase. To further understand these observations, we labeled bulk DNA in BF cells with BrdU for the last 24 h of total TbORC1 RNAi induction time. During this labeling period, we expected that replicating cells were BrdU-positive while cells that had arrested before the labeling period would remain BrdU-negative. Without TbORC1 depletion, 90% of cells incorporated BrdU. Upon TbORC1 depletion for 3 days, 73% of cells did not incorporate BrdU, indicating impaired DNA replication. In addition, there was an increase in cells with aberrant DNA content, such as cells with multiple nuclei (BrdU experiments were performed and analyzed by Concepción-Acevedo, J). Collectively, this indicates that TbORC1 plays an important role in DNA replication.

Prior to our cell-cycle studies, we expected that the depletion of TbORC1 would arrest cells in S-phase, and hence we would observe a dramatic increase of cells in the S-

phase. However, this was not the case in our cell cycle analysis. There are two possible explanations for these observations. First, although TbORC1 was the first DNA replication homolog identified in *T. brucei,* there are additional factors that have been identified, Orc1-like Orc4, and Orc1b (Dang and Li 2011; Tiengwe et al. 2012b), and these factors can proceed with DNA replication in the absence of TbORC1 –although not efficiently. The second explanation, which is more likely, is that TbORC1 depletion is not equivalent in all the cells in an unsynchronized population, where cells with greater depletion of TbORC1 arrested at S-phase and the cells with moderate depletion of TbORC1 was able to escape an S-phase arrest.

Replication is regulated in budding yeast by the regulation of CDC6, where the CDC6 is phosphorylated and targeted for degradation preventing re-replication (Elsasser et al. 1999; Drury et al. 2000). Also, replication is regulated in mammals as described earlier (Mendez et al. 2002). However, little is known about the regulation of replication in *T. brucei*. TbORC1 was able to complement the temperature sensitive phenotype of a budding yeast *cdc6* mutant (Goody et al. 2009) and therefore may function as a CDC6 as well. This could explain why cells with aberrant DNA content arise upon the depletion of TbORC1 in BF cells. It is possible that TbORC1 is not only required for replication, but also to regulate replication, and although other DNA replication factors are present (Orc4 and Orc1b), the absence of regulating the entry to S-phase creates cells with aberrant DNA content. Cells with aberrant DNA content cannot divide and hence a dramatic G2/M arrest was observed. We observed cells with multiple nuclei in BF cells upon the depletion of TbORC1, consistent with the lack of the regulation of DNA replication. Studies have just begun to understand nuclear DNA replication in *T. brucei* and further

studies are required to address the possibilities presented. For instance, is the function of TbORC1 in nuclear DNA replication affected if Orc4 and Orc1b genes were deleted? What happens to replication if Orc4 was depleted or Orc1b? Is this phenotype stronger upon the depletion of TbORC1? These studies are necessary to explain the phenotypes observed in this study. Future experiments should address these questions.

TbORC1 and antigenic variation

The ORC complex is known to play important roles not only in DNA replication but other cellular processes including heterochromatin organization, mitotic checkpoint assembly and cell-cycle progression (Sasaki and Gilbert 2007; Chakraborty et al. 2011). The association of ORC subunits with HP1 in *Drosophila* and *Xenopus* (Pak et al. 1997; Huang et al. 1998), recruitment of Sir1 in budding yeast to establish heterochromatin in mating type silencing (Triolo and Sternglanz 1996), the binding of Orc1 to HM silencer and the cooperation of Orc1 with Sir2 and Sir4 in *Kluyvereromyces lactis* for the formation of heterochromatin structure at telomeres (Hickman and Rusche 2010) illustrates the importance of the role of the ORC complex and subunits in heterochromatin organization.

Trypanosoma brucei regulates *VSG* expression through mono-allelic expression of *VSG*. The regulation involves multiple pathways and multiple proteins, including heterochromatin organization (Hughes et al. 2007; Figueiredo and Cross 2010; Stanne and Rudenko 2010; Wang et al. 2010; Denninger et al. 2010). In this study we show that depletion of TbORC1 resulted in a significant increase in silent B-ES linked *VSGs* in both insect stage form and bloodstream form stage. Nevertheless, how TbORC1 influences

VSG silencing is not known. It is possible that the role of ORC in heterochromatin organization is conserved from protozoans to mammals. We did test the possibility that the depletion of TbORC1 results in the opening of heterochromatin through FAIRE analysis (data not shown); however, our data did not illustrate such a phenotype. The FAIRE assay, however, is probably not sensitive enough to detect subtle changes in chromatin structure in TbORC1-defective cells.

In addition, it is tempting to speculate that TbSir2rp1 may play a role in establishing the heterochromatin, once its recruitment is initiated via TbORC1 (such as the case in *K. lactis*), but two forces oppose this idea. First, the depletion of TbSir2rp1 in *T. brucei* did not result in an increase in B-ES linked *VSG* transcripts (Alsford et al. 2007). Second, there is a lack of a necessary bromo-adjacent homology domain (BAH) in TbORC1 (Tiengwe et al. 2012b). This domain is necessary for binding to nucleosomes, such as the case in budding yeast (Triolo and Sternglanz 1996). It is also possible that TbORC1 interacts with a yet un-identified factor that harbors a heterochromatin remodeling activity such as methyltransferase, where the recruitment of TbORC1 to replication origins and its interaction with this unknown protein modifies the histones on chromatin for silencing as its been shown in yeast (Krogan et al. 2002). Many possibilities remain to be tested in order to unwind the molecular mechanism by which TbORC1 affects *VSG* silencing. We only showed that TbORC1 associates with telomeres and it remains possible that this recruitment is facilitated by a role of TbORC1 in heterochromatin organization at telomeres that is yet not studied. Nevertheless, TbORC1's conserved function in DNA replication, its effect on *VSG* silencing, and its divergence from mammalian ORC1 (Godoy et al. 2009) makes the targeting of pre-

replication machinery in trypanosomes a future therapeutic intervention (Calderano et al. 2011).

TbORC1 at telomeres

ORC interacts with mammalian TRF2 (Atanasiu et al. 2006; Deng et al. 2009) and maintains heterochromatin structure at telomeres (Hickman and Rusche 2010). Since *VSG* genes are located at sub-telomeres (De Lange and Borst 1982), we postulated that TbORC1's role in antigenic variation could be due to its association with telomeres. Indeed, we show that TbORC1 associates with telomeres in both life stages, but not as strongly as TbTRF, the telomere binding protein. Recently it was shown that TbORC1 appears to associate with subtelomeric regions containing *VSG* expression sites at a subset of *T. brucei* megabase chromosomes (Tiengwe et al. 2012a). The association of TbORC1 with *VSG* expression sites and telomeres may be important for TbORC1's function in *T. brucei* antigenic variation.

We also investigated whether this recruitment is dependent on one of the only two known telomere factors in *T. brucei* TbRAP1 (Yang et al. 2009), or TbTRF (Li et al. 2005) or both. Since the role of TbRAP1 in the regulation of antigenic variation is well documented (Yang et al. 2009), we hypothesized that TbORC1's role in antigenic variation may be due to its direct interaction with TbRAP1, consequently, its deletion affected either the protein levels of TbRAP1 or TbRAP1's recruitment to telomeres. However, we did not observe any significant changes in TbRAP1 protein levels or its recruitment to telomeres upon the depletion of TbORC1. This illustrates that the role of TbORC1 in antigenic variation is probably independent of TbRAP1 pathway.

Another telomere protein that may facilitate the recruitment of TbORC1 to telomeres is TbTRF. In addition, TbTRF is important for the regulation of *VSG* switching (chapter IV). Since hORC1 was shown to directly interact with hTRF2 but not hTRF1 or hRAP1 (Atanasiu et al. 2006), and TbTRF and hTRF2 have a similarity in function (Li et al. 2005), we hypothesized that TbORC1 is recruited to telomeres through the interaction with TbTRF. We tested the interaction between TbTRF and TbORC1 using *in vivo* and *in vitro* approaches, and we did not detect any interaction. We also tested the possibility that the depletion of TbORC1 may affect TbTRF association at telomeres or TbTRF's protein levels, and since the protein interaction data provided no support for such a possibility, it was not surprising that we did not report any changes in TbTRF protein levels or recruitment to telomeres upon the depletion of TbORC1. This is also not surprising, since hORC1 interacts with the N-terminus of hTRF2 (Atanasiu et al. 2006; Deng et al. 2009), and TbTRF lacks this domain. How TbORC1 goes to the telomeres is a question for active investigation. Future experiments should provide answers to these questions.

CHAPTER IV

CHARACTERIZE THE FUNCTIONS OF TTAGGG REPEAT BINDING FACTOR IN TRYPANOSOMA BRUCEI

Imaan Benmerzouga et al.

ABSTRACT

Trypanosoma brucei is a protozoan parasite that causes sleeping sickness in humans and nagana in cattle. When inside the mammalian host, *T. brucei* cells stay in extracellular spaces and regularly switch their surface antigen, Variant Surface Glycoprotein (*VSG*), to escape the host's immune responses. *T. brucei* expresses a single type of *VSG* at any time exclusively from one of nearly 20 identical *VSG* expression sites located next to the telomere. Monoallelic expression of *VSG* ensures that *VSG* switching is effective. We have recently found that RAP1, an intrinsic component of the *T. brucei* telomere complex, is essential for silencing subtelomeric *VSG* genes, indicating that the telomere structure is important for antigenic variation in *T. brucei*.

Telomeres are nucleoprotein complexes located at the ends of linear chromosomes. Telomeres are essential for maintaining genomic integrity. We have identified *T. brucei* TRF as a duplex telomere DNA binding factor. However, its function in antigenic variation has not been elucidated. We successfully established *T. brucei's*

strains with transient depletion of TbTRF. These cells will be used for further studies. Also, we solved the NMR structure of TbTRF DNA binding domain (MYB). We identified point mutations that weaken the DNA binding activity *in vitro*. These point mutations were successfully targeted *in vivo* in two independent *T. brucei* strains. Finally, we studied the DNA binding activity of TbTRF in the presence or absence of base J, the modified thymidine (beta-D-glucosyl-hydroxymethyluracil) found in Kinetoplastids, *in vitro* and we report no difference.

INTRODUCTION

Telomeres are specialized nucleoprotein complexes that protect the termini of chromosomes (Blackburn 1991). Mammalian telomeres are bound by TRF1 and TRF2 (Zhong et al. 1992; Broccoli et al. 1997; Bilaud et al. 1997), both of which recognize the same sequence TAGGGTT (Court et al. 2005) and are essential for the integrity and function of telomeres (van Steensel and de Lange 1997; van Steensel et al. 1998; Karlseder et al. 1999; Smogorzewska et al. 2000; Sfeir et al. 2009). *Trypanosoma brucei* TRF binds telomeres and is important for end protection (Li et al. 2005).

Both hTRF1 and hTRF2 were identified through the ability of each protein to bind telomere DNA through a distinct MYB DNA binding motif (Zhong et al. 1992; Broccoli et al. 1997; Bilaud et al. 1997). The hTRF1 binds telomere DNA through a single MYB domain composed of 62 amino acids at its C-terminus (Broccoli et al. 1997). The MYB domain in hTRF1 is homologous to the c-Myb DNA binding domain (Klempnauer and Sippel 1987). The c-Myb protein belongs to the family of myb protein, is constituted of 3 repeats R1-R3, where only R2 and R3 are required for DNA binding

(Bianchi et al. 1999). The c-Myb transcription factor is a sequence specific DNA binding protein that binds to TTACNG (Biedenkapp et al. 1988).

The solution structure of hTRF2 and hTRF1 with telomere DNA showed similar results with a minor significant difference in that hTRF1 binds to telomere DNA more strongly than hTRF2 (Hanaoka et al. 2005). The hTRF1 and hTRF2 proteins have critical functions in telomere length regulation (Smogorzewska et al. 2000). In addition, mammalian TRF1 is important for telomere replication (Sfeir et al. 2009). In murine embryonic stem cells (mESs), TRF1 is critical for telomere integrity and chromosomal stability (Iwano et al. 2004). However, hTRF2 is most crucial for end-protection (van Steensel et al. 1998; Karlseder et al. 1999;), a role that has been well conserved even in ancient protozoa (Li et al. 2005). Particularly, both the dimerization domain and the hinge domain are critical for the role of hTRF2 in end-protection (Okamoto et al. 2013). In addition to end protection, hTRF2 promotes heterochromatin formation through TERRA and ORC recruitment at telomeres, particularly through its N-terminal domain where it is required for ORC1 interaction (Deng et al. 2009). The TRF2 homodimerization domain, in addition to the MYB domain, enhances strand invasion that may aid in T-loop formation (Amiard et al. 2007).

Telomeres have long been proposed to regulate the expression of *VSGs* (Barry et al. 2003; Lira et al. 2007; Dreesen et al. 2007). Evidently, recent breakthrough findings showed an essential role for *T. brucei* telomeric protein RAP1 in silencing all silent ES-linked *VSGs* (Yang et al. 2009). The structure of telomeres and the location of virulent genes adjacent to telomeres are means developed by parasites for survival (Li 2010).

Putative TTAGGG Repeat Binding Factor (TRF) was identified in *T. brucei* (Li et al 2005). TbTRF has significant sequence similarity to hTRF1 and hTRF2 at its C-terminus, but low sequence similarity at its N-terminus (Li et al. 2005). In addition, TbTRF lacks the acidic or basic domain present in hTRF1 and hTRF2 respectively (Figure: 4-1).

Figure 4-1: TbTRF domains. Schematic representation of the two domains in TbTRF: TRFH and MYB. TRFH domain is less conserved among other TRFs, but the MYB domain is quite conserved. For sequence identity similarity see (Li et al. 2005).

Early characterization of TbTRF documented the significant role of TbTRF in telomere end protection, where depletion of TbTRF resulted in a dramatic loss of G-overhang signal (Li et al. 2005). However, a role for TbTRF in antigenic variation was not reported.

In this chapter, I present the successful transient depletion of TbTRF in four independent clones generated by the author, the TbTRF NMR structure generated by our collaborator, the identification of specific point mutations that affected the DNA binding activity of TbTRF *in vitro* generated by our collaborator, the targeting of these particular point mutations in the MYB domain of TbTRF in two different strains generated by the author, the role of TbTRF in *VSG* silencing generated by the author, the binding of TbTRF to base J *in vitro* generated by our collaborator and finally, the successful depletion of base J *in vivo* generated by the author.

MATERIALS AND METHODS

Plasmids generated for these studies and *T. brucei* strains generated for these studies can be found in the corresponding sections in chapter II. ITC analysis, ChIP analysis, Southern blot analysis, genomic DNA isolation and Western analysis detailed methods may be found in their corresponding sections in material and methods in chapter II.

RESULTS

The successful transient depletion of TbTRF in four independent clones in HSTB261 strain

TbTRF-RNAi cells were established in the HSTB261 reporter strain (refer to chapter II) by introducing an inducible RNAi expression vector PZJMβ-TbTRF (Li et al. 2005). HSTB261-TbTRF-RNAi clones were screened for doxycycline sensitivity at 200 ng/ml. Clones that showed a reproducible arrest at 24 hours were further utilized and carefully monitored for growth by generating a growth curve (Figure 4-2).

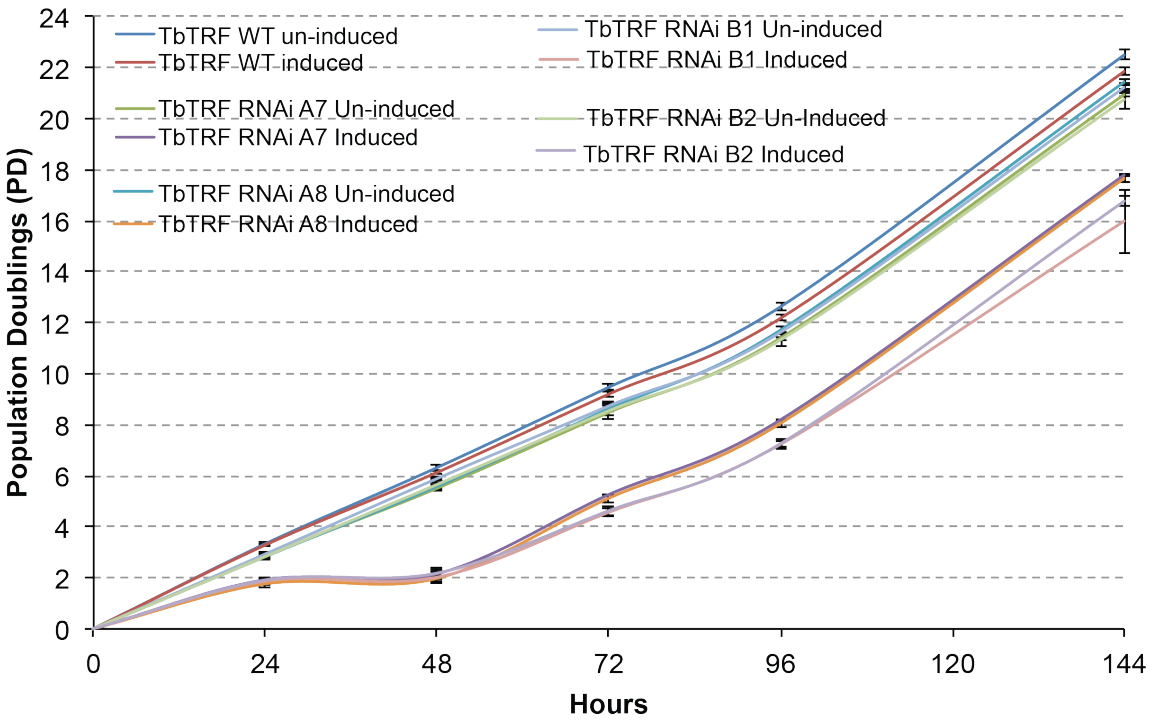

Figure 4-2: Growth curve analysis for all TbTRF-RNAi clones. Four independent clones were established for TbTRF-RNAi studies: A7, A8, B1 and B2. For each clone, cells were induced with 200 ng/ml of doxycycline for 24 hours. Cells were then recovered by washing away doxycycline. As a control, wild-type cells were treated with doxycycline and washed following the same conditions as TbTRF-RNAi cells. Only cells with TbTRF-RNAi showed a growth arrest at 24 hours and not wild-type cells.

TbTRF protein levels were examined upon the induction and recovery of TbTRF-RNAi. As expected, TbTRF protein levels decrease at 24 hours, and upon the removal of doxycycline, cells recover and protein levels return to wild-type levels at 72 hours. Histone 3 (H3) or Elongation Factor-2 (EF-2) was used as a loading control (Figure: 4-3).

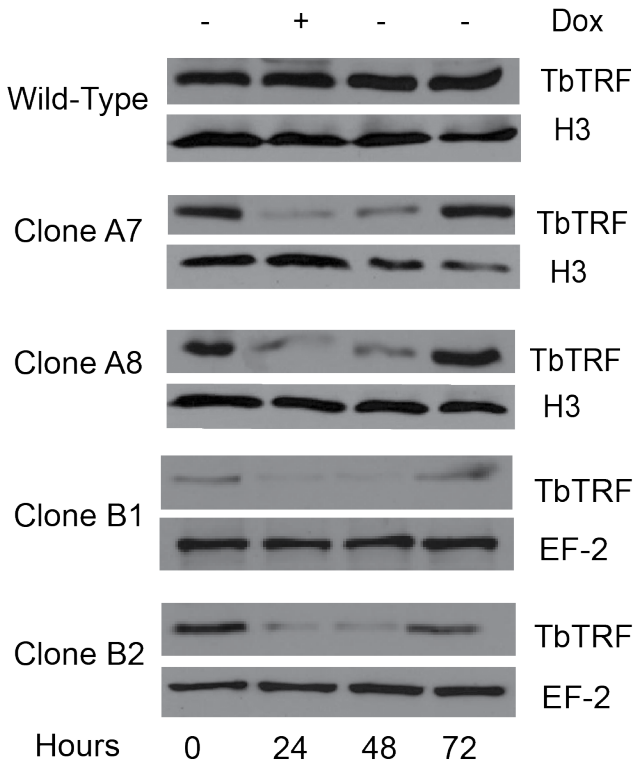

Figure 4-3: Western analysis for TbTRF in all TbTRF-RNAi clones to confirm the transient depletion of TbTRF. Cells were induced for 24 hours and doxycycline was washed away at 24 hours. Protein samples were collected for 24, 48 and 72 hours. TbTRF protein levels decrease at 24 hours and slowly increase to wild-type levels. At 72 hours, TbTRF protein levels return to wild-type levels (in agreement with the growth curve analysis).

NMR structure of TbTRF MYB domain

TbTRF has two domains that are essential for its DNA binding activity, the homodimerization domain TRFH and the MYB domain. In order for TRF to bind to DNA, two MYB domains must recognize the (TTAGGG)n sequence at telomeres in each strand of the DNA and homodimerization must occur between the two subunits that are already bound to DNA. As the MYB domain is the smaller domain (~ 100 bp), we utilized it and solved its NMR structure in collaboration with Dr. Zhao from Hong Kong Polytechnic University in China. The TbTRF MYB domain structure was compared with

its homologs (human and yeast species). The amino acid sequence of the TbTRF MYB domain is significantly different from that of other MYB domains. Nevertheless, the tertiary structure of the DNA binding domain of TbTRF consists of three helices. Helix 1 is composed of 13 amino acid residues (S304-F316), helix 2 is composed of 9 amino acid residues (F323-R331) and helix 3 is composed of 11 residues (V339-G349) (Figure 4-4).

These helices are organized in the Helix-Turn-Helix (HTH) motif commonly seen in DNA-binding proteins (Figure 4-5a). To determine point mutations that would affect TbTRF's DNA binding activity, the solved 3-D structure of the TbTRF MYB domain was compared with its homologs (human and yeast species) with respect to DNA interaction points. The following residues were found to be possibly critical for TbTRF's DNA binding activity: R298, Q320, Q321, H346, R348 and R352 (Figure 4-4). The R298 residue is critical for TbTRF's DNA binding function because it implies the N-terminal loop of the HTH motif. The R348 residue specifically recognizes the G base in the major groove of DNA. Residues Q320, Q321 and R352 are critical for sugar-phosphate backbone recognition, while H346 forms salt bridges with the NT of TbTRF (Figure 4-5b).

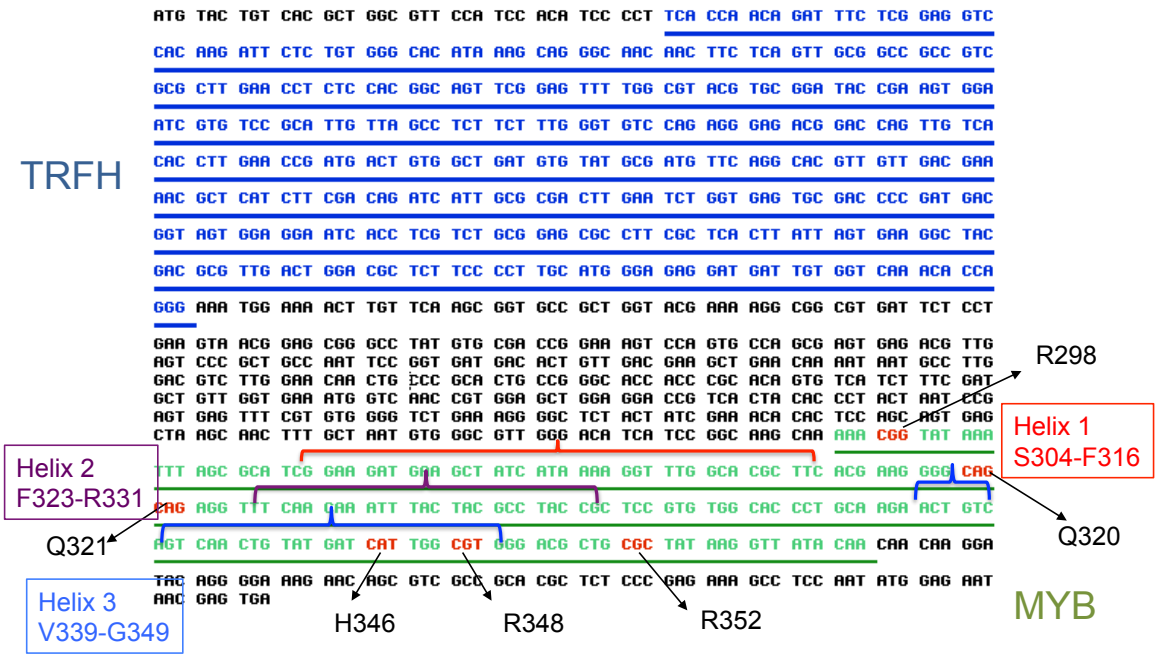

Figure 4-4: TbTRF amino acid sequence. The three helices are indicated in brackets with helix 1 in red, helix 2 in purple and helix 3 in blue. The entire MYB domain is in green. The residues selected for mutational studies are indicated in red. Note that R298, Q320, Q321 and R352 are outside of any helix. Only H346 and R348 are located in helix 3. The location of each residue with respect to TbTRF's MYB domain HTH motif is indicated in figure (4-7b).

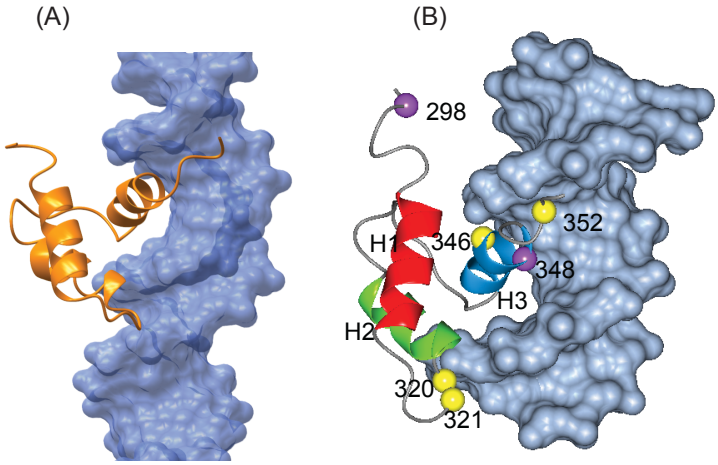

Figure 4-5: NMR structure of TbTRF MYB domain. (Experiments and analysis were performed by Li, X). (A) TbTRF MYB domain NMR structure in orange; simulation of MYB domain (orange) binding to DNA (blue). (B) Identification of residues that may affect the DNA binding activity of TbTRF.

Based on the TbTRF MYB domain NMR structure, point mutations were generated with the goal of finding mutations that either weaken or abolish TbTRF's DNA binding function *in vitro*. The ultimate goal of these mutational studies was to successfully obtain viable *T. brucei* cells with these point mutations when they were targeted *in vivo*. The mutational studies had two directions: one was to change the original amino acid to an amino acid that had a side chain with an opposite charge, for instance, mutating arginine (R) to glutamic acid (E). The second direction of the mutational studies was to change the original amino acid to an amino acid that had a side chain with a similar charge, for instance: R to lysine (K). In the cases where changing the original amino acid to an amino acid holding an opposite charge, and the functional analysis did not exhibit dramatic changes in TbTRF's DNA binding activity, no further mutations were carried out for that particular residue, for instance glutamine (Q) to serine (S) point mutation. In addition, if the *in vitro* expression of the MYB domain mutation was not successful (the protein was insoluble in *E. coli*), no further experiments could be carried out for that particular residue (ex. H346E). The following point mutations were generated and tested for the DNA binding activity *in vitro* R298E, R298K, Q320S, Q321S, H346R, R348E, R348K, R352E and finally R352K.

DNA binding activity of TbTRF MYB domain mutants in vitro

The following isothermal titration calorimetry (ITC) experiments and analysis were performed by Li, X. To analyze the DNA binding activity of the MYB domain mutations, ITC was used to measure the extent of binding by each presented mutation. Approximately 200 μM of protein (MYB wild-type or with a point mutation) was titrated

onto 10 μM of sequence of TTAGGG (double stranded DNA) or negative DNA (5' GAA TCT GGT GAG AGC GAC CCC GAT GAC GG 3'). Binding was measured as the heat interaction generated from the titration of protein onto telomeric DNA. Both wild-type and negative controls were carried out prior to testing the point mutations (Figure 4-6). These experiments concluded that the conditions used were optimal to measure the interaction of MYB with telomere DNA.

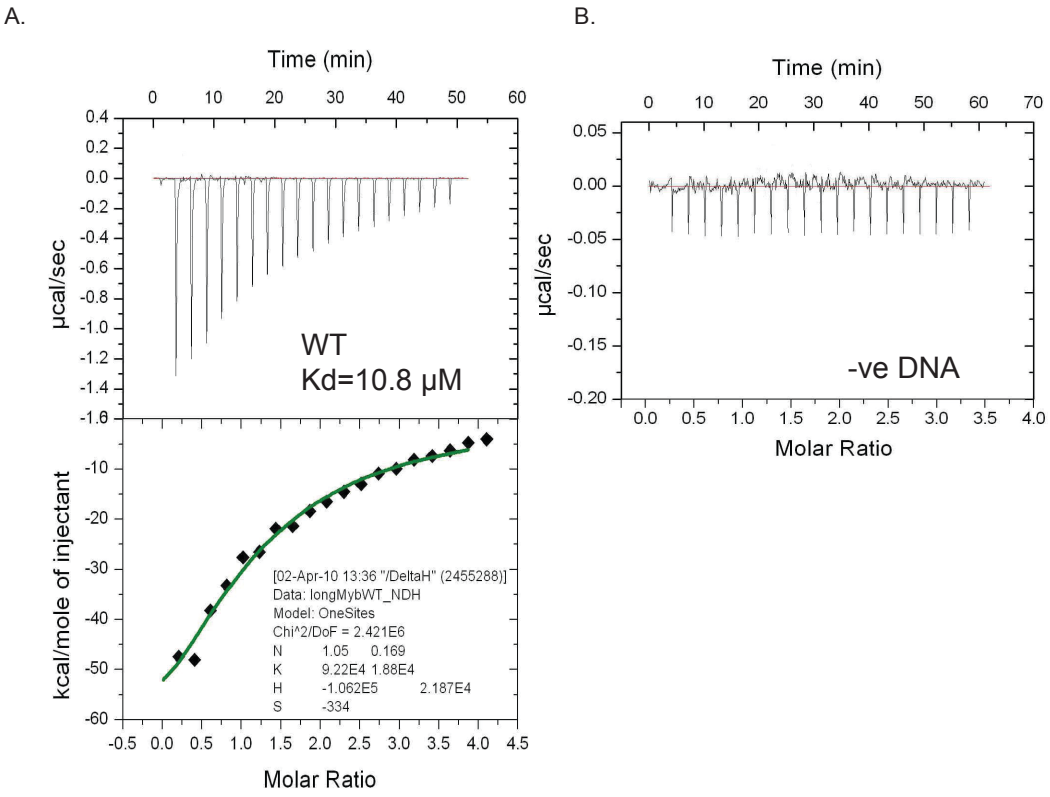

Figure 4-6: *In vitro* DNA binding activity of TbTRF mutants using Isothermal Titration Calorimetry (ITC). (Experiments and analysis were performed by Li, X). (A) Interaction of wild-type MYB with telomeric DNA. The well- shaped curve indicates progressive heat transfer as shown in wild-type telomeric DNA. In addition the Kd was calculated from the heat curve using Origin 7.0. Tight interaction is translated by a low Kd value. (B) Lack of interaction of wild-type MYB with non-telomeric DNA (negative control). The Kd value could not be determined because there was no curve generated due to the lack of interaction.

The dissociation constant (Kd) was extrapolated from the generated heat curves using the software origin 7.0, as long as the heat curve could fit to some mode. The dissociation constant indicated the extent of binding, where a stronger interaction had a lower Kd value (Kd = (A) (B)/ (AB), where AB is complex formation). Due to the lack of interaction in some of the TbTRF MYB domain mutants with telomeric DNA, the Kd could not be determined. These mutations were classified as point mutations that abolished the DNA binding activity *in vitro*. These point mutations were R298E, R298K, R348E and R348K (Figure: 4-7).

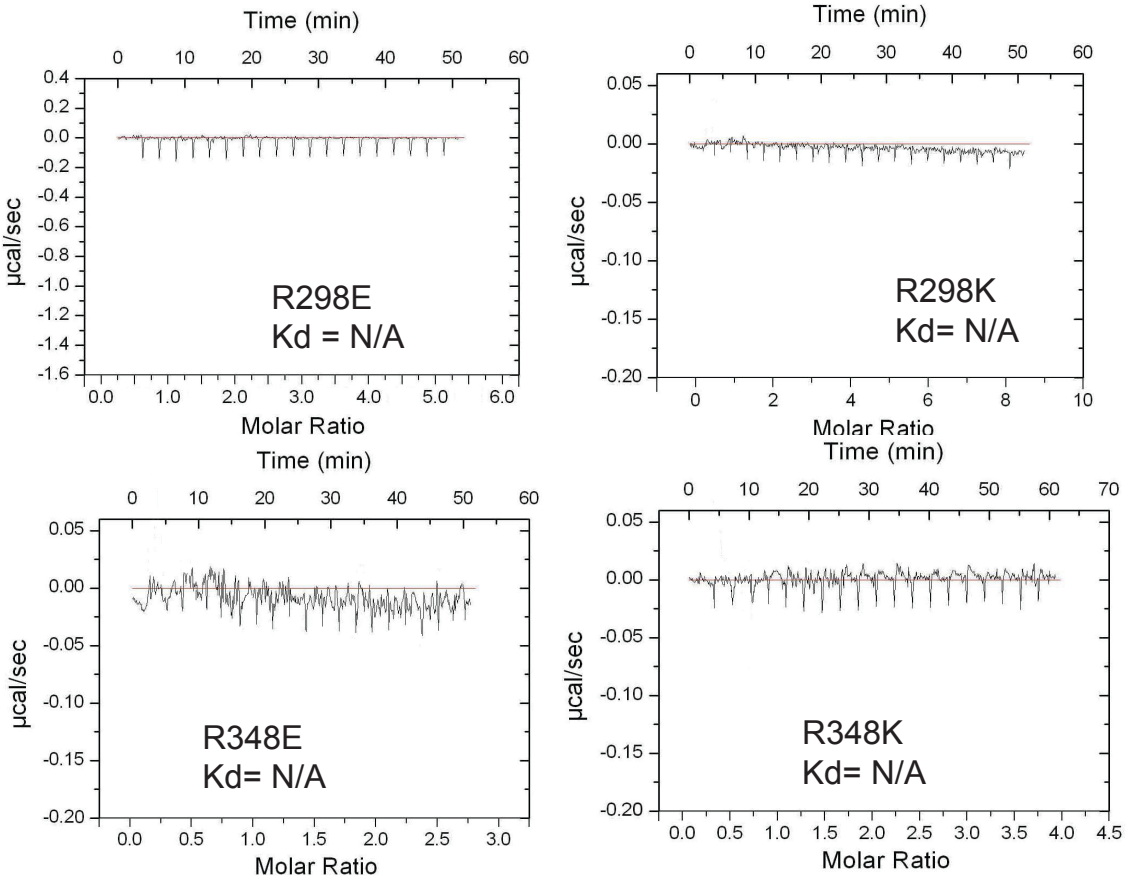

Figure 4-7: TbTRF MYB domain mutants with abolished DNA binding activity *in vitro*. (Experiments and analysis were performed by Li, X). Measurement of the interaction between TbTRF MYB domain mutants and telomeric DNA. Due to the lack of interaction, no heat curve was generated and hence Kd could not be determined. R298 and R348 residues are critical for telomere DNA interaction *in vitro*.

The Kd was calculated for the remaining point mutations, because there was some interaction and a heat curve was generated. These mutations were classified as point mutations that weaken the DNA binding activity of TbTRF *in vitro*. The point mutations were: Q320S, Q321S, H346R and R352K (Figure 4-8).

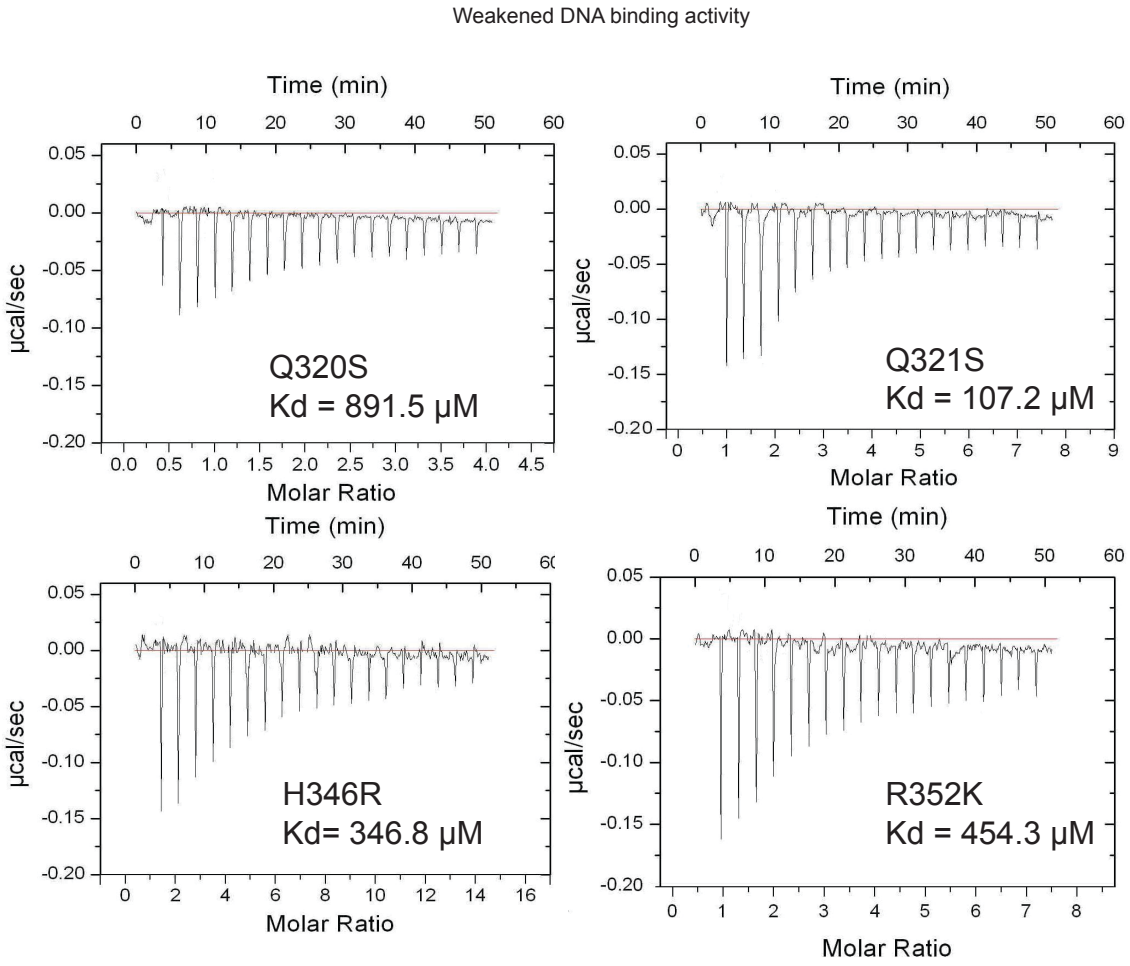

Figure 4-8: TbTRF MYB domain mutants with weakened DNA binding activity *in vitro*. (Experiments and analysis were performed by Li, X). The progressive heat curve indicates interaction between TbTRF MYB domain mutants and telomeric DNA. The Kd was calculated from the heat curve using Origin 7.0. The Kd values were compared to the WT Kd value and these mutants were classified as mutations with weakened DNA binding activity *in vitro*. Note the high Kd value compared to WT.

Generation of TbTRF DNA binding mutants in vivo

To generate TbTRF point mutations *in vivo*, we constructed targeting constructs that harbour the point mutations via two-step PCR as described in materials and methods (chapter II). The targeting constructs were introduced in a TbTRF -/+ strain, so that the only allele present for TbTRF would be the TbTRF allele harbouring the particular point mutation (Figure: 4-9).

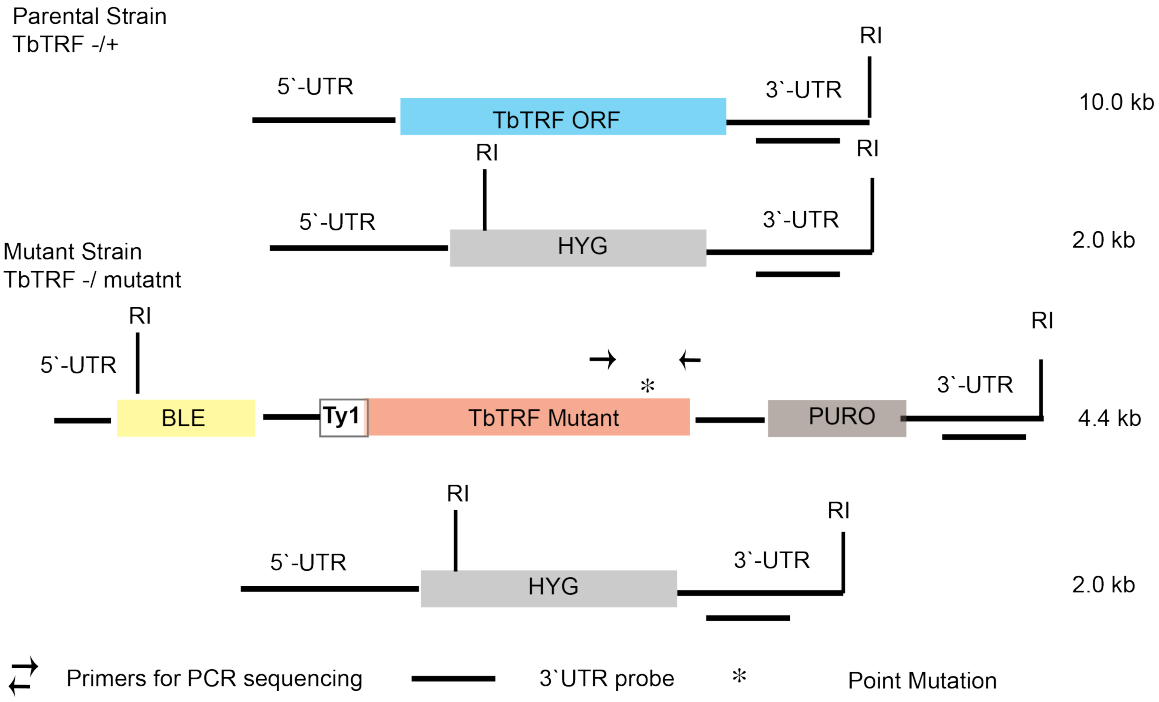

Figure 4-9: Generation of TbTRF MYB domain mutants *in vivo*. First a parental strain was generated where a single allele of TbTRF was replaced with the *HYG* gene. Amplification of the mutants is described in chapter II (material and methods; plasmids section). The constructs harbouring the specified point mutations were targeted into the parental cells (TbTRF -/+). Because the mutant allele was doubly marked with *BLE* and *PUR*, drug selection was utilized to obtain correctly incorporated mutants. Only cells that survived in a medium containing hygromycin, puromycin and phelomycin were collected. In addition, a quick PCR analysis was used to validate the incorporation of the point mutation prior to further validations. The following mutants were viable: R298K, Q320S, Q321S, H346R, R348K, R352K. However R298E, R348E and R352E cells were not viable, although we tried the targeting multiple times. TbTRF is an essential gene and we expected that cells would not be viable, if the point mutation was of great severity to TbTRF's DNA binding activity *in vivo*.

All viable cells harboring specific point mutations were confirmed via Southern using the *EcoRI* enzyme for digestion and a 3'-UTR probe to differentiate between the WT allele and the mutant allele (Figure 4-9). Only two independent clones per mutation were sequenced. To sequence *T. brucei's* clones, genomic DNA was isolated from each clone and the TbTRF MYB domain was amplified using primers 15 and 13 (Figure 4-10 and appendix B). The samples were purified and sent to *Genwiz* for sequencing. The sequencing data were aligned with the wild-type MYB domain of TbTRF. Each mutation was incorporated at the expected position and no other mutations were present. Sample sequencing data is presented in (Figure 4-10).

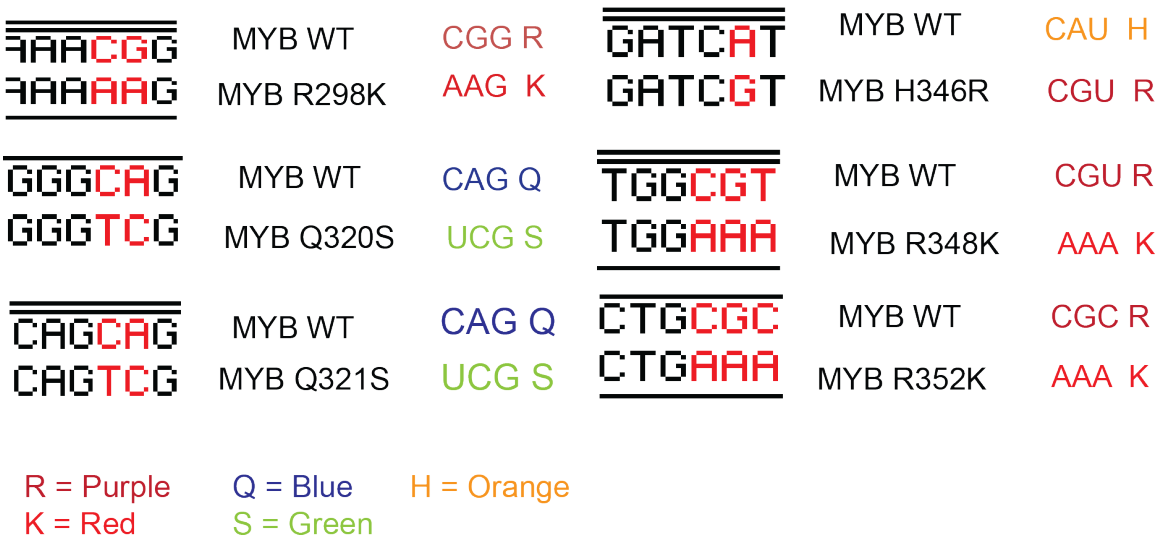

Figure 4-10: Representative sequencing data of TbTRF MYB domain mutations in *T. brucei* cells. Sequencing data of TbTRF MYB domain mutants were aligned with the wild-type MYB domain. Base pairs in red indicate the 3 or 2 or 1 base changes of the particular point mutation. Different amino acids are indicated in different colors.

Finally, Western analysis was performed for one clone per mutation. Cells were tested for the presence of the mutant allele, which is Ty1-tagged, where the parental cells (TbTRF -/+) were not. Cells were tested for the presence of the tagged allele by hybridization with an antibody specific for Ty1. All mutants express Ty1-TbTRF (mutant) equally; wild-type Ty1-TbTRF was used as a positive control to compare the

expression and molecular weight of the mutants (Figure 4-11a). When an antibody against TbTRF was used, the Ty1-tagged mutants were detected by their change in molecular weight, where they were slightly larger in size (Ty1-TbTRF is ~50 Kda and wild-type TbTRF is ~ 45 Kda; Figure: 4-11b).

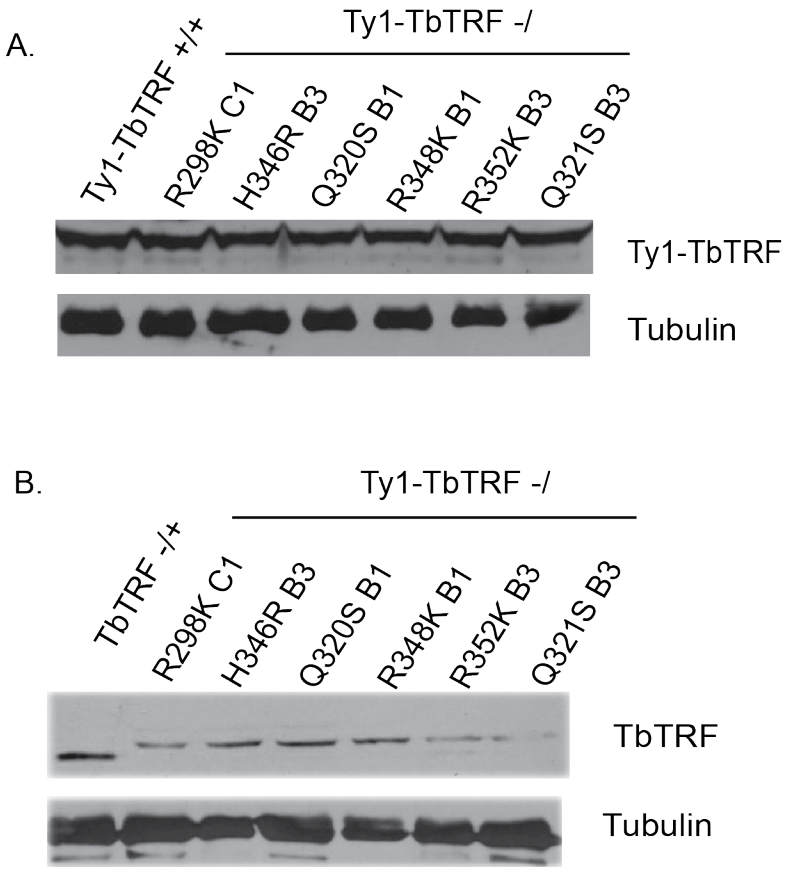

Figure 4-11: Western confirmation of *T. brucei* cells harboring indicated point mutation in the MYB domain. Western blot analysis to examine the presence of functional TbTRF in TbTRF MYB domain mutants. Cells were detected for the presence of (A) Ty1-TbTRF or (B) TbTRF (see text for details). Overall, there were no significant changes in the expression levels of mutant TbTRF compared to wild-type.

Upon the confirmation of each DNA binding point mutation, detailed growth analysis was performed for all the viable cells harboring particular point mutations in TbTRF's MYB domain. We did not observe a significant overall change in the growth of these mutants (Figure 4-12).

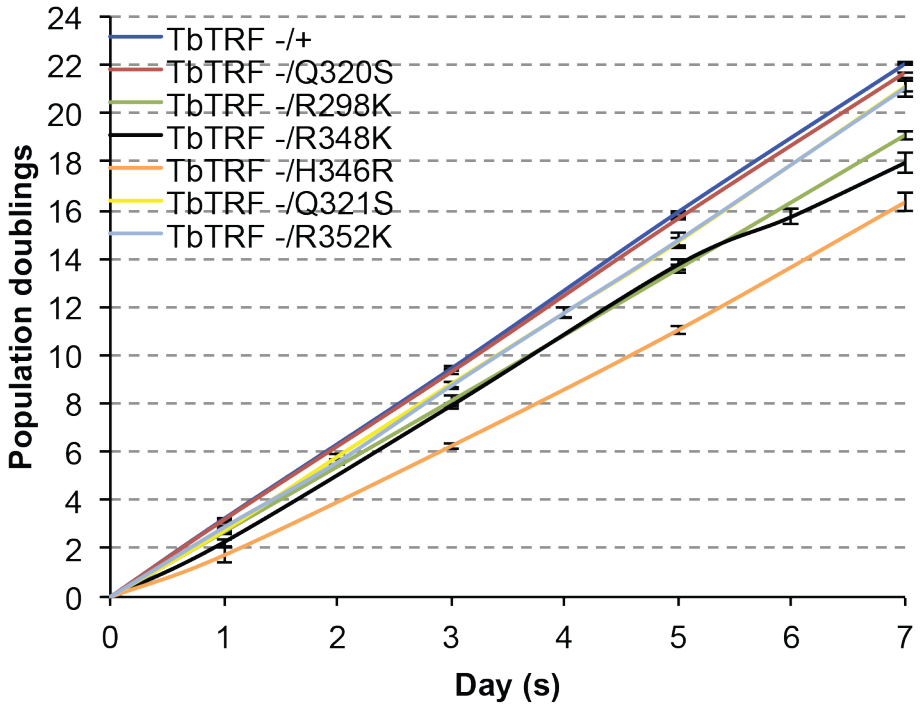

Figure 4-12: Growth curve analysis of TbTRF MYB domain mutants. Growth progression of all mutants was carefully characterized over 7 days. No overall significant changes were observed in the growth of TbTRF mutants. However, we did observe that the mutants that had weakened DNA binding activity compared to WT (R298K, H346R and R348K) had a slightly slower growth rate compared to the remaining mutants. However, the overall changes were not significant.

Analysis of VSG silencing in TbTRF DNA binding mutants

In order to detect any possible role for TbTRF DNA binding mutants in *VSG* silencing, Western blot was carried out to look at the expression of a different ES-linked VSG other than the active VSG (VSG2). Only TbTRF-/R348K expressed VSG13 in addition to the originally active VSG2. This hinted to the possibility that perhaps this particular mutant is affecting *VSG* switching rather than silencing (Figure: 4-13a). In addition, VSG13 was detected in a Northern analysis for some sub-clones of TbTRF -/R348K mutant (Figure 4-13b), further supporting our hypothesis that TbTRF DNA

binding mutants affect *VSG* switching and not *VSG* silencing. These data are in agreement with previous observations (Yang et al. 2009).

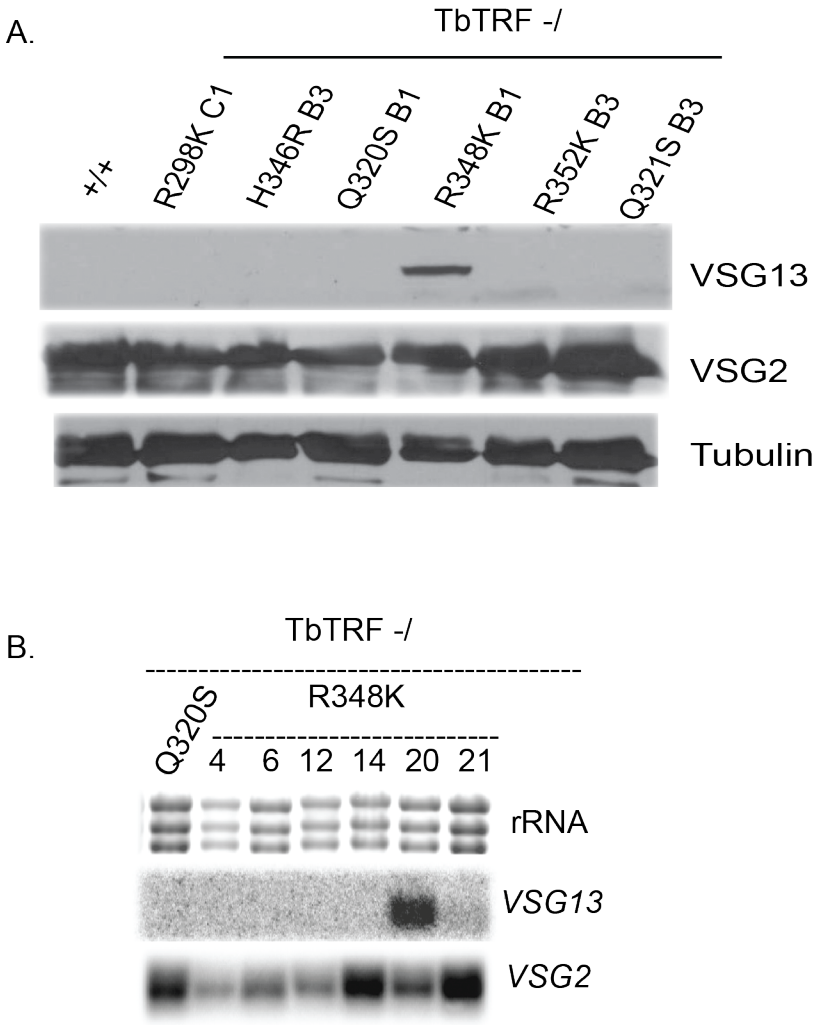

Figure 4-13: Analysis of *VSG* silencing in TbTRF DNA binding mutants. (A) Western analysis of VSG2 and VSG13 expression in TbTRF mutants. Only TbTRF -/R348K expressed VSG13 in addition to VSG2, further supporting our hypothesis that TbTRF may play a role in *VSG* switching and not *VSG* silencing. (B) Northern analysis of TbTRF -/R348K sub-clones. The TbTRF -/R348K mutant was sub-cloned and mRNA was isolated for several sub-clones. The expression of *VSG13* was tested for several sub-clones and *VSG13* was detected only in TbTRF -/R348K sub-clone #20. TbTRF -/Q320S was used as a control (Western analysis did not detect any VSG13 expression in TbTRF -/Q320S).

Targeting TbTRF MYB domain mutants into HSTB261 reporter strain

TbTRF MYB domain mutants R298K, H346R, R348K and Q320S were introduced in HSTB261 starter strain with minor modifications (see material and methods section and figure: 4-14). Each mutant was confirmed with PCR, Western blot and sequencing. At least two different clones were generated per mutation. These clones will be used to perform future switching assays.

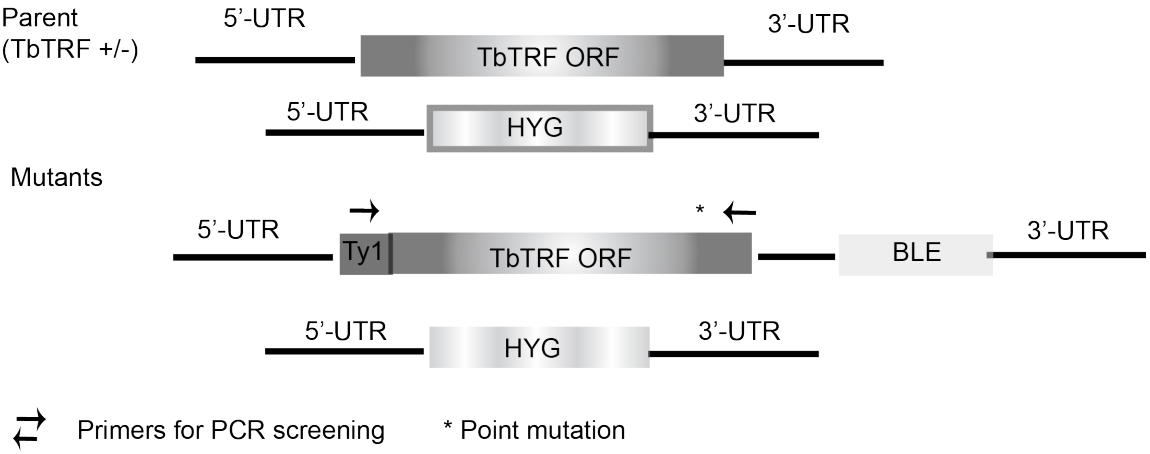

Figure 4-14: Strategy to target TbTRF MYB domain mutants in the starter strain HSTB261. A single knockout allele of TbTRF was established as described in figure 4-14. The point mutations were introduced into a construct that was marked with a *BLE* downstream of TbTRF ORF.

J-modification in T. brucei does not affect TbTRF DNA binding activity in vitro and in vivo

J base is a modification present at telomeres, where a thymidine residue is modified to J base. Since TbTRF is the only known direct telomere DNA binding factor, we sought to investigate TbTRF binding to J-modification at telomeres and whether or not TbTRF is indifferent to the presence of J modification at telomeres. Using ITC to measure the DNA binding activity of TbTRF in the presence or absence of J *in vitro*, we reported no difference (Figure: 4-15). TbTRF MYB domain was titrated onto a telomeric

sequence containing J (5`-GGT**J**AGGTTAGG-3`). The interaction was measured as described previously, where a well-shaped curve indicates interaction. In addition, a Kd value was determined from the heat curves. Whether TbTRF MYB was titrated onto a telomeric sequence containing J base or not containing J-base, the heat curves generated from the interaction did not differ significantly nor did the Kds. These curves were generated in collaboration with Dr. Zhao at Hong Kong Polytechnic University (Experiments were performed and analyzed by Li, X).

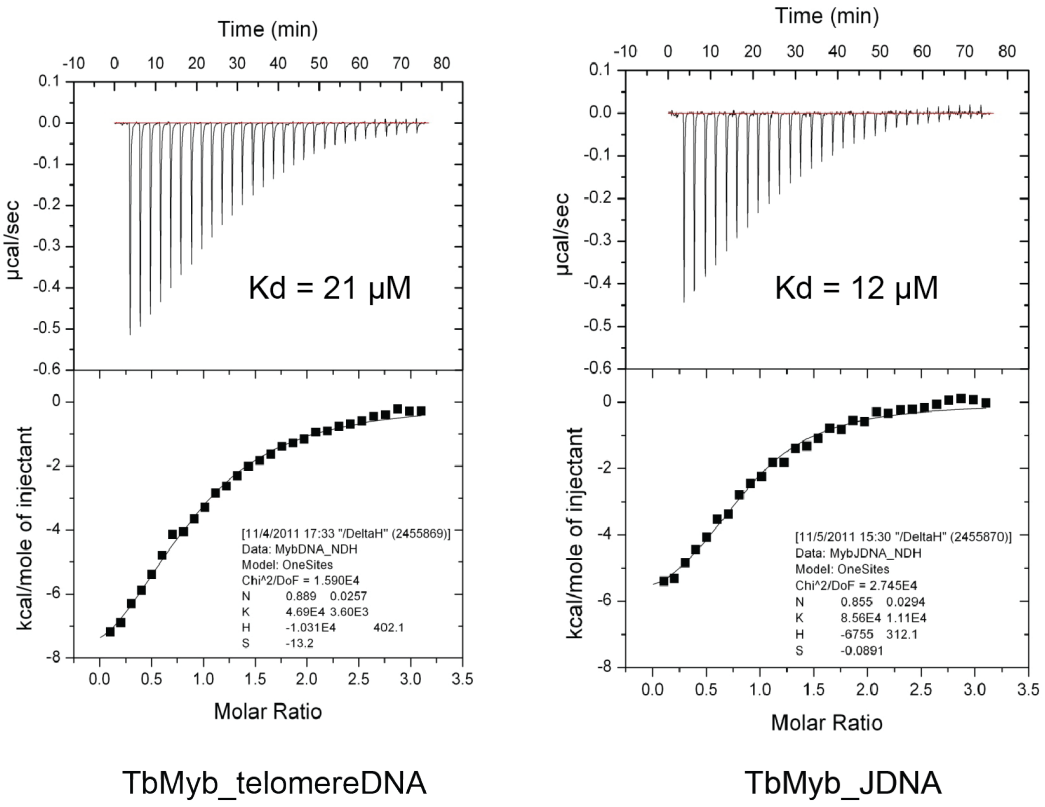

Figure 4-15: J modification does not affect the telomere DNA binding activity of TbTRF *in vitro*. The TbTRF MYB domain interaction with telomere DNA was measured using ITC. TbTRF's MYB domain was titrated onto a telomeric sequence containing J. The overall interaction did not differ significantly when compared to TbTRF's MYB domain interaction with a telomeric sequence lacking J (Experiments and analysis were done by Li, X).

Successful depletion of J-base in vivo.

To further investigate if this result was reproduced *in vivo*, first, successful depletion of J must be established. To deplete J, cells were treated with DMOG for 6 days at a 0.5 mM concentration. DMOG is a J synthesis inhibitor (Cliffe et al. 2012). As a control, cells were treated with DMSO in the same manner and for the same time length. As a control to either treatment, cells with no treatment were grown for the same time length. No growth defects were observed upon the addition of DMOG in two different strains SM and PVS-3-2-OD-1-1 (Figure 4-16), in agreement with previous observations (Cliffe et al. 2012).

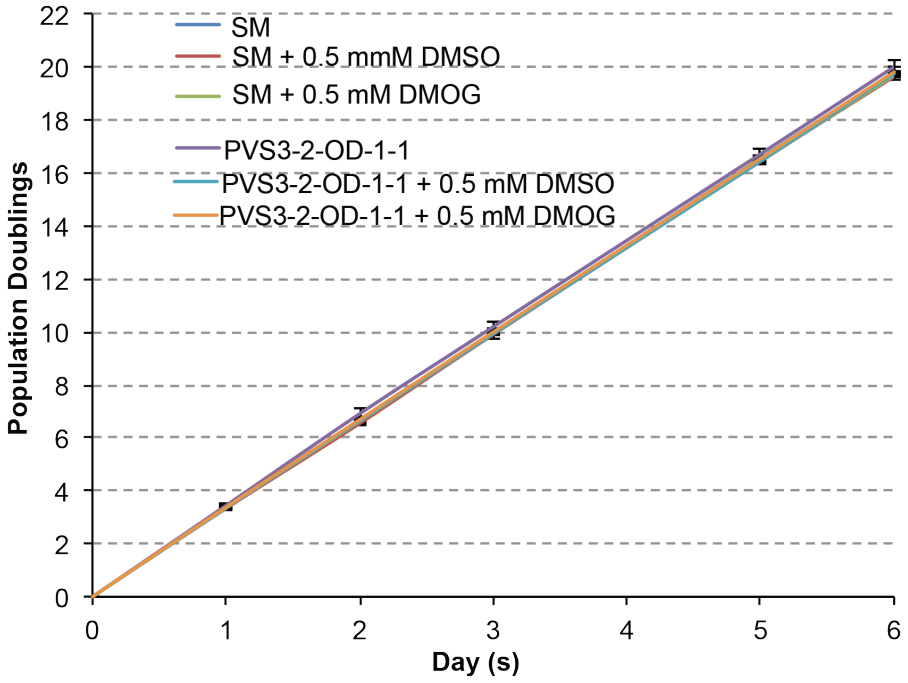

Figure 4-16: Growth curve analysis upon the addition of J-synthesis inhibitor (DMOG). No growth defects were observed when treating the cells with 0.5 mM of DMOG. Cells without treatment or DMSO treatment were carried out as controls.

Finally, J-synthesis depletion was confirmed by looking at the *VSG2* locus after *PstI* digestion in PVS-3-2-OD-1-1 strain, where *VSG2* is silent. Recall that J is present in silent but not active ES. Therefore, we used this discrepancy to determine if our depletion

of J was successful. If J is present in the *PstI* digestion site, *PstI* enzyme cannot cleave that site and will cleave the following *PstI* site (as long as there is no J modification). If J is absent complete cleavage of *PstI* sites takes place. Because we used VSG2 NT as a probe, we were able to differentiate between partial and full cleavage of *PstI* sites. In the absence of J, only one band is observed at 1.6kb due to complete cleavage. In the presence of J, some *PstI* sites are modified and therefore, partial cleavage is observed whenever there is J (see map for expected or possible sizes of partial cleavage, figure 4-17a).

Upon treatment with DMOG, the absence of J, we clearly observed the complete cleavage of *PstI* site at silent *VSG2* locus. As a control, we ran PVS-3-2-OD-1-1 strain genomic DNA digested with *PstI*. Also we ran PVS-3-2-OD-1-1 strain genomic DNA treated with DMSO and digested with *PstI*. In both cases we observed partial cleavage of *PstI* site in *VSG2* locus (9.6kb band) indicating the presence of J at one of the *PstI* sites present in the *VSG2* locus. To validate the digestion pattern of the *VSG2* locus SM strain, where *VSG2* is active, genomic DNA was run as a positive control. The expected size of full cleavage, 1.6 kb, was observed. In addition, procyclic WT427 (cells that lack J-modification) was carried out as a positive control. The expected size of full cleavage when *PstI* site is not modified was observed (Figure: 4-17b).

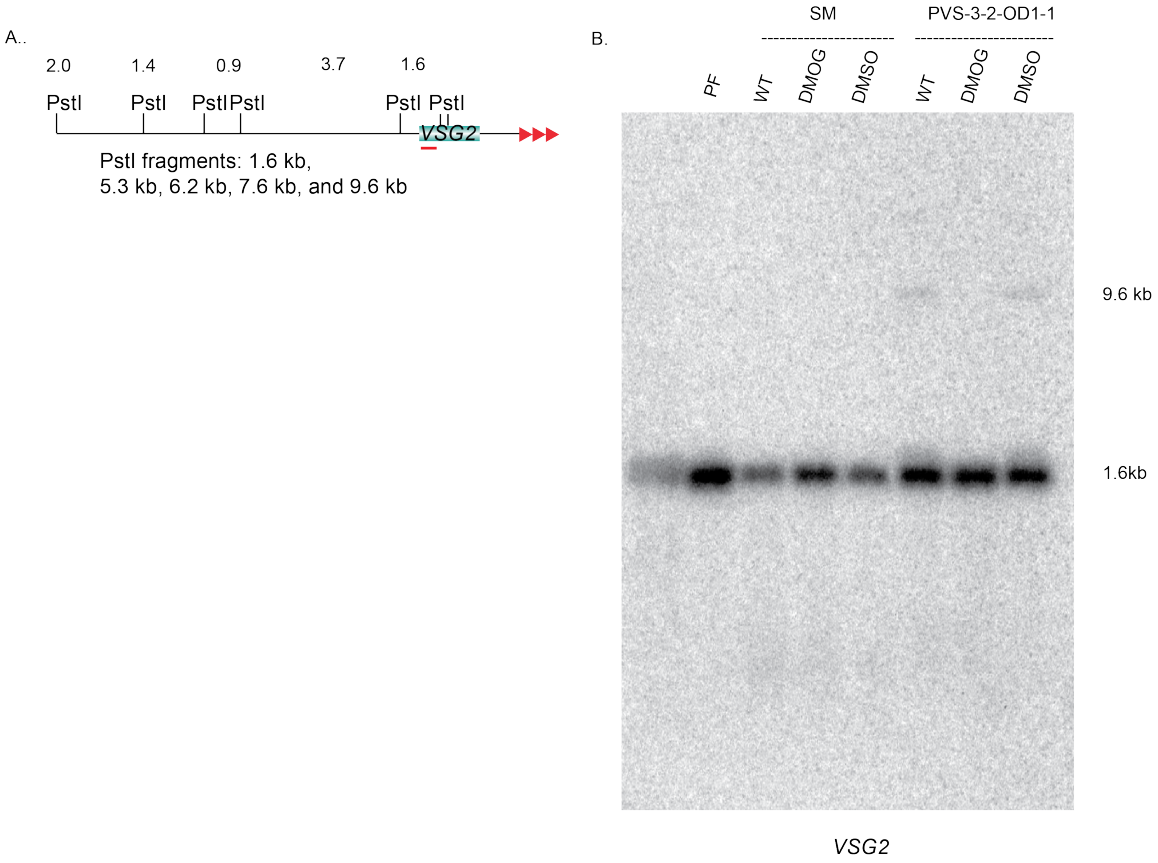

Figure 4-17: Confirmation of the depletion of J *in vivo* upon addition of the J-synthesis inhibitor DMOG. (A) Map of *VSG2* locus and expected bands upon *PstI* digestion. NT probe was used (pink line on map). If the *PstI* site is fully cleaved, only the 1.6 kb band is observed. If J modification is present and depending on what *PstI* site is modified, various bands may be observed. See map. (B) Southern Blot analysis to confirm the loss of J-modification upon DMOG treatment. The expected 1.6 kb band when *PstI* sites were fully cleaved and when *VSG2* NT was used as a probe was observed in the following sample: 1) cells lacking J (WT427), 2) in cells where *VSG2* is active (SM), 3) Upon DMOG treatment in cells where *VSG2* is silent (depletion of J). Partial cleavage is observed only in the PVS-3-2-OD-1-1 WT cells and cells treated with DMSO, indicating the presence of J in some of the population at a particular *PstI* site. (See text for more details).

DISCUSSION:

Trypanosoma brucei TTAGGG repeat binding factor

Telomeres in *T. brucei*, like humans, consist of TTAGGG repeat tracts. However, only one telomere DNA binding protein was identified (Li et al. 2005). TbTRF was

specifically shown to bind to duplex TTAGGG DNA through EMSA experiments (Li et al. 2005). TbTRF was also shown to bind telomere DNA *in vivo* through ChIP analyses. Depletion of TbTRF led to dramatically reduced G-overhang signal characterized through in-gel hybridization studies. Therefore, TbTRF is a homologue of hTRF2 and, like hTRF2, is important for end protection (Li et al. 2005). TbTRF depleted cells acutely arrested at 24 hours, making the analysis of *VSG* silencing or *VSG* switching hard to perform. TbTRF like hTRF1 and hTRF2 contains a single MYB domain, a homodimerization domain, but lacks an N-terminal domain and has a less conserved hinge domain (Li et al. 2005). Despite the differences, hTRF1 was able to localize to the *T. brucei* telomere when expressed (Munoz-Jordan and Cross 2001). TbTRF is a homodimer, so in order for TbTRF to bind to telomeres, TbTRF needs both a MYB domain on each strand and the homodimerization activity of TbTRF. Therefore, we proposed that the disruption of TbTRF's major function (DNA binding activity) through its MYB domain or homodimerization domain will provide us with a mechanistic understanding of the functions of TbTRF in *VSG* regulation. Being a small domain of only 60 amino acids (Li et al. 2005), we solved its NMR structure in collaboration with Dr. Zhao at Hong Kong Polytechnic University in China. The MYB domain of TbTRF forms a Helix-Turn-Helix (HTH) motif, a typical motif found in DNA binding proteins. Studies are on-going to solve the TbTRF homodimerization domain, which is ~ 150 amino acids in length.

Several point mutations were identified to weaken or abolish DNA binding activity *in vitro*. These point mutations were successfully targeted *in vivo*. Attempts to obtain the following TbTRF MYB domain mutants, R298E, R348E and R352E were not

successful. It is possible that the point mutation is deleterious and no viable cells could be obtained. However, further attempts to obtain these cells must be conducted prior to making this conclusion.

We observed the expression of VSG13 in addition to VSG2 in TbTRF -/R348K. However, we did not observe this phenotype in other TbTRF MYB domain mutants. It is possible that the VSG expressed in the other mutants is not VSG13. To further examine this, a q-RT-PCR analysis for various ES-linked silent *VSGs* must be carried out and as an expectation, an expression of an additional *VSG* other than VSG13 should be observed. Another explanation could be the DNA binding activity of these mutants varies *in vivo*, where mutants with significantly less DNA binding activity affect *VSG* silencing. These studies will lead to an explanation to why only TbTRF -/R348K showed an increase in *VSG13* mRNA levels and not any other mutant.

TbTRF and antigenic variation

VSG regulation is a crucial mechanism for *T. brucei* pathogenesis. There are two independent pathways for *VSG* regulation: *VSG* silencing and *VSG* switching. Many factors are involved in the regulation of *VSG* silencing including telomere proteins (Yang et al. 2009). In addition, *VSG* switching is regulated via telomere length (Hovel-Miner et al. 2012). Here we successfully established four independent clones where we can transiently deplete TbTRF in all four independent clones; these clones will be used to study the role of TbTRF in *VSG* switching. If TbTRF plays a role in *VSG* switching, then it is of great interest to study if any of the TbTRF DNA binding mutants affects *VSG* switching. To date, I successfully established some of TbTRF DNA binding mutants in

HSTB261 reporter strain. These point mutations weakened or abolished DNA binding activity of TbTRF *in vitro*. Point mutation in R348 and R298 to R348K and R298K, respectively, had abolished DNA binding activity *in vitro*. However, mutations in Q320 and H346 to Q320S and H346R had weakened DNA binding activity *in vitro,* when compared to wild-type. All clones should be utilized to study antigenic variation controlled by TbTRF's MYB domain.

No *VSG* derepression was detected in TbTRF depleted cells (Yang et al. 2009). However, when the TbTRF DNA binding mutants were tested for a potential role in *VSG* silencing, only VSG13 expression was observed in TbTRF -/R348K mutant. We sub-cloned the TbTRF -/R348K population, in order to understand the expression of VSG13 in the TbTRF -/R348K population. Sub-cloning of TbTRF -/R348K resulted in one clone expressing *VSG13* and the other clones did not. There are two possible explanations to these differences. The first explanation is that the mRNA of *VSG13* in some sub-clones is not abundant and hence could not be detected with a Northern analysis. The second explanation is that the sub-clones that did not express *VSG13* switched to a different *VSG*, other than *VSG13*. In order to determine what explanation is true, a q-RT-PCR analysis must be carried out for all TbTRF -/R348K sub-clones. If the first explanation were true, we would observe a significant fold change in the mRNA levels of *VSG13* among the sub-clones, when compared to the sub-clones where *VSG13* was not detected. If the second explanation were true, the q-RT-PCR analysis would not detect any fold changes in *VSG13* expression in the sub-clones where *VSG13* was not detected and instead the expression of a different *VSG* is observed. Further experiments will provide an answer to our observations.

TbTRF and base J

Base J is quite abundant at telomeres (van Leeuwen et al. 1998b) and TbTRF is the only duplex TTAGGG binding factor known in *T. brucei*. However, for a long time it was not known whether the presence of this modification at telomeres affects the binding of TbTRF to telomeres. We analyzed the association of TbTRF with telomere DNA in the presence or absence of J both *in vitro* (experiments performed by Li, X). The titration of wild-type TbTRF onto telomeric sequence contacting J did not differ significantly from the titration of wild-type TbTRF onto telomeric sequence lacking J (data collected and analyzed by Li, X). We further will study this association *in vivo* using ChIP analysis. To do so, successful depletion of J must be established. We successfully depleted J using a J-synthesis inhibitor DMOG (Cliffe et al. 2012). DMOG was shown previously to deplete all J present in the genome (Cliffe et al. 2012). The absence of J did not affect cell viability (Cliffe et al. 2012).

Since the absence of J did not affect cell viability, we expect that the binding of TbTRF to telomere DNA *in vivo* will not affected by the presence or absence of J. If TbTRF required the presence of J to bind to telomeres, it is expected that upon the depletion of J, cells are not viable, because TbTRF is essential (Li et al. 2005). Nevertheless, it was not the case previously (Cliffe et al. 2012) and it is not the case in our study, where the depletion of J did not affect cell growth. Taken these data together, it is evident that the presence of J in telomeric repeats in *T. brucei* does not affect TbTRF's binding to telomeric DNA *in vitro* and the absence of J does not affect cell viability. Future studies will be needed to analyze the association of TbTRF to telomeres in the presence or absence of J *in vivo*.

CHAPTER V

CHARACTERIZATION OF TRYPANOSOMA BRUCEI TEL2

Imaan Benmerzouga

ABSTRACT

Trypanosoma brucei is a protozoan parasite that causes African trypanosomiasis. In their mammalian host, *T. brucei* cells regularly switch their surface antigen, Variant Surface Glycoprotein (VSG), to evade host immune attack. To maximize the efficiency of *VSG* switching, *T. brucei* expresses a single VSG exclusively from one of ~20 nearly identical *VSG* expression sites (ESs) located next to the telomere. Telomeres are specialized nucleoprotein complexes located at the ends of linear chromosomes. They are essential for chromosome stability and form a heterochromatic structure that can influence the transcription of genes located nearby. We have shown that one of the telomere-specific proteins (TbRAP1) is essential for *VSG* expression control, indicating that telomeres are important for virulence mechanisms in *T. brucei*. Tel2 was first identified in yeast and has been shown to be essential for telomere length maintenance. Subsequently, Tel2 homologues have been identified in different organisms including worm and human. However, different Tel2 homologues seem to have different functions, including circadian rhythm regulation, growth control, and telomere maintenance. Recent

studies showed that mammalian and yeast Tel2s regulate the protein stability of PI3-K related kinases (PIKK), which are key signal transducers in multiple signal transduction pathways involved in DNA damage repair/cell cycle checkpoint, degradation of mRNA, and gene expression control, explaining the versatility of Tel2 functions.

An *in silico* approach was used to find putative TEL2 in *T. brucei's* genome. Because telomeres are important for antigenic variation, we explored the potential role of putative TbTEL2 in telomere length maintenance, regulation of the protein stability of *T. brucei's* PIKKs, which in turn, may be critical for telomere recombination, a major pathway for *VSG* switching. Inducible TbTEL2 RNAi cells have been established and only one *T. brucei* PIKK homologue was tagged with epitopes. The protein levels of TbTOR1 were examined after depletion of TbTEL2. Preliminary data suggest that putative TbTEL2 is indeed the TEL2 homolog in *T. brucei*.

INTRODUCTION

In 1986, Lustig and Petes identified mutant strains that exhibited shorter telomeres. They named them *tel1* and *tel2*. Ten years later, the genes were cloned. In *Saccharomyces cervisiae* Tel2 mutants showed shortening in their telomeres (Lustig and Petes 1986; Runge and Zakian 1996). Tel2 caused the reversible repression of transcription genes located near telomeres, a phenomenon known as telomere position effect (Runge and Zakian, 1996). ScTel2 is important for cell viability. Cells lacking ScTel2 did not survive (Runge and Zakian 1996). In addition, ScTel2 encodes a protein that binds telomeric DNA (Kota and Runge 1998). ScTel2p binds to single stranded telomeric DNA *in vitro* (Kota and Runge 1999). ScTel2 functions during DNA damage at

a specific step in the ATM/Tel1 pathway, it mediates the activation and localization of ATM/Tel1 to double strand break (Anderson et al. 2008). In *Schizosaccharoyces pombe* Tel2 physically interacts with all the phosphoinositide 3-kinase- related kinases (PIKKs) (Hayashi et al. 2007). In *Caenorhabditis elegans*, *clk-2* encodes protein homologous to budding yeast Tel2p. It functions in telomere regulation, where *clk-2* mutants have elongated telomeres and *clk-2* over-expression leads to telomere shortening (Benard et al. 2001). *Clk-2 a*ffects embryonic development and the temperature sensitive mutant leads to embryonic lethality at 25 ºC (Benard et al. 2001). In mammalian cells Tel2 had no obvious telomere-related functions, however, it was essential for embryonic development, cell growth and the stability of ATM, mTOR and other PIKKs (Takai et al. 2007). In addition, Tel2 can interact with each of the six mammalian PIKKs (Takai et al. 2007).

Telomeres are nucleoprotein complexes located at the ends of linear chromosomes and are essential for protection of chromosome ends. In addition, the telomeric heterochromatic structure affects transcription of genes located in subtelomric regions, phenomenon known as TPE. Several functions have been reported for Tel2 homologs in different organisms, including telomere homeostasis.

Putative TbTEL2 was identified by Dr. George Cross and in this chapter, the author shows preliminary data for the role of TbTEL2 in cell viability, telomere homeostasis, TbTOR1 stability and finally *VSG* regulation. My preliminary data suggest that like budding yeast Tel2, TbTEL2 is essential for cell growth and telomere hemostasis. Like mammalian TEL2, TbTEL2 affects the stability of TbTOR1 protein and finally, TbTEL2 affects *VSG* switching.

MATERIAL AND METHODS

Plasmids and *T. brucei* strains generated for these studies can be found in chapter II. Western blot analysis, *VSG* switching and G-overhang analysis are described in materials and methods (Chapter II).

RESULTS

Depletion of TbTEL2 resulted in a growth defect

Dr. George Cross from the Rockefeller University identified a putative TbTEl2. The identification was established by the alignment of several published TEL2 sequences including TEL2 in budding yeast (Runge and Zakian 1996), TEL2 in *S. pombe* (Hayashi et al. 2007), human TEL2 (Takai et al. 2007) and TEL2 homolog in *C. elegans* (Ahmed et al., 2001) with putative TbTEL2, which indicated a sequence similarity that is not highly conserved, yet was similar enough so we named it TbTEL2.

In order to deplete TbTEL2, we generated a strain harboring a single allele of TbTEL2, where the other allele was replaced with the blasticidin marker (TbTEL2 +/-). An inducible TbTEL2 RNAi construct was targeted into the *rDNA* locus. To deplete TbTEL2, a dsRNA was generated under the Tet operon regulated T7 promoter, where the Tet repressor bound to the Tet operon in the absence of doxycyclin, thereby inhibiting transcription of TbTEL2 dsRNA. When doxcyclin was added, it bound to the Tet repressor, thereby allowing T7 transcription of TbTEL2 dsRNA. The generation of dsRNA targets TbTEL2 to the RNAi pathway of degradation.

Upon induction of TbTEL2 dsRNA with 100 ng/ml of doxycycline, a transient growth arrest was observed followed by a slow recovery in clone C6 (Figure: 5-1a). In

contrast, a growth arrest was observed for clones A7 and A8 (Figure: 5-1c). For clone C6, the growth curve was more carefully characterized compared to clones A7 and A9, where only days 0, 2, 4 and 6 were analyzed. The following time points were carried out for clone C6: days 0, 1, 2, 3, 4 and 5. It is possible that slow recovery cannot be captured from spread out time-points. Only clone C6 harbors a tagged allele of TbTEL2 (F2H-TbTEL2) and a Western blot analysis was performed to confirm the depletion of TbTEL2 (Figure 5-1b).

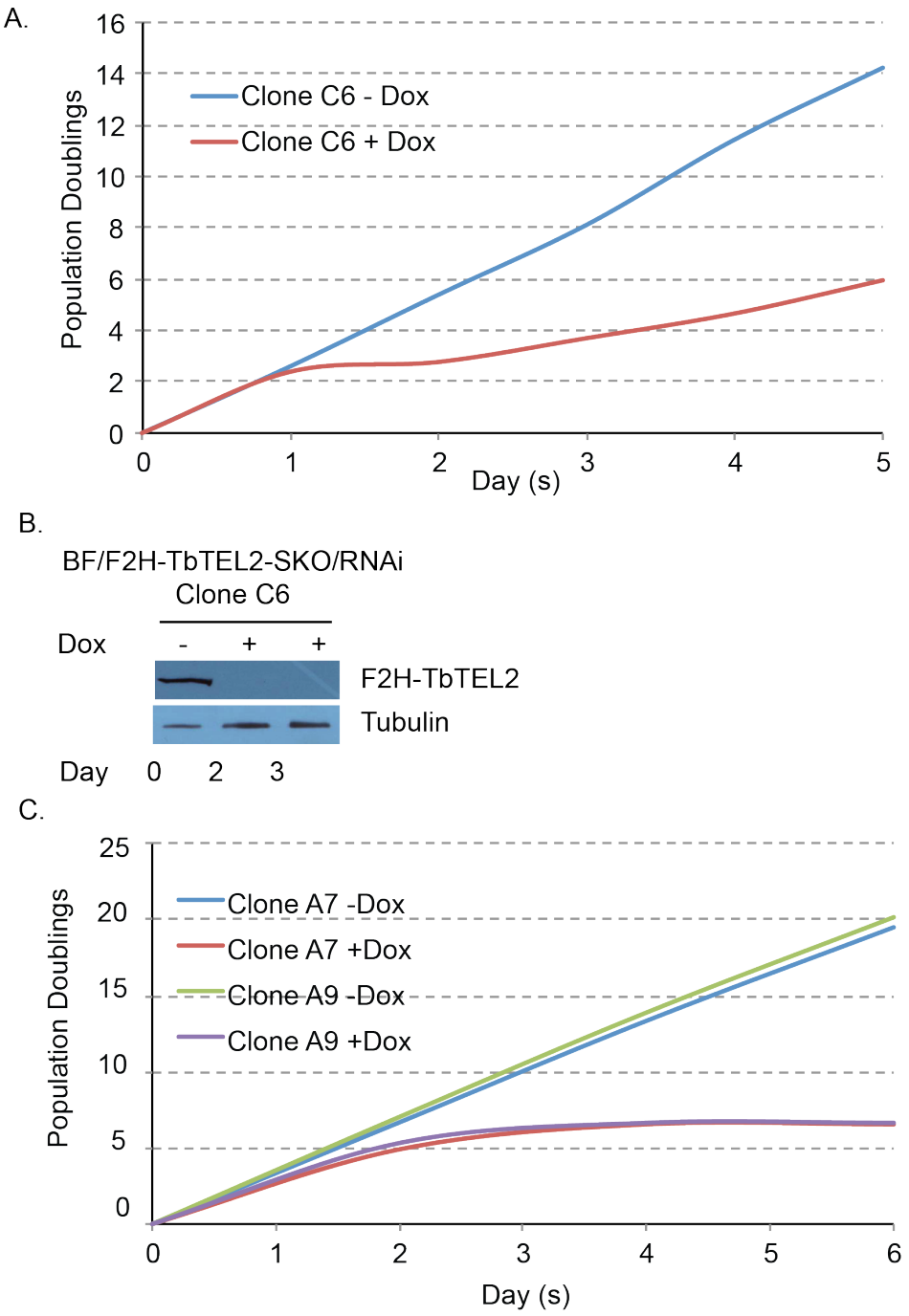

Figure 5-1: Growth curve analysis upon the depletion of TbTEL2. (A) RNAi induction for TbTEL2 was carried out in a single knockout background; clone C6 was analyzed from day 0 to day 5. Transient growth arrest with slow growth recovery was observed. (B) Western analysis for the depletion of TbTEL2. TbTEL2 was not detected after 48 hours. 12CA5 antibody was used to detect F2H-TbTEL2; tubulin was used as a loading control. (C) Additional RNAi induction for TbTEL2 was performed in a single knockout background. Clones A7 and A9 were analyzed at day 0, 2, 4 and 6 after

depletion of TbTEL2. Complete growth arrest was observed in these clones. The arrest occurred within 24 hours.

Depletion of TbTEL2 led to decrease in G-overhang signal

In *Saccharomyces cerevisiae*, Tel2 is important for telomere length maintenance, (Lustig and Petes 1986) and telomere position effect (Runge and Zakian 1996), where a *tel2-1* mutation reduced telomere position effect. In light of these findings, we questioned if TbTEL2 played any role in telomere homoeostasis in *T. brucei*. Characterization of G-overhang signal, in the presence or absence of TbTEL2, illustrated that indeed, TbTEL2 is important for G-overhang maintenance. G-overhang signal was reduced gradually suggesting that the affect of TbTEL2 is additive. Within 48 hours of TbTEL2 depletion, G-overhang signal was reduced to ~ %80 (Figure: 5-2).

Although mammalian TEL2 does not have any obvious telomeric functions (Takai et al. 2007), it seems that TbTEL2 resembles *Sc*Tel2 in its telomeric phenotype. It is too premature to make any conclusions about TbTEL2's role in telomere protection, but preliminary data suggests that TbTEL2 is important for telomere homoeostasis.

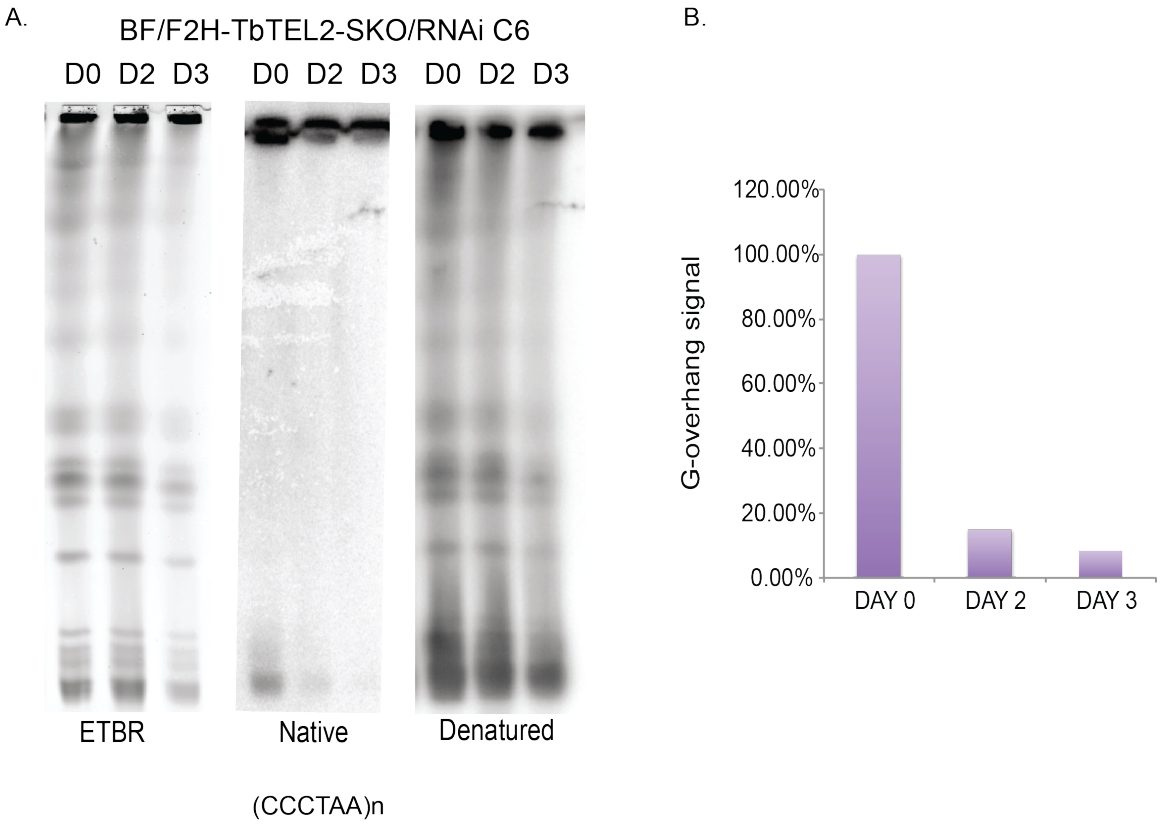

Figure 5-2: Depletion of TbTEL2 leads to a decrease of G-overhang signal. (A) In-gel hybridization of TbTEL2 plugs prepared at 0 hours, 48 hours after induction and 72 hours after induction. The native gel was used to determine the G-overhang signal that is normalized against the total DNA (denatured gel) (B) Quantification of G-overhang signal from native and denatured gels (consult Appendix A for calculation).

TbTEL2 affected the stability of TbTOR1

Mammalian Tel2 was shown to be important for the protein stability of the PI3-related kinases but not their mRNA levels (Takai et al. 2007; Chang and Lingner 2008). To test the possibility that TbTEL2 affects the stability of PI3-related kinases, several putative PI3-kinases were tagged: TbTOR1 (Tb10.6k15.2060), TbTOR2 (Tb927.4.420) and ATM (Tb11.01.6300). Only TbTOR1 was successfully tagged in the previously described single knockout and RNAi TbTEL2 cells. Several tries to obtain F2H-TbTOR2 and F2H-ATM were not successful in TbTEL2 -/+ only. We did not try to tag these in

TbTEL2 +/+ background. TbTOR1 was detected with anti-F2H antibody: 12CA5. Protein samples were collected to assess the stability of TbTOR1 upon the depletion of TbTEL2 at 24 and 48 hours. TbTOR1 protein levels decreased upon the depletion of TbTEL2 (Figure: 5-3a). However, the depletion of TbTEL2 did not affect the protein levels of TbTRF (Figure: 5-3b).

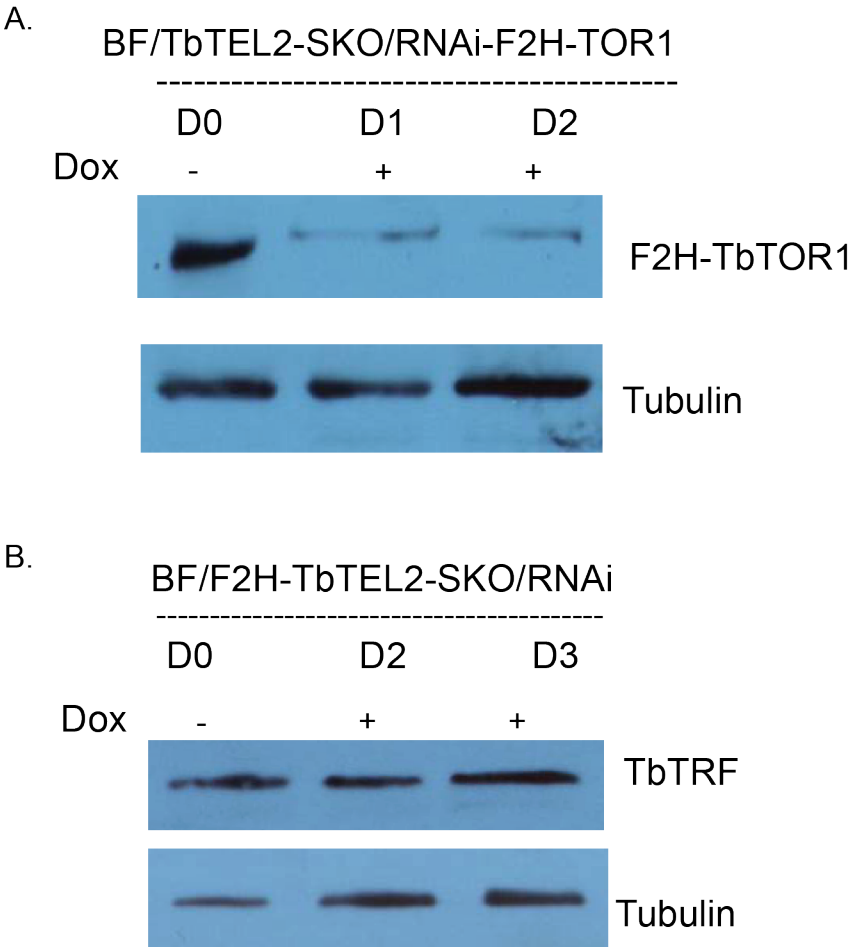

Figure 5-3: Western blot analysis of TbTOR1 and TbTRF protein levels upon the depletion of TbTEL2. (A) TbTOR1 protein level decreased dramatically upon the depletion of TbTEL2. (B) TbTRF protein level was not affected. Tubulin was used as a loading control.

TbTEL2 is important for VSG switching

VSG switching is regulated by several factors including telomere length (Hovel-Miner et al. 2012), DNA recombination (McCulloch and Barry 1999; Proudfoot and McCulloch 2005; Kim and Cross 2010; Kim and Cross 2011) and DNA replication (Benmerzouga et al. 2013). In addition, ScTel2 was shown to be important for TPE (Runge and Zakian 1996), a phenomenon that has been shown to be critical for *VSG* silencing (Yang et al. 2009). Therefore, we questioned whether TbTEL2 played any role in antigenic variation.

We tested the expression of several silent VSGs upon the depletion of TbTEL2: VSG9 and VSG13 (Figure: 5-4a). Upon the depletion of TbTEL2 we observed the expression of VSG9 but not VSG13, suggesting that there may be a switching phenomenon that is taking place (Figure: 5-4a). In order to address this question, a TbTEL2 RNAi construct was introduced into the HSTB261 strain (the doubly marked reporter strain). Only one switching assay was performed as a screen for the potential role of TbTEL2 in *VSG* switching regulation. TbTEL2 RNAi cells did not arrest as dramatically as in a single knockout background (compare to Figure: 5-1). Instead, they had a slower growth phenotype (Figure: 5-4b). We depleted TbTEL2 for 72 hours prior to conducting the switching assays. On the other hand, the *VSG* switching assay was performed for cells without induction as a control. Indeed, upon the depletion of TbTEL2, *VSG* switching frequency increased by ~ 6 fold.

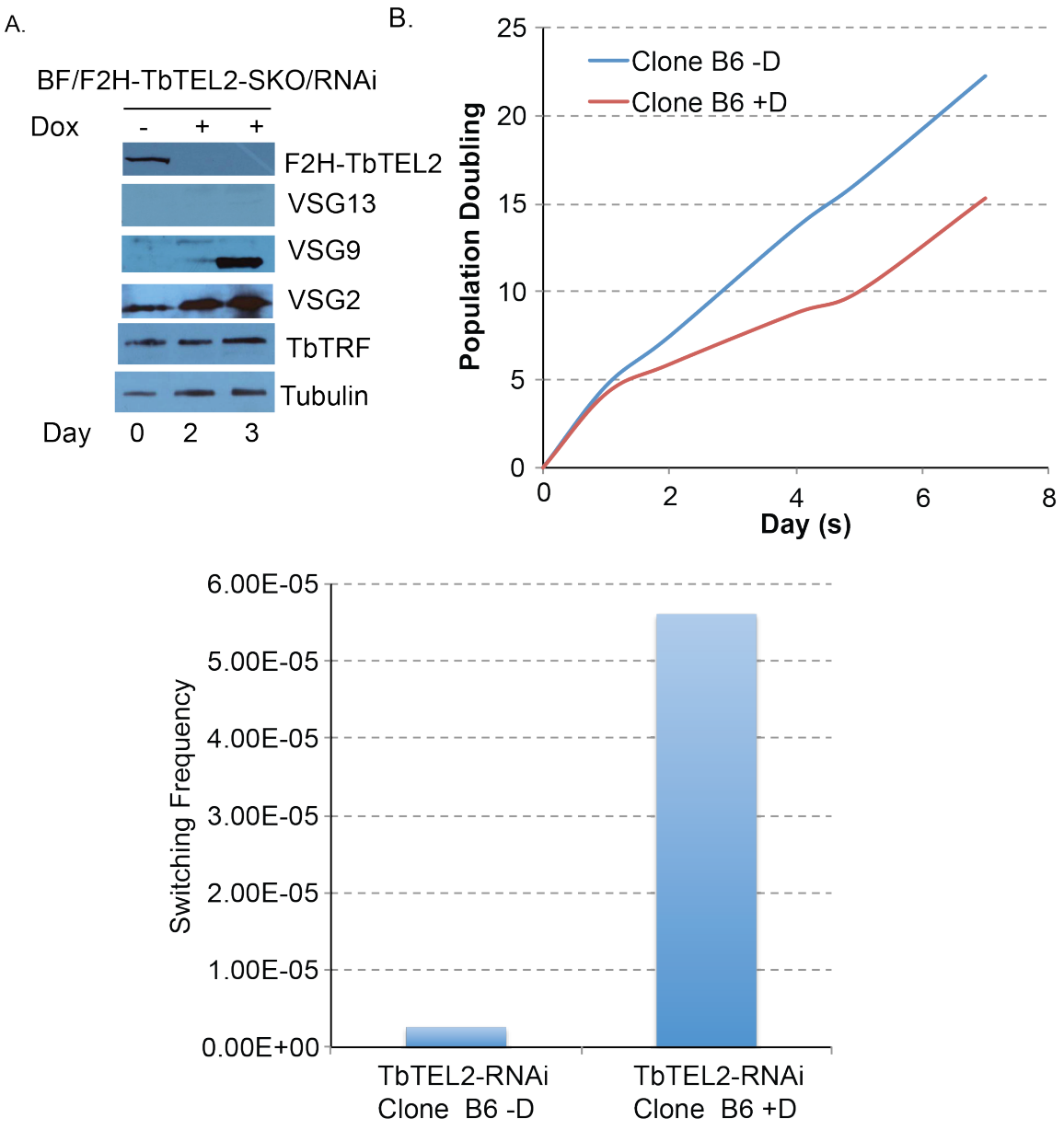

Figure 5-4: Depletion of TbTEL2 led to increase in *VSG* switching frequency. (A) Western blot analysis of silent VSG9 upon the depletion of TbTEL2. In addition, TbTEL2 depletion did not affect TbTRF protein levels. (B) Growth analysis of HSTB261-TbTEL2-RNAi clones B6 and B12. Slow growth was observed upon TbTEL2 depletion. (C) Depletion of TbTEL2 results in an increase in *VSG* switching frequency.

DISCUSSION

Tel2 was first identified in budding yeast as a negative telomere length regulator (Lustig and Petes 1986). Further studies were done to characterize the role of ScTel2 and studies showed that ScTel2 is essential for cell viability, telomere position effect and telomere homeostasis (Runge and Zakian 1996). In addition, studies in budding yeast have shown that Tel2 binds telomeric DNA (Kota and Runge 1998; Kota and Runge 1999). In *Schizosaccharoyces pombe,* Tel2 was shown to physically interact with all the phosphoinositide 3-kinase- related kinases (PIKKs) (Hayashi et al. 2007). In *Caenorhabditis elegans*, *clk-2 (*a budding yeast tel2 homolog) was critical for telomere homeostasis (Benard et al. 2001). In mammalian cells, Tel2 was shown to be important for embryonic stem cell viability and to affect the stability of all six PI3-related kinases (Takai et al. 2007).

In *T. brucei*, a protozoan parasite that causes human sleeping sickness disease, a putative TbTEL2 homolog was identified through an *in silico* approach. However, TbTEL2 was not characterized and to date nothing is really known about TbTEL2. Since budding yeast Tel2 and *C. elegans clk-2* were shown to be important for telomere length regulation, we speculated that TbTEL2 might play a role in telomere homeostasis. To test this, we analyzed the G-overhang signal upon the depletion of TbTEL2 and we observed a substantial decrease in G-overhang signal, suggesting that TbTEL2 plays a role in telomere homeostasis. Further experiments need to be done to support this hypothesis.

PIKKs are key signal transducers that function in multiple pathways. They are involved in DNA repair, cell cycle arrest, cell cycle progression and cell cycle checkpoints. There are 6 known mammalian PIKKs: Ataxia telagiectasia mutated (ATM),

ATM and Rad3 related (ATR), DNA-dependent protein kinase catalytic subunit ataxia (DNA-Pkcs), Mammalian target of rapamycin (mTOR), Suppressor with morphological effect on genitalia 1 (SMG1) and transformation/transcription domain-associated protein (TRRAP). Mammalian Tel2 affects the stability of all six PI3-related kinases (Takai et al. 2007). We tested the potential role of TbTEL2 in the stability of known PI3-kinases by tagging TbTOR1, TbTOR2 and Tb6300 (a possible ATM homolog); only TbTOR1 was successfully tagged and used for the screen. Tagging of TbTOR2 and Tb6300 should be carried out in a wild-type background to test for the possibility that a single allele of TbTEL2 hindered their tagging with F2H tag.

If TbTEL2 affects the stability of TbTOR1, we expect that upon the depletion of TbTEL2, TbTOR1 protein levels will substantially decrease. Indeed, upon the depletion of TbTEL2, and within 24 hours, TbTOR1 protein levels decrease dramatically compared to TbTOR1 levels in the presence of TbTEL2. This suggests that TbTEL2, like mammalian Tel2, plays a role in the stability of PI3-related kinases. Further experiments should test the stability of TbTOR2 and Tb6300 and the mRNA levels of TbTOR1, TbTOR2 and Tb6300 upon the depletion of TbTEL2. These experiments must be conducted in order to substantialize this conclusion.

Finally, one of the most interesting aspects of *T. brucei* is how it regulates mono-allelic expression and *VSG* switching. Several factors have been described that regulate either mono-allelic expression or *VSG* switching or both. Since TbTEL2 might play a role in telomere homeostasis, and telomeric proteins have been reported to play an essential role in *VSG* regulation, we investigated if TbTEL2 played a role in antigenic variation. A Western blot analysis for the expression of multiple silent VSGs at one time is a standard

indication of a *VSG* derepression phenotype. Upon the depletion of TbTEL2, silent VSG9 and VSG13 protein levels were analyzed, in addition to the originally active VSG2. Only the expression of VSG9 was observed but not VSG13, suggesting that it is not a de-repression phenotype that was observed, rather a *VSG* switching phenotype. To address this, we introduced TbTEL2-RNAi vector into the HSTB261 reporter strain. Upon the depletion of TbTEL2, we observed an increase in *VSG* switching frequency, in agreement with our hypothesis. However, additional switching assays must be performed and detailed analysis of *VSG* switching mechanisms must be characterized in order to solidify this conclusion.

In summary, the putative TbTEL2 phenotypes indicate that indeed, this may be the TEL2 homolog in *T. brucei*. Further experiments need to elucidate if TbTEL2 associates with the telomere or not, if TbTEL2 binds dsDNA or ssDNA as is the case in budding yeast (Runge and Zakian 1996) and if TbTEL2 affects telomere length. These studies are needed in order to firmly conclude that the putative TbTEL2 is indeed TbTEL2. Constructs for these studies have been prepared and are in the laboratory lab plasmid stock. Successful expression of TbTEL2 is needed to conduct gel shift experiments to test TbTEL2's binding to telomere DNA.

CHAPTER VI

PRELIMINARY DATA FOR FUTURE STUDIES

Imaan Benmerzouga

Trypanosoma brucei Origin Recognition Complex 1 (TbORC1)

Origin Recognition Complex, a critical DNA replication initiation complex, has been thoroughly studied in yeast and mammals. Although, it is not well conserved in *T. brucei,* components of the ORC complex exist in *T. brucei* such as Orc1, Orc4, Orc1-like protein or Orc1b and couple of other novel ORC components that are yet not classified (Godoy et al. 2009; Dang and Li 2011; Tiengwe et al. 2012b). Among these components, TbORC1 was reported to affect antigenic variation in two independent studies and collectively, the function of TbORC1 in antigenic variation was found across all life stages of *T. brucei* (Tiengwe et al. 2012a; Benmerzouga et al. 2013).

In yeast, ORC1 possesses the nucleosome binding BAH domain that interacts with key silencers to form the heterochromain at telomeres (Hickman and Rusche 2010). TbORC1 lacks the BAH domain (Tiengwe et al. 2012b) suggesting functional differences in TbORC1. In addition, TbORC1 does not interact with TbRAP1 (Benmerzouga et al. 2013), a major silencer in *T. brucei* (Yang et al. 2009) suggesting that TbORC1 plays an independent role in *VSG* silencing.

ORC associates with heterochromain protein 1 (HP1), an important component of tightly packed telomeres and centromeres in Drosophila (Huang et al. 1998) and this interaction mediates heterochromatin induced silencing (Shareef et al. 2001). Therefore, it is possible that TbORC1 regulates *VSG* silencing via heterochromatin and through a direct interaction with a homologue of HP1. To date, there are no homologues of HP1 in *T. brucei* but sequence alignments suggest the presence of the chromosome organization modifier) or chromo domain in histone acetyltransferases HAT-1 and HAT-2 that are analogous to the chromo domain present in HP1 (Kawahara et al. 2008). Depletion of HAT-1 affected telomeric silencing but not VSG expression and is essential for cell growth (Kawahara et al. 2008). HAT-1 knockdown cells proceed to mitosis without nuclear DNA replication, suggesting an impaired DNA replication progression. Therefore, it is possible that TbORC1 and TbHAT-1 directly interact at heterochromatin regions for both silencing and replication progression. Direct interaction studies must be carried out for both proteins and the localization of TbORC1 upon the depletion of HAT-1 and the localization of HAT-1 upon the depletion of TbORC1 would provide insights to whether TbORC1 affects heterochromatin and if so, whether heterochromatin organization is mediated via a chromo domain containing protein in *T. brucei* HAT-1, a function that has been observed in higher eukaryotes (Pak et al. 1997).

Our study did not report any changes in heterochromatin status (Benmerzouga et al. 2013) and the analysis of derepression at the promoter (Figure: 6-1) failed to provide an explanation for the derepression phenotype of sub-telomeric *VSGs*. However, the promoter is 40-60 kb upstream of VSG and hence TbORC1's effect is exclusively at sub-telomeres.

A recent study by Deng et al. (2009) showed that TERRA (telomere repeat containing RNA), TRF2 and ORC1 form a ternary complex at telomeres, which is crucial for heterochromatin formation. Attempts to study the expression of TelRNA or TERRA in TbORC1 depleted cells and preliminary data suggest that the depletion of TbORC1 resulted affect TERRA transcripts (data not shown), however, optimization of the protocol to detect TERRA must be established prior to making any conclusive results. Therefore, it is possible that TbORC1 may affect TERRA in *T. brucei* and hence TbORC1 association at telomeres, which is a mechanism whereby TbORC1 affects VSG silencing. Future experiments should test this possibility.

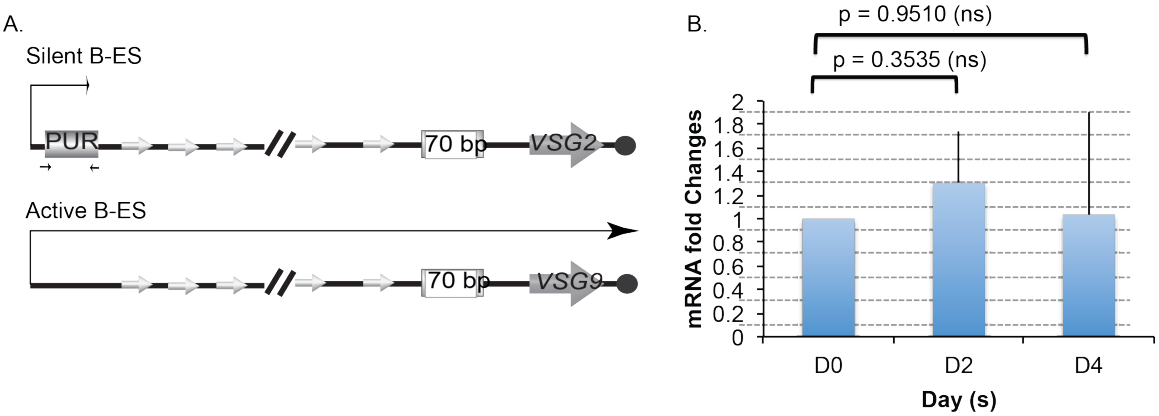

Figure 6-1: No changes in the transcription of PURO reporter gene upon the depletion of TbORC1. (A) Schematic representation of the strain utilized for promoter analysis study. Silent *VSG2* ES promoter site is tagged with *PURO* gene. Any derepression of silent *VSG2* promoter can be detected by the amplification of *PURO* from cDNA. (B) Quantification of *PURO* expression changes with and without TbORC1. D0 expression is set arbitrary at 1 and any changes to the transcription of *PURO* is normalized against D0.

Studies on ORC complex in *T. brucei* will provide insights into the role of replication at sub-telomeres, which affects VSG silencing. These findings can be utilized along with other telomere silencing factors to eliminate *T. brucei* and other fatal parasites

that use telomereic silencing to regulate antigenic variation to escape the host immune system (Li 2012).

Trypanosoma brucei TTAGGG Repeat Binding Factor (TbTRF)

Although not all the shelterin complex proteins have been identified in *T. brucei,* the two identified proteins exhibit effects on antigenic variation (Yang et al. 2009; chapter IV). Homologue of TRF2 in *T. brucei* was identified by Li et al. (2005) and TbTRF lacks the acidic or basic domain present in mammalian TRF1 and TRF2 respectively and constitutes of only two domains: TRFH domain and MYB domain, both the TRFH domain and MYB domain are required for TRF telomere DNA binding activity. TbTRF MYB domain structure is composed of three helices making a helix-turn-helix motif. Like mammalian TRF1 and TRF2 (Hanaoka et al. 2005), the third helix recognizes telomeric DNA. Domain interaction and domain functional studies have been extensively dissected for hTRF1 and hTRF2 (for review, see Diotti and Loayza 2011). However, there are no reported roles for TbTRF MYB domain or TRFH domain.

To date, studies that reported regulation of antigenic variation through regulating *VSG* switching were 1) telomere length (Hovel-Miner et al. 2012), 2) DNA replication (Benmerzouga et al. 2013) and 3) DNA recombination factors (Kim and Cross 2010), (Kim and Cross 2011). Therefore, if TbTRF affects *VSG* switching, telomeric proteins will be an additional factor that regulates *VSG* switching.

Trypanosoma brucei TTAGGG Repeat Binding Factor (TbTRF) and G-overhang

Telomeres end with a G-rich single stranded DNA (Wellinger and Sen 1997). A specialized structure known as a T-loop, where the G-rich strand invades the double

stranded telomere ends making a loop, sequesters the single stranded DNA end from being recognized as Double Strand Breaks (DSBs) (Murti and Prescott 1999). T-loops are detected in *T. brucei* nevertheless, they are smaller in size ~ 1 kb compared to mammalian T-loops which can be ~ 25 kb (Munoz-Jordan et al. 2001). TRF2 protects telomeres from end to end fusions (van Steensel et al. 1998). TRF2 binding to the proximity of 3`-overhang is required for the assembly of the T-loop *in vitro* (Stansel et al. 2001). TbTRF resembles mammalian TRF2, for its depletion resulted in the loss of G-overhang signal. If T-loops are a conserved structure to protect telomeres and are stimulated by TRF2 binding towards the telomere end, close to 3`-G-overhang, then the DNA binding activity of TRF2 is indeed an important regulator of this function. T-loop studies utilizing the telomere-binding mutants will solidify the mechanistic formation of T-loops at chromosome ends in *T. brucei* as well as the role of TbTRF DNA binding activity in G-overhang maintenance. After prolonged attempts, the preliminary data suggest that not all the DNA binding mutants affect G-overhang signal (Figure: 6-2). Further G-overhang analysis should be carried out for each mutant, although highly discouraged due to the significant variation in the results. The application of a more sensitive assay is needed to characterize the differences in G-overhang length among the mutants. The standardization of such an assay is on-going in the lab.

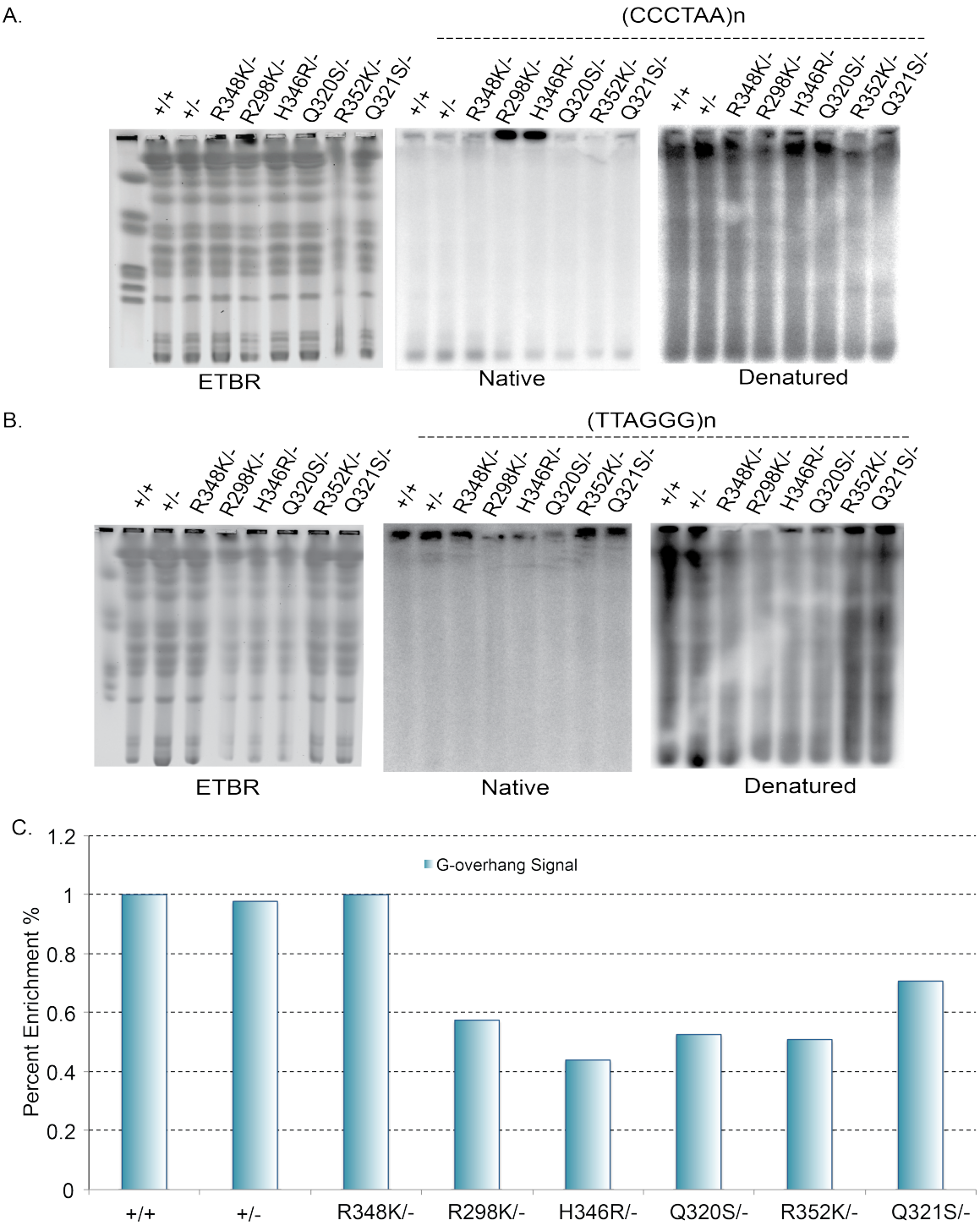

Figure 6-2: G-overhang analysis in TbTRF mutants. Mutants were grown for 13 weeks and analyzed for G-overhang signal compared to WT. (A) C-strand hybridized gel to show G-overhang (B) G-strand hybridized control gel to show the specificity of the C-strand gel signal (C) Quantification of (a) G overhang signal. Probes used are indicated on top.

Characterization of TbTRF and TbRAP1 interaction in vitro

TbRAP1 is an integral telomeric component that plays an essential role in *VSG* silencing. Our studies have suggested that TbRAP1 depends on TbTRF to be targeted to telomeres, which is critical for its function. In addition, changes in this interaction may influence *VSG* switching. Therefore, the interaction of TbRAP1 with TbTRF mutants was characterized *in vitro* using yeast-two-hybrid analysis. Since TbRAP1 interacts with the MYB domain of TbTRF directly, the characterization was dissected into the interaction with full-length TbTRF and the interaction with the MYB domain only.

For TbTRF-R348K and TbTRF-Q320S, yeast-two-hybrid analysis was carried out for 9 independent clones from 3 independent transformations. The interactions were averaged and plotted and a standard deviation was determined. TbRAP1 interaction with the MYB domain of TbTRF-R348K mutant was significantly affected (Figure: 6-3a), however, when the interaction was characterized with full-length TbTRF harboring R348K as a point mutation, the over-all interaction with TbRAP1 did not change significantly (Figure: 6-3b). Therefore, it is unlikely that the weakened TbRAP1 interaction with TbTRF MYB domain can be recapitulated *in vivo* using Co-IP, due to insignificant changes in the overall interaction *in vitro*.

For TbTRF-R298K and TbTRF- H346R, the interaction of TbRAP1 with the MYB domain of the mutants did not differ significantly (Figure: 6-4a). In addition, the overall interaction with TbRAP1 was not affected (Figure: 6-4b). This illustrates that TbTRF mutants do not affect TbRAP1's interaction with TbTRF. Therefore we presume that the role of TbTRF in antigenic variation is independent of TbRAP1 and therefore, no future work is encouraged.

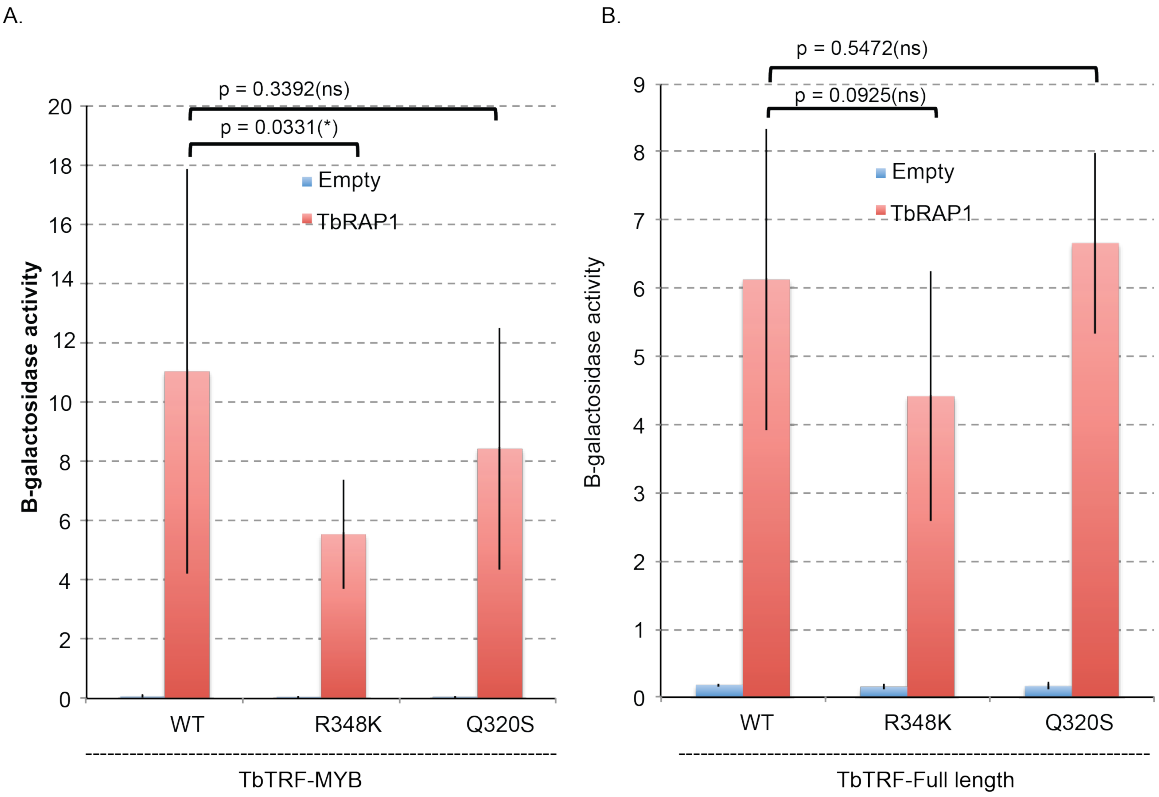

Figure 6-3: Yeast-two hybrid analysis of the interaction of TbTRF-R348K or TbTRF-Q320S with TbRAP1. (A) Interaction of the MYB domain only of TbTRF-R348K or TbTRF-Q320S mutant with TbRAP1. TbTRF-R348K had significantly weaker interaction with TbRAP1. No significant changes were observed in TbRAP1's interaction with TbTRF-Q320S. (B) Interaction of full-length TbTRF-R348K mutant with TbRAP1 or TbTRF-Q320S with TbRAP1. No significant changes were observed. Overall, the interaction of TbRAP1 with TbTRF-R348K or TbTRF-Q320S was not affected.

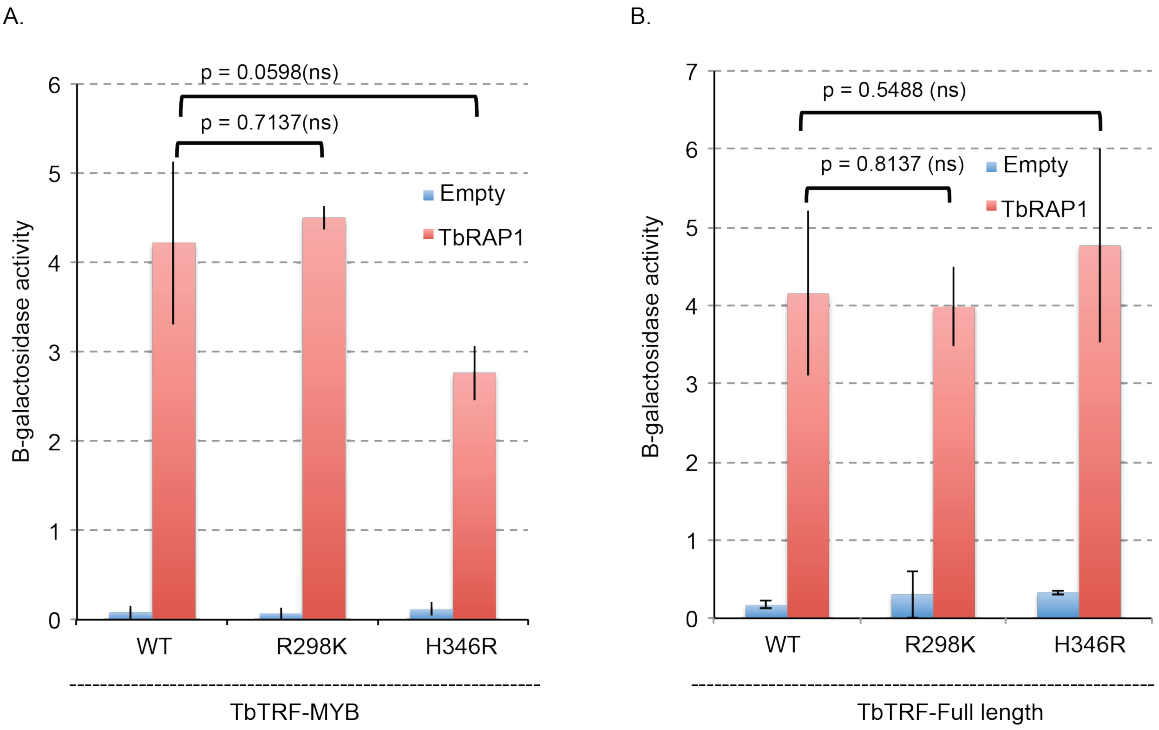

Figure 6-4: Yeast-two hybrid analysis of the interaction of TbTRF-R298K or TbTRF H346R with TbRAP1. (A) Interaction of the MYB domain only of TbTRF-R298K or TbTRF-H346R mutants with TbRAP1. No significant changes were observed in the interaction of TbRAP1 with TbTRF mutants compared to wild-type TbTRF. (B) Interaction of full-length TbTRF-R298K or TbTRF-H346R mutants with TbRAP1. No significant changes were observed in the interaction of TbRAP1 with TbTRF mutants compared to wild-type TbTRF.

TbRAP1 recruitment to telomeres in TbTRF mutant

To determine if weakened DNA binding activity of TbTRF affects the recruitment of TbRAP1 to telomeres, we performed ChIP analysis of TbRAP1 in a wild-type background and in the background of TbTRF -/R348K mutant. We do notice the increase of TbRAP1 at telomeres in TbTRF -/R348K, however careful analysis must be carried out in order to make such a conclusion. It is possible that TbRAP1 is recruited more to telomeres due to the changes in TbTRF binding to telomeres (Figure: 6-5). However, as a control to the recruitment of TbRAP1 to telomeres in TbTRF -/R348K, ChIP of TbRAP1 in a single knockout background of TbTRF is required to tell us if this phenotype is

because of the mutation itself or because of knocking out a single allele of TbTRF. In addition, ChIP analysis of TbTRF -/R348K must be carried out to determine how much TbTRF is at the telomeres in this particular mutation *in vivo*.

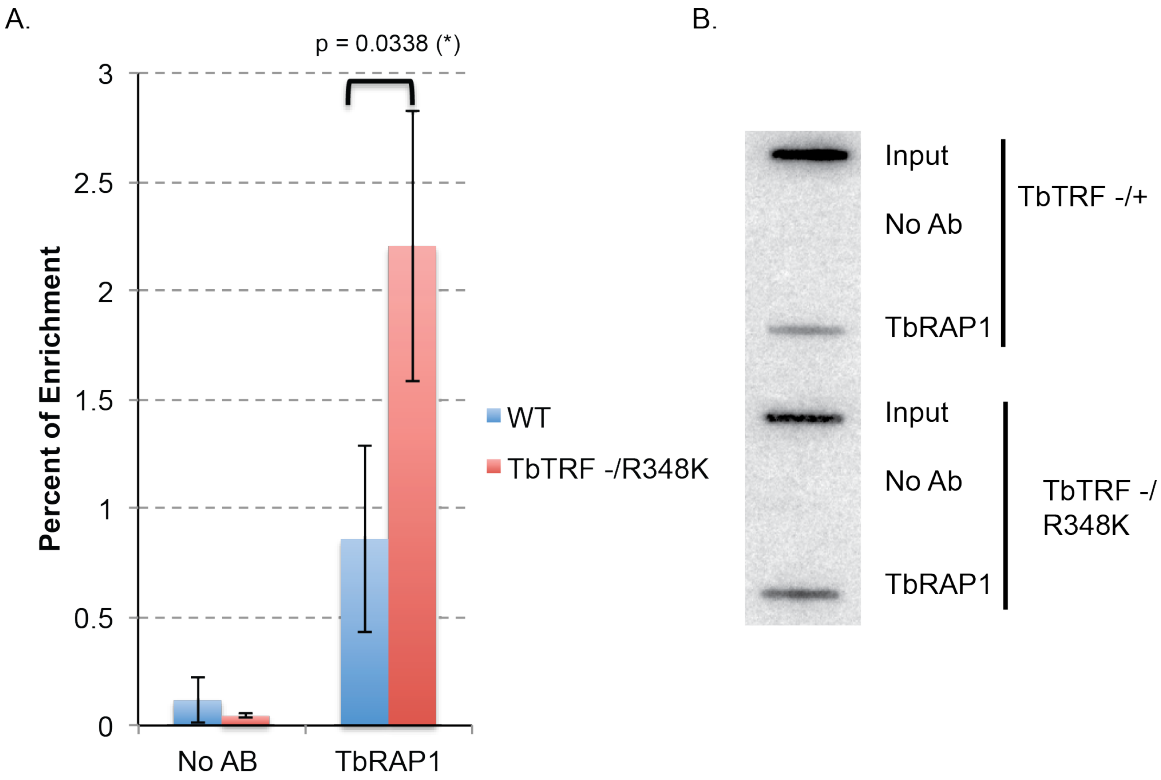

Figure 6-5: ChIP analysis of TbRAP1 at telomeres. We analyzed the recruitment of TbRAP1 in TbTRF wild-type background and in TbTRF -/R348K mutant. We observe a significant increase in TbRAP1 recruitment to telomeres in the TbTRF -/R348K mutant. (A) Quantification of 3 independent ChIPs for TbRAP1 in wild-type and in TbTRF -/R348K backgrounds, respectively. (B) Representative slot blots used to quantify TbRAP1's binding to TTAGGG.

TbTRF and *VSG* switching

VSG switching analysis was performed upon the depletion of TbTRF. Two sets of experiments were performed, *VSG* switching assays without induction and *VSG* switching assays with induction (Figure 6-6). For each clone, at least 7 experiments were carried out for the transient depletion of TbTRF and at least 3 experiments were carried out without any induction. Cells were induced for 24 hours with 200 ng/ml doxycycline

and recovered by the removal of doxycycline though several washes with media. In both cases, cells were allowed to undergo the same population doublings and the same washing conditions. HSTB261-TbTRF-RNAi without induction recovered a day prior to HSTB261-TbTRF-RNAi with induction. Switching frequencies were calculated as described (see chapter II). TbTRF depletion resulted in a significant (~ 5-10 fold) increase in *VSG* switching frequency in all four clones as illustrated in (Figure: 6-7).

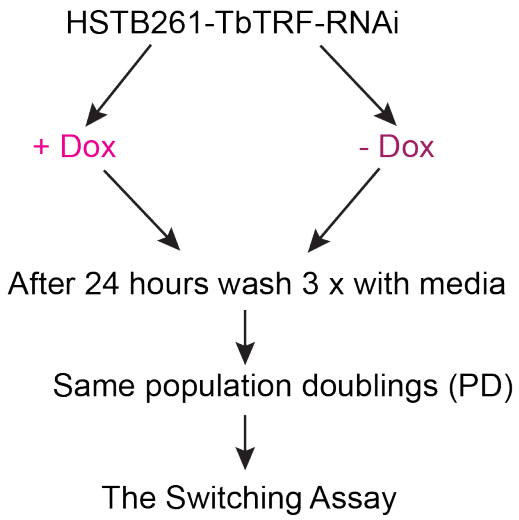

Figure 6-6: Diagram of TbTRF-RNAi method in preparation for the switching assay. Cells were induced or un-induced for 24 hours. After 24 hours, cells were washed with media lacking selective drugs (see chapter II). When cells reached the same population doublings, the switching assay was performed for both induced and un-induced cells (see chapter II).

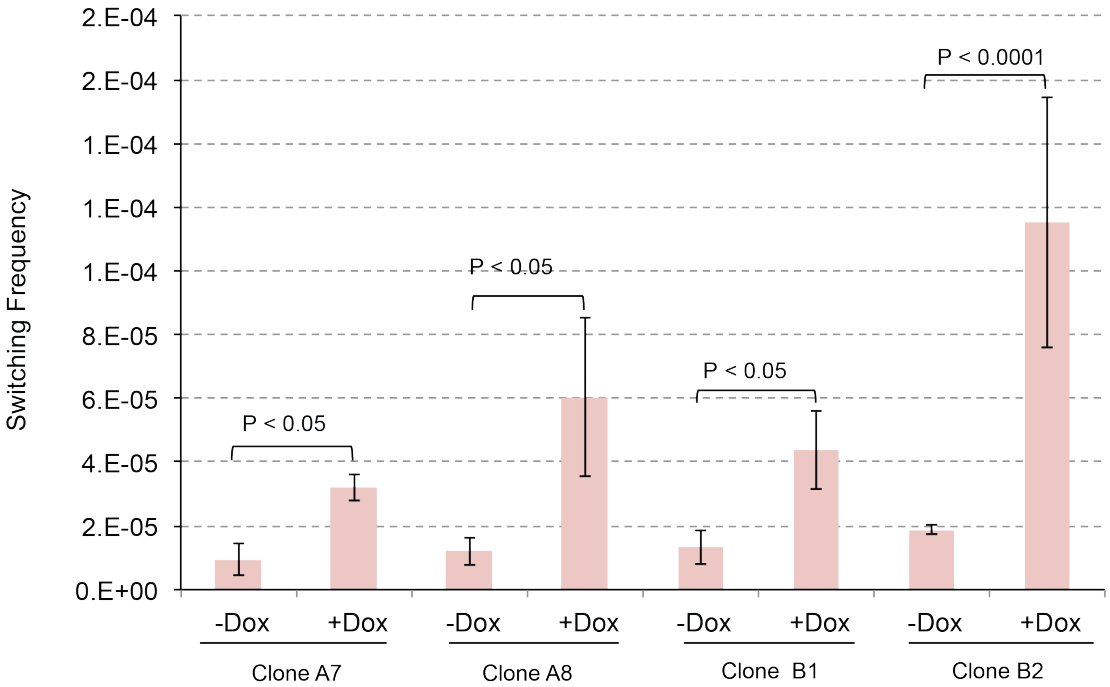

Figure 6-7: *VSG* switching frequency upon the transient depletion of TbTRF. Switching assays were performed for all four clones established and confirmed for the transient depletion of TbTRF as described in chapter IV. Preliminary data suggest that there is a significant increase in *VSG* switching frequency in clones A7, A8, B1 and B2 upon the transient depletion of TbTRF for 24 hours.

These data suggest that the transient depletion of TbTRF affects *VSG* switching frequency. These data need to be further validated. Since telomere length affects VSG switching frequency (Hovel-Miner et al. 2012), it is strongly suggested that telomere length is examined upon the transient depletion of TbTRF. Although no changes in telomere length were observed upon the depletion of TbTRF (Li et al. 2005), it is possible to detect these changes upon the transient depletion of TbTRF, which was not performed by Li et al. (2005). These experiments are needed, primarily to detect if the transient depletion of TbTRF affects *VSG* switching frequency, and if so, it is essential to determine if telomere length is affected upon the transient depletion of TbTRF. If telomere length is affected, then the changes in *VSG* switching frequency observed upon

the transient depletion of TbTRF is a consequence of changes in telomere length. Future experiments will provide insights into these possibilities.

TbTRF MYB domain mutants and VSG switching

We investigated if the expression of VSG13 in TbTRF -/R348K was due to *VSG* switching events. To do so, these point mutations were introduced into a reporter strain to study *VSG* switching frequency. Also, we performed switching assays in TbTRF -/+ cells to control for the possibility that the deletion of a single allele of TbTRF resulted in *VSG* switching frequency changes. If *VSG* switching frequency increased in TbTRF -/+ cells, then a single knockout allele of TbTRF is affecting the *VSG* switching frequency and not the introduced point mutations. For each mutant, at least two different clones were tested and for each clone, the assay was carried out multiple times (4-7 assays per clone). Clones from the same mutant showed comparable changes in the switching frequency, allowing us to pool the switching frequency changes into one bar representing the average of both clones from one mutant, therefore at least 8-14 assays are presented per bar.

An unpaired t-test was used to determine the P-values of the *VSG* switching frequency changes. In the unpaired t-test, the resulting frequencies from TbTRF -/R298K, TbTRF -/Q320S, TbTRF -/H346R, TbTRF -/R348K and TbTRF -/+ were compared to the wild-type switching frequency. P-values are indicated on each bar (Figure 6-8).

The highest average of switching frequency was observed in TbTRF -/H346R with ~ 4.45 x10^-5 events/cell generation. Switching assays for TbTRF -/Q320S were performed in the same fashion and no increase in *VSG* switching frequency was observed. Finally, we also performed switching assays in wild-type cells having both

alleles of TbTRF (TbTRF +/+) and in the parental cells having one allele of TbTRF (TbTRF -/+). We did not observe any significant changes in previously reported wild-type switching frequency (Kim and Cross 2010) in both TbTRF +/+ cells and TbTRF +/- cells. In addition, the difference in the switching frequency of TbTRF -/+ from TbTRF +/+ cells was not significant. The latter supports that the changes in switching frequency observed in the TbTRF DNA binding mutants R298K, H346R and R348K were not a consequence of the knockout of an allele of TbTRF (Figure 6-8).

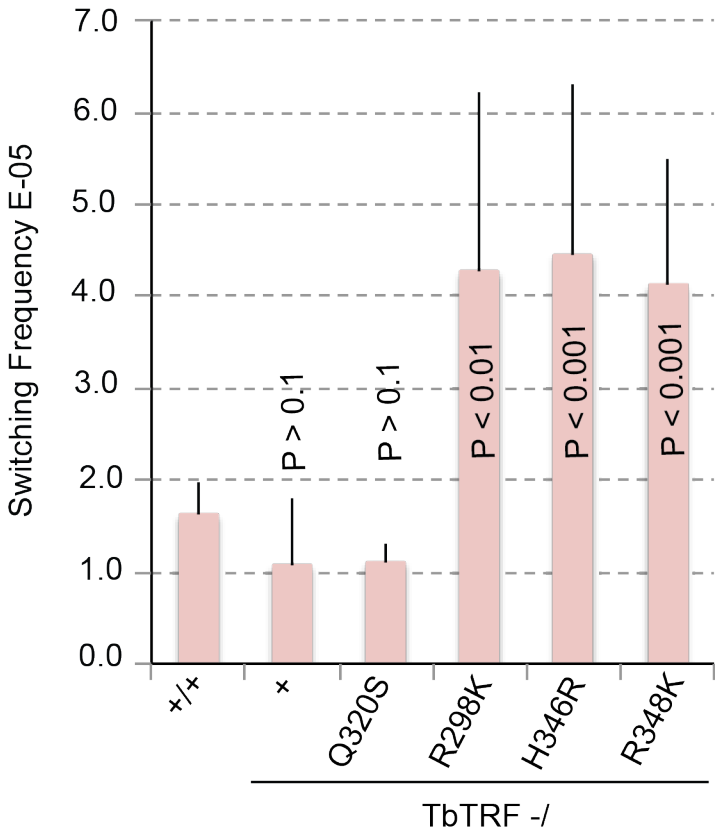

Figure 6-8: *VSG* switching frequency in TbTRF mutants. Preliminary data suggest that some TbTRF MYB domain mutants showed on average a 3-fold increase in *VSG* switching frequency. No increase in *VSG* switching frequency was observed in TbTRF -/Q320S. There were no significant changes in the *VSG* switching frequency in parental cells (TbTRF -/+). Each bar represents an average of at least 14 experiments from 2 independent clones per mutant, except switching assays performed for TbTRF -/+ where only 6 assays were performed. Each bar was compared to TbTRF +/+ switching frequency in an unpaired t-test. P-values are indicated on bars.

These observations suggest that TbTRF MYB domain mutants affect *VSG* switching frequency. Nevertheless, further assays must be carried out to validate these observations. In addition, future experiments must analyze the *VSG* switching frequency in the remaining mutants Q321S and R352K in order to support our hypothesis that the DNA binding domain of TbTRF affects *VSG* switching frequency. However, the question remains to as why not all DNA binding mutants affected *VSG* switching frequency.

These differences cannot be explained from the *in vitro* DNA binding studies, because the Kd value for TbTRF-MYB-H346R is lower than the Kd value for TbTRF-MYB-Q320S, making TbTRF-MYB-Q320S a stronger mutant. Nevertheless, we did not observe any changes in *VSG* switching frequency in TbTRF -/Q320S strain. It is possible that the DNA binding activity of TbTRF -./Q320S is not affected *in vivo*. However, ChIP analysis must be performed in order to test this hypothesis. In addition, it is possible that the telomere length in the TbTRF -/R298K, TbTRF -/H346R and TbTRF -/R348K is affected but not in the TbTRF -/Q320S and hence we do not observe changes in *VSG* switching frequency in the TbTRF -/Q320S. These experiments will explain the differences observed in the *VSG* switching frequency among the TbTRF mutants.

TbTRF binding to telomeres in the absence of J in vivo

As describe in chapter IV, we successfully established cells where J was depleted. However, only three ChIP experiments were performed. ChIP was performed after treating the cells with DMOG for 6 days at a 0.5 mM or with DMSO in the same manner and for the same time length or without any treatment grown for the same time length.

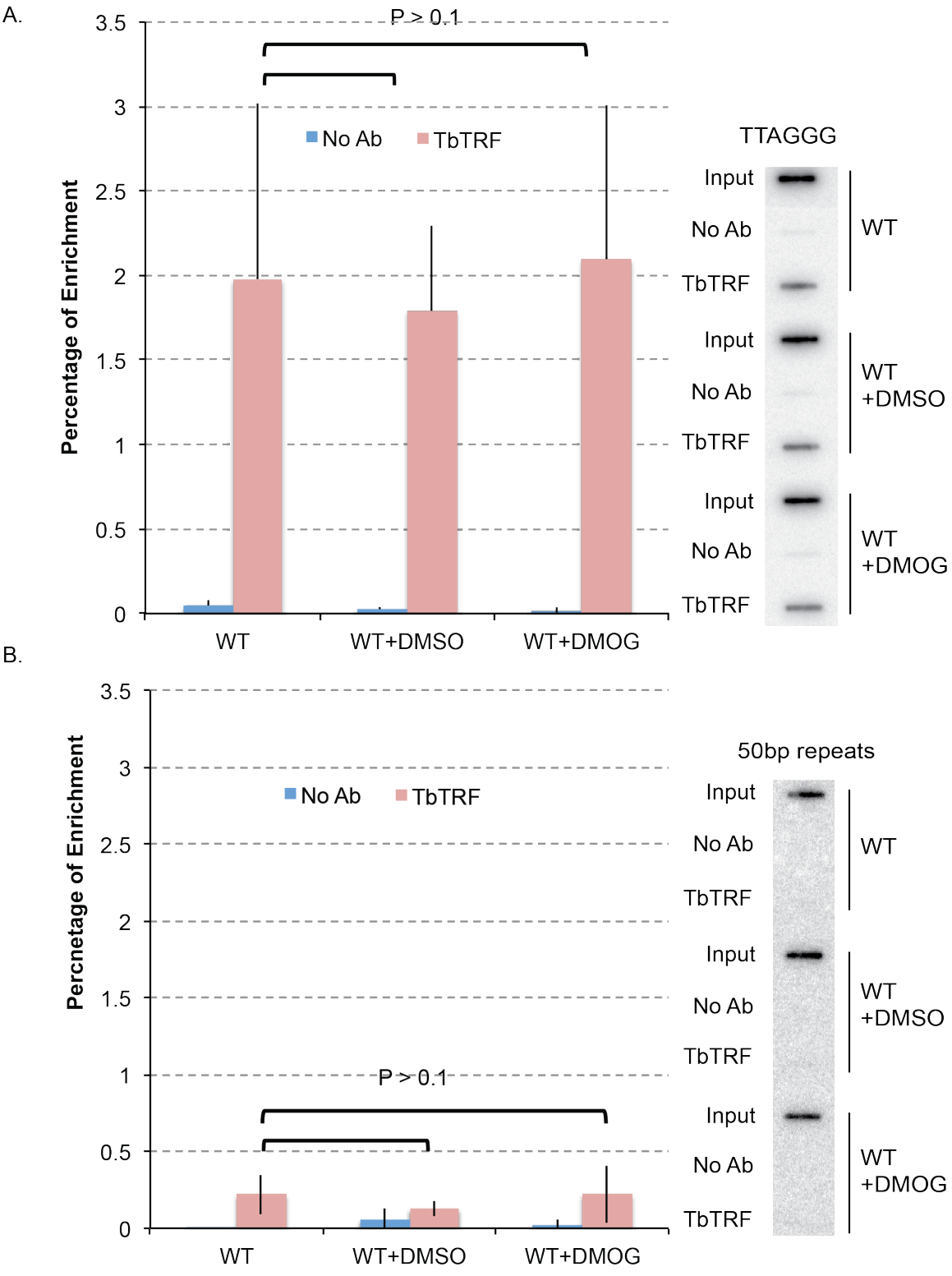

Figure 6-9: ChIP of TbTRF in the presence or absence of J-base. (A) ChIP analysis of TbTRF binding to telomere DNA in the presence (wild-type and DMSO treatment) or absence of J (DMOG treatment). At least three independent ChIPs were performed. An un-paired t-test was used to determine the significance of the changes. No significant

changes were observed in TbTRF association with telomere DNA in the presence or absence of J. (B) Quantification and representative slot blot of 50bp repeats hybridization. These data were generated for binding specificity control.

ChIP products were normalized against input to obtain the percent of enrichment (see appendix A for details). To date, there were no significant changes in the binding of TbTRF to telomeres in the absence of J (Figure: 6-9a). As a control to the specificity of binding, blots were hybridized with 50bp repeats. No binding was detected in any scenario, validating that TbTRF specifically pulls down telomeric DNA and not any other sequence (Figure 6-9b). Further ChIPs must be carried out in order to firmly conclude that the binding of TbTRF to telomeres is not affected by the presence of J *in vivo*.

TbTRF mutants, VSG switching and mouse studies

If TbTRF affects *VSG* switching and if this effect is a consequence of TbTRF's DNA binding activity, then the TbTRF DNA binding mutant will be a unique tool to investigate the consequence of targeting *VSG* switching in mouse models. Whether *T. brucei* manages to escape host immune detection despite the elevation in *VSG* switching frequency, or whether targeting *VSG* switching allows the host's immune system to effectively eliminate *T. brucei,* these mutants and other studies that characterized *VSG* switching changes will provide insights to whether targeting *VSG* switching is indeed a therapeutic intervention.

Finally, these mutants will provide answers to a long-term hypothesis that telomere proteins play an important role in the pathogenesis of not only *T. brucei*, but also other parasites that utilize antigenic variation. These mutants provide a direct

measure to investments in therapeutic discovery and targeting the telomeric proteins of parasites as a mean to eliminate *T. brucei* and other parasites.

BIBLIOGRAPHY

Alarcon, C.M., Son, H.J., Hall, T., and Donelson, J.E. (1994) A monocistronic transcript for a trypanosome variant surface glycoprotein. *Mol Cell Biol* **14**: 5579-5591.

Alexandre, S., Guyaux, M., Murphy, N.B., Coquelet, H., Pays, A., Steinert, M., and Pays, E. (1988) Putative genes of a variant-specific antigen gene transcription unit in Trypanosoma brucei. *Mol Cell Biol* **8**: 2367-2378.

Alirol, E., Schrumpf, D., Amici Heradi, J., Riedel, A., de Patoul, C., Quere, M., and Chappuis, F. (2013) Nifurtimox-eflornithine combination therapy for second-stage gambiense human African trypanosomiasis: Medecins Sans Frontieres experience in the Democratic Republic of the Congo. *Clin Infect Dis* **56**: 195-203.

Alsford, S., Kawahara, T., Isamah, C., and Horn, D. (2007) A sirtuin in the African trypanosome is involved in both DNA repair and telomeric gene silencing but is not required for antigenic variation. *Mol Microbiol* **63**: 724-736.

Alsford, S., Wickstead, B., Ersfeld, K., and Gull, K. (2001) Diversity and dynamics of the minichromosomal karyotype in Trypanosoma brucei. *Mol Biochem Parasitol* **113**: 79-88.

Anderson, C.M., and Blackburn, E.H. (2008) Mec1 function in the DNA damage response does not require its interaction with Tel2. *Cell Cycle* **7**: 3695-3698.

Atanasiu, C., Deng, Z., Wiedmer, A., Norseen, J., and Lieberman, P.M. (2006) ORC binding to TRF2 stimulates OriP replication. *EMBO Rep* **7**: 716-721.

Bacchi, C.J. (2009) Chemotherapy of human african trypanosomiasis. *Interdiscip Perspect Infect Dis* **2009**: 195040.

Barry, J.D., Ginger, M.L., Burton, P., and McCulloch, R. (2003) Why are parasite contingency genes often associated with telomeres? *Int J Parasitol* **33**: 29-45.

Bell, S.P. (2002) The origin recognition complex: from simple origins to complex functions. *Genes Dev* **16**: 659-672.

Bell, S.P., Kobayashi, R., and Stillman, B. (1993) Yeast origin recognition complex functions in transcription silencing and DNA replication. *Science* **262**: 1844-1849.

Benard, C., McCright, B., Zhang, Y., Felkai, S., Lakowski, B., and Hekimi, S. (2001) The C. elegans maternal-effect gene clk-2 is essential for embryonic development, encodes a protein homologous to yeast Tel2p and affects telomere length. *Development* **128**: 4045-4055.

Benmerzouga, I., Concepcion-Acevedo, J., Kim, H.S., Vandoros, A.V., Cross, G.A., Klingbeil, M.M., and Li, B. (2013) Trypanosoma brucei Orc1 is essential for nuclear DNA replication and affects both VSG silencing and VSG switching. *Mol Microbiol* **87**: 196-210.

Bernards, A., van Harten-Loosbroek, N., and Borst, P. (1984) Modification of telomeric DNA in Trypanosoma brucei; a role in antigenic variation? *Nucleic Acids Res* **12**: 4153-4170.

Berriman, M., Ghedin, E., Hertz-Fowler, C., Blandin, G., Renauld, H., Bartholomeu, D.C., Lennard, N.J., Caler, E., Hamlin, N.E., Haas, B., Bohme, U., Hannick, L., Aslett, M.A., Shallom, J., Marcello, L., Hou, L., Wickstead, B., Alsmark, U.C., Arrowsmith, C., Atkin, R.J., Barron, A.J., Bringaud, F., Brooks, K., Carrington, M., Cherevach, I., Chillingworth, T.J., Churcher, C., Clark, L.N., Corton, C.H., Cronin, A., Davies, R.M., Doggett, J., Djikeng, A., Feldblyum, T., Field, M.C., Fraser, A., Goodhead, I., Hance, Z.,

Harper, D., Harris, B.R., Hauser, H., Hostetler, J., Ivens, A., Jagels, K., Johnson, D., Johnson, J., Jones, K., Kerhornou, A.X., Koo, H., Larke, N., Landfear, S., Larkin, C., Leech, V., Line, A., Lord, A., Macleod, A., Mooney, P.J., Moule, S., Martin, D.M., Morgan, G.W., Mungall, K., Norbertczak, H., Ormond, D., Pai, G., Peacock, C.S., Peterson, J., Quail, M.A., Rabbinowitsch, E., Rajandream, M.A., Reitter, C., Salzberg, S.L., Sanders, M., Schobel, S., Sharp, S., Simmonds, M., Simpson, A.J., Tallon, L., Turner, C.M., Tait, A., Tivey, A.R., Van Aken, S., Walker, D., Wanless, D., Wang, S., White, B., White, O., Whitehead, S., Woodward, J., Wortman, J., Adams, M.D., Embley, T.M., Gull, K., Ullu, E., Barry, J.D., Fairlamb, A.H., Opperdoes, F., Barrell, B.G., Donelson, J.E., Hall, N., Fraser, C.M., Melville, S.E., and El-Sayed, N.M. (2005) The genome of the African trypanosome Trypanosoma brucei. *Science* **309**: 416-422.

Berriman, M., Hall, N., Sheader, K., Bringaud, F., Tiwari, B., Isobe, T., Bowman, S., Corton, C., Clark, L., Cross, G.A., Hoek, M., Zanders, T., Berberof, M., Borst, P., and Rudenko, G. (2002) The architecture of variant surface glycoprotein gene expression sites in Trypanosoma brucei. *Mol Biochem Parasitol* **122**: 131-140.

Bilaud, T., Brun, C., Ancelin, K., Koering, C.E., Laroche, T., and Gilson, E. (1997) Telomeric localization of TRF2, a novel human telobox protein. *Nat Genet* **17**: 236-239.

Bisser, S., and Courtioux, B. (2012) [Sleeping sickness: end of the epidemic outbreak?]. *Rev Neurol (Paris)* **168**: 230-238.

Blackburn, E.H. (1991) Structure and function of telomeres. *Nature* **350**: 569-573.

Blackburn, E.H. (2001) Switching and signaling at the telomere. *Cell* **106**: 661-673.

Blow, J.J., and Dutta, A. (2005) Preventing re-replication of chromosomal DNA. *Nat Rev Mol Cell Biol* **6**: 476-486.

Blum, J.A., Neumayr, A.L., and Hatz, C.F. (2012) Human African trypanosomiasis in endemic populations and travellers. *Eur J Clin Microbiol Infect Dis* **31**: 905-913.

Borst, P., and Rudenko, G. (1994) Antigenic variation in African trypanosomes. *Science* **264**: 1872-1873.

Borst, P., and Sabatini, R. (2008) Base J: discovery, biosynthesis, and possible functions. *Annu Rev Microbiol* **62**: 235-251.

Broccoli, D., Smogorzewska, A., Chong, L., and de Lange, T. (1997) Human telomeres contain two distinct Myb-related proteins, TRF1 and TRF2. *Nat Genet* **17**: 231-235.

Calderano, S.G., de Melo Godoy, P.D., da Cunha, J.P., and Elias, M.C. (2011) Trypanosome prereplication machinery: a potential new target for an old problem. *Enzyme Res* **2011**: 518258.

Carrington, M., Miller, N., Blum, M., Roditi, I., Wiley, D., and Turner, M. (1991) Variant specific glycoprotein of Trypanosoma brucei consists of two domains each having an independently conserved pattern of cysteine residues. *J Mol Biol* **221**: 823-835.

Chakraborty, A., Shen, Z., and Prasanth, S.G. (2011) "ORCanization" on heterochromatin: linking DNA replication initiation to chromatin organization. *Epigenetics* **6**: 665-670.

Chang, M., and Lingner, J. (2008) Cell signaling. Tel2 finally tells one story. *Science* **320**: 60-61.

Chappuis, F. (2007) Melarsoprol-free drug combinations for second-stage Gambian sleeping sickness: the way to go. *Clin Infect Dis* **45**: 1443-1445.

Chen, S., de Vries, M.A., and Bell, S.P. (2007) Orc6 is required for dynamic recruitment of Cdt1 during repeated Mcm2-7 loading. *Genes Dev* **21**: 2897-2907.

Cliffe, L.J., Kieft, R., Southern, T., Birkeland, S.R., Marshall, M., Sweeney, K., and Sabatini, R. (2009) JBP1 and JBP2 are two distinct thymidine hydroxylases involved in J biosynthesis in genomic DNA of African trypanosomes. *Nucleic Acids Res* **37**: 1452-1462.

Court, R., Chapman, L., Fairall, L., and Rhodes, D. (2005) How the human telomeric proteins TRF1 and TRF2 recognize telomeric DNA: a view from high-resolution crystal structures. *EMBO Rep* **6**: 39-45.

Dang, H.Q., and Li, Z. (2011) The Cdc45.Mcm2-7.GINS protein complex in trypanosomes regulates DNA replication and interacts with two Orc1-like proteins in the origin recognition complex. *J Biol Chem* **286**: 32424-32435.

De Greef, C., Imberechts, H., Matthyssens, G., Van Meirvenne, N., and Hamers, R. (1989) A gene expressed only in serum-resistant variants of Trypanosoma brucei rhodesiense. *Mol Biochem Parasitol* **36**: 169-176.

de Lange, T. (2005) Shelterin: the protein complex that shapes and safeguards human telomeres. *Genes Dev* **19**: 2100-2110.

De Lange, T., and Borst, P. (1982) Genomic environment of the expression-linked extra copies of genes for surface antigens of Trypanosoma brucei resembles the end of a chromosome. *Nature* **299**: 451-453.

DeJesus, E., Kieft, R., Albright, B., Stephens, N.A., and Hajduk, S.L. (2013) A single amino acid substitution in the group 1 Trypanosoma brucei gambiense haptoglobin-hemoglobin receptor abolishes TLF-1 binding. *PLoS Pathog* **9**: e1003317.

Deng, Z., Norseen, J., Wiedmer, A., Riethman, H., and Lieberman, P.M. (2009) TERRA RNA binding to TRF2 facilitates heterochromatin formation and ORC recruitment at telomeres. *Mol Cell* **35**: 403-413.

Denninger, V., Fullbrook, A., Bessat, M., Ersfeld, K., and Rudenko, G. (2010) The FACT subunit TbSpt16 is involved in cell cycle specific control of VSG expression sites in Trypanosoma brucei. *Mol Microbiol* **78**: 459-474.

Diffley, J.F. (2004) Regulation of early events in chromosome replication. *Curr Biol* **14**: R778-86.

Diffley, J.F., Cocker, J.H., Dowell, S.J., and Rowley, A. (1994) Two steps in the assembly of complexes at yeast replication origins in vivo. *Cell* **78**: 303-316.

Diotti, R., and Loayza, D. (2011) Shelterin complex and associated factors at human telomeres. *Nucleus* **2**: 119-135.

Dreesen, O., Li, B., and Cross, G.A. (2007) Telomere structure and function in trypanosomes: a proposal. *Nat Rev Microbiol* **5**: 70-75.

Drury, L.S., Perkins, G., and Diffley, J.F. (2000) The cyclin-dependent kinase Cdc28p regulates distinct modes of Cdc6p proteolysis during the budding yeast cell cycle. *Curr Biol* **10**: 231-240.

Dubois, M.E., Demick, K.P., and Mansfield, J.M. (2005) Trypanosomes expressing a mosaic variant surface glycoprotein coat escape early detection by the immune system. *Infect Immun* **73**: 2690-2697.

Ekanayake, D.K., Minning, T., Weatherly, B., Gunasekera, K., Nilsson, D., Tarleton, R., Ochsenreiter, T., and Sabatini, R. (2011) Epigenetic regulation of transcription and

virulence in Trypanosoma cruzi by O-linked thymine glucosylation of DNA. *Mol Cell Biol* **31**: 1690-1700.

El-Sayed, N.M., Hegde, P., Quackenbush, J., Melville, S.E., and Donelson, J.E. (2000) The African trypanosome genome. *Int J Parasitol* **30**: 329-345.

Elsasser, S., Chi, Y., Yang, P., and Campbell, J.L. (1999) Phosphorylation controls timing of Cdc6p destruction: A biochemical analysis. *Mol Biol Cell* **10**: 3263-3277.

Figueiredo, L.M., and Cross, G.A. (2010) Nucleosomes are depleted at the VSG expression site transcribed by RNA polymerase I in African trypanosomes. *Eukaryot Cell* **9**: 148-154.

Foss, M., McNally, F.J., Laurenson, P., and Rine, J. (1993) Origin recognition complex (ORC) in transcriptional silencing and DNA replication in S. cerevisiae. *Science* **262**: 1838-1844.

Frevert, U., Movila, A., Nikolskaia, O.V., Raper, J., Mackey, Z.B., Abdulla, M., McKerrow, J., and Grab, D.J. (2012) Early invasion of brain parenchyma by African trypanosomes. *PLoS One* **7**: e43913.

Gajiwala, K.S., and Burley, S.K. (2000) Winged helix proteins. *Curr Opin Struct Biol* **10**: 110-116.

Genest, P.A., Ter Riet, B., Cijsouw, T., van Luenen, H.G., and Borst, P. (2007) Telomeric localization of the modified DNA base J in the genome of the protozoan parasite Leishmania. *Nucleic Acids Res* **35**: 2116-2124.

Gilbert, D.M. (2001) Making sense of eukaryotic DNA replication origins. *Science* **294**: 96-100.

Glover, L., and Horn, D. (2006) Repression of polymerase I-mediated gene expression at Trypanosoma brucei telomeres. *EMBO Rep* **7**: 93-99.

Godoy, P.D., Nogueira-Junior, L.A., Paes, L.S., Cornejo, A., Martins, R.M., Silber, A.M., Schenkman, S., and Elias, M.C. (2009) Trypanosome prereplication machinery contains a single functional orc1/cdc6 protein, which is typical of archaea. *Eukaryot Cell* **8**: 1592-1603.

Gommers-Ampt, J., Lutgerink, J., and Borst, P. (1991) A novel DNA nucleotide in Trypanosoma brucei only present in the mammalian phase of the life-cycle. *Nucleic Acids Res* **19**: 1745-1751.

Gommers-Ampt, J.H., Van Leeuwen, F., de Beer, A.L., Vliegenthart, J.F., Dizdaroglu, M., Kowalak, J.A., Crain, P.F., and Borst, P. (1993) beta-D-glucosyl-hydroxymethyluracil: a novel modified base present in the DNA of the parasitic protozoan T. brucei. *Cell* **75**: 1129-1136.

Graham, S.V., and Barry, J.D. (1995) Transcriptional regulation of metacyclic variant surface glycoprotein gene expression during the life cycle of Trypanosoma brucei. *Mol Cell Biol* **15**: 5945-5956.

Gruszynski, A.E., van Deursen, F.J., Albareda, M.C., Best, A., Chaudhary, K., Cliffe, L.J., del Rio, L., Dunn, J.D., Ellis, L., Evans, K.J., Figueiredo, J.M., Malmquist, N.A., Omosun, Y., Palenchar, J.B., Prickett, S., Punkosdy, G.A., van Dooren, G., Wang, Q., Menon, A.K., Matthews, K.R., and Bangs, J.D. (2006) Regulation of surface coat exchange by differentiating African trypanosomes. *Mol Biochem Parasitol* **147**: 211-223.

Hanaoka, S., Nagadoi, A., and Nishimura, Y. (2005) Comparison between TRF2 and TRF1 of their telomeric DNA-bound structures and DNA-binding activities. *Protein Sci* **14**: 119-130.

Hartley, C.L., and McCulloch, R. (2008) Trypanosoma brucei BRCA2 acts in antigenic variation and has undergone a recent expansion in BRC repeat number that is important during homologous recombination. *Mol Microbiol* **68**: 1237-1251.

Hayashi, T., Hatanaka, M., Nagao, K., Nakaseko, Y., Kanoh, J., Kokubu, A., Ebe, M., and Yanagida, M. (2007) Rapamycin sensitivity of the Schizosaccharomyces pombe tor2 mutant and organization of two highly phosphorylated TOR complexes by specific and common subunits. *Genes Cells* **12**: 1357-1370.

Hemerly, A.S., Prasanth, S.G., Siddiqui, K., and Stillman, B. (2009) Orc1 controls centriole and centrosome copy number in human cells. *Science* **323**: 789-793.

Hickman, M.A., and Rusche, L.N. (2010) Transcriptional silencing functions of the yeast protein Orc1/Sir3 subfunctionalized after gene duplication. *Proc Natl Acad Sci U S A* **107**: 19384-19389.

Hovel-Miner, G.A., Boothroyd, C.E., Mugnier, M., Dreesen, O., Cross, G.A., and Papavasiliou, F.N. (2012) Telomere length affects the frequency and mechanism of antigenic variation in Trypanosoma brucei. *PLoS Pathog* **8**: e1002900.

Huang, D.W., Fanti, L., Pak, D.T., Botchan, M.R., Pimpinelli, S., and Kellum, R. (1998) Distinct cytoplasmic and nuclear fractions of Drosophila heterochromatin protein 1: their phosphorylation levels and associations with origin recognition complex proteins. *J Cell Biol* **142**: 307-318.

Hughes, K., Wand, M., Foulston, L., Young, R., Harley, K., Terry, S., Ersfeld, K., and Rudenko, G. (2007) A novel ISWI is involved in VSG expression site downregulation in African trypanosomes. *EMBO J* **26**: 2400-2410.

Janzen, C.J., Hake, S.B., Lowell, J.E., and Cross, G.A. (2006) Selective di- or trimethylation of histone H3 lysine 76 by two DOT1 homologs is important for cell cycle regulation in Trypanosoma brucei. *Mol Cell* **23**: 497-507.

Karlseder, J., Broccoli, D., Dai, Y., Hardy, S., and de Lange, T. (1999) p53- and ATM-dependent apoptosis induced by telomeres lacking TRF2. *Science* **283**: 1321-1325.

Kawahara, T., Siegel, T.N., Ingram, A.K., Alsford, S., Cross, G.A., and Horn, D. (2008) Two essential MYST-family proteins display distinct roles in histone H4K10 acetylation and telomeric silencing in trypanosomes. *Mol Microbiol* **69**: 1054-1068.

Kim, H.S., and Cross, G.A. (2010) TOPO3alpha influences antigenic variation by monitoring expression-site-associated VSG switching in Trypanosoma brucei. *PLoS Pathog* **6**: e1000992.

Kim, H.S., and Cross, G.A. (2011) Identification of Trypanosoma brucei RMI1/BLAP75 homologue and its roles in antigenic variation. *PLoS One* **6**: e25313.

Koren, A., Tsai, H.J., Tirosh, I., Burrack, L.S., Barkai, N., and Berman, J. (2010) Epigenetically-inherited centromere and neocentromere DNA replicates earliest in S-phase. *PLoS Genet* **6**: e1001068.

Kota, R.S., and Runge, K.W. (1998) The yeast telomere length regulator TEL2 encodes a protein that binds to telomeric DNA. *Nucleic Acids Res* **26**: 1528-1535.

Kota, R.S., and Runge, K.W. (1999) Tel2p, a regulator of yeast telomeric length in vivo, binds to single-stranded telomeric DNA in vitro. *Chromosoma* **108**: 278-290.

Lee, S.H., Stephens, J.L., and Englund, P.T. (2007) A fatty-acid synthesis mechanism specialized for parasitism. *Nat Rev Microbiol* **5**: 287-297.

Li, B. (2010) A newly discovered role of telomeres in an ancient organism. *Nucleus* **1**: 260-263.

Li, B. (2012) Telomere components as potential therapeutic targets for treating microbial pathogen infections. *Front Oncol* **2**: 156.

Li, B., Espinal, A., and Cross, G.A. (2005) Trypanosome telomeres are protected by a homologue of mammalian TRF2. *Mol Cell Biol* **25**: 5011-5021.

Lira, C.B., Giardini, M.A., Neto, J.L., Conte, F.F., and Cano, M.I. (2007) Telomere biology of trypanosomatids: beginning to answer some questions. *Trends Parasitol* **23**: 357-362.

Lowell, J.E., and Cross, G.A. (2004) A variant histone H3 is enriched at telomeres in Trypanosoma brucei. *J Cell Sci* **117**: 5937-5947.

Lustig, A.J., and Petes, T.D. (1986) Identification of yeast mutants with altered telomere structure. *Proc Natl Acad Sci U S A* **83**: 1398-1402.

Mancio-Silva, L., Rojas-Meza, A.P., Vargas, M., Scherf, A., and Hernandez-Rivas, R. (2008) Differential association of Orc1 and Sir2 proteins to telomeric domains in Plasmodium falciparum. *J Cell Sci* **121**: 2046-2053.

Marcello, L., Menon, S., Ward, P., Wilkes, J.M., Jones, N.G., Carrington, M., and Barry, J.D. (2007) VSGdb: a database for trypanosome variant surface glycoproteins, a large and diverse family of coiled coil proteins. *BMC Bioinformatics* **8**: 143.

McCulloch, R., and Barry, J.D. (1999) A role for RAD51 and homologous recombination in Trypanosoma brucei antigenic variation. *Genes Dev* **13**: 2875-2888.

Melville, S.E., Leech, V., Gerrard, C.S., Tait, A., and Blackwell, J.M. (1998) The molecular karyotype of the megabase chromosomes of Trypanosoma brucei and the assignment of chromosome markers. *Mol Biochem Parasitol* **94**: 155-173.

Metcalf, P., Blum, M., Freymann, D., Turner, M., and Wiley, D.C. (1987) Two variant surface glycoproteins of Trypanosoma brucei of different sequence classes have similar 6 A resolution X-ray structures. *Nature* **325**: 84-86.

Micklem, G., Rowley, A., Harwood, J., Nasmyth, K., and Diffley, J.F. (1993) Yeast origin recognition complex is involved in DNA replication and transcriptional silencing. *Nature* **366**: 87-89.

Morrison, L.J. (2011) Parasite-driven pathogenesis in Trypanosoma brucei infections. *Parasite Immunol* **33**: 448-455.

Munoz-Jordan, J.L., and Cross, G.A. (2001) Telomere shortening and cell cycle arrest in Trypanosoma brucei expressing human telomeric repeat factor TRF1. *Mol Biochem Parasitol* **114**: 169-181.

Munoz-Jordan, J.L., Cross, G.A., de Lange, T., and Griffith, J.D. (2001) t-loops at trypanosome telomeres. *EMBO J* **20**: 579-588.

Murti, K.G., and Prescott, D.M. (1999) Telomeres of polytene chromosomes in a ciliated protozoan terminate in duplex DNA loops. *Proc Natl Acad Sci U S A* **96**: 14436-14439.

Namangala, B. (2011) How the African trypanosomes evade host immune killing. *Parasite Immunol* **33**: 430-437.

Narayanan, M.S., Kushwaha, M., Ersfeld, K., Fullbrook, A., Stanne, T.M., and Rudenko, G. (2011) NLP is a novel transcription regulator involved in VSG expression site control in Trypanosoma brucei. *Nucleic Acids Res* **39**: 2018-2031.

Nasheuer, H.P., Smith, R., Bauerschmidt, C., Grosse, F., and Weisshart, K. (2002) Initiation of eukaryotic DNA replication: regulation and mechanisms. *Prog Nucleic Acid Res Mol Biol* **72**: 41-94.

Pak, D.T., Pflumm, M., Chesnokov, I., Huang, D.W., Kellum, R., Marr, J., Romanowski, P., and Botchan, M.R. (1997) Association of the origin recognition complex with heterochromatin and HP1 in higher eukaryotes. *Cell* **91**: 311-323.

Pays, E., Tebabi, P., Pays, A., Coquelet, H., Revelard, P., Salmon, D., and Steinert, M. (1989) The genes and transcripts of an antigen gene expression site from T. brucei. *Cell* **57**: 835-845.

Pays, E., Vanhamme, L., and Perez-Morga, D. (2004) Antigenic variation in Trypanosoma brucei: facts, challenges and mysteries. *Curr Opin Microbiol* **7**: 369-374.

Povelones, M.L., Gluenz, E., Dembek, M., Gull, K., and Rudenko, G. (2012) Histone H1 plays a role in heterochromatin formation and VSG expression site silencing in Trypanosoma brucei. *PLoS Pathog* **8**: e1003010.

Prasanth, S.G., Prasanth, K.V., Siddiqui, K., Spector, D.L., and Stillman, B. (2004) Human Orc2 localizes to centrosomes, centromeres and heterochromatin during chromosome inheritance. *EMBO J* **23**: 2651-2663.

Prasanth, S.G., Prasanth, K.V., and Stillman, B. (2002) Orc6 involved in DNA replication, chromosome segregation, and cytokinesis. *Science* **297**: 1026-1031.

Prasanth, S.G., Shen, Z., Prasanth, K.V., and Stillman, B. (2010) Human origin recognition complex is essential for HP1 binding to chromatin and heterochromatin organization. *Proc Natl Acad Sci U S A* **107**: 15093-15098.

Proudfoot, C., and McCulloch, R. (2005) Distinct roles for two RAD51-related genes in Trypanosoma brucei antigenic variation. *Nucleic Acids Res* **33**: 6906-6919.

Roberts, L., Janovy, J., Schmidt, G., and Larry, S. (2009) Roberts' Foundations of Parasitology.

Rudenko, G. (2010) Epigenetics and transcriptional control in African trypanosomes. *Essays Biochem* **48**: 201-219.

Rudenko, G. (2011) African trypanosomes: the genome and adaptations for immune evasion. *Essays Biochem* **51**: 47-62.

Rudenko, G., Cross, M., and Borst, P. (1998) Changing the end: antigenic variation orchestrated at the telomeres of African trypanosomes. *Trends Microbiol* **6**: 113-116.

Runge, K.W., and Zakian, V.A. (1996) TEL2, an essential gene required for telomere length regulation and telomere position effect in Saccharomyces cerevisiae. *Mol Cell Biol* **16**: 3094-3105.

Sfeir, A., Kosiyatrakul, S.T., Hockemeyer, D., MacRae, S.L., Karlseder, J., Schildkraut, C.L., and de Lange, T. (2009) Mammalian telomeres resemble fragile sites and require TRF1 for efficient replication. *Cell* **138**: 90-103.

Shareef, M.M., King, C., Damaj, M., Badagu, R., Huang, D.W., and Kellum, R. (2001) Drosophila heterochromatin protein 1 (HP1)/origin recognition complex (ORC) protein is associated with HP1 and ORC and functions in heterochromatin-induced silencing. *Mol Biol Cell* **12**: 1671-1685.

Sherwin, T., and Gull, K. (1989) The cell division cycle of Trypanosoma brucei brucei: timing of event markers and cytoskeletal modulations. *Philos Trans R Soc Lond B Biol Sci* **323**: 573-588.

Siegel, T.N., Hekstra, D.R., Kemp, L.E., Figueiredo, L.M., Lowell, J.E., Fenyo, D., Wang, X., Dewell, S., and Cross, G.A. (2009) Four histone variants mark the boundaries of polycistronic transcription units in Trypanosoma brucei. *Genes Dev* **23**: 1063-1076.

Simarro, P.P., Jannin, J., and Cattand, P. (2008) Eliminating human African trypanosomiasis: where do we stand and what comes next? *PLoS Med* **5**: e55.

Smogorzewska, A., van Steensel, B., Bianchi, A., Oelmann, S., Schaefer, M.R., Schnapp, G., and de Lange, T. (2000) Control of human telomere length by TRF1 and TRF2. *Mol Cell Biol* **20**: 1659-1668.

Speck, C., Chen, Z., Li, H., and Stillman, B. (2005) ATPase-dependent cooperative binding of ORC and Cdc6 to origin DNA. *Nat Struct Mol Biol* **12**: 965-971.

Stanne, T.M., and Rudenko, G. (2010) Active VSG expression sites in Trypanosoma brucei are depleted of nucleosomes. *Eukaryot Cell* **9**: 136-147.

Stansel, R.M., de Lange, T., and Griffith, J.D. (2001) T-loop assembly in vitro involves binding of TRF2 near the 3' telomeric overhang. *EMBO J* **20**: 5532-5540.

Stephens, N.A., Kieft, R., Macleod, A., and Hajduk, S.L. (2012) Trypanosome resistance to human innate immunity: targeting Achilles' heel. *Trends Parasitol* **28**: 539-545.

Stillman, B. (2005) Origin recognition and the chromosome cycle. *FEBS Lett* **579**: 877-884.

Stockdale, C., Swiderski, M.R., Barry, J.D., and McCulloch, R. (2008) Antigenic variation in Trypanosoma brucei: joining the DOTs. *PLoS Biol* **6**: e185.

Takai, H., Wang, R.C., Takai, K.K., Yang, H., and de Lange, T. (2007) Tel2 regulates the stability of PI3K-related protein kinases. *Cell* **131**: 1248-1259.

Tatsumi, Y., Ezura, K., Yoshida, K., Yugawa, T., Narisawa-Saito, M., Kiyono, T., Ohta, S., Obuse, C., and Fujita, M. (2008) Involvement of human ORC and TRF2 in pre-replication complex assembly at telomeres. *Genes Cells* **13**: 1045-1059.

Taylor, J.E., and Rudenko, G. (2006) Switching trypanosome coats: what's in the wardrobe? *Trends Genet* **22**: 614-620.

Tiengwe, C., Marcello, L., Farr, H., Dickens, N., Kelly, S., Swiderski, M., Vaughan, D., Gull, K., Barry, J.D., Bell, S.D., and McCulloch, R. (2012a) Genome-wide analysis reveals extensive functional interaction between DNA replication initiation and transcription in the genome of Trypanosoma brucei. *Cell Rep* **2**: 185-197.

Tiengwe, C., Marcello, L., Farr, H., Gadelha, C., Burchmore, R., Barry, J.D., Bell, S.D., and McCulloch, R. (2012b) Identification of ORC1/CDC6-interacting factors in Trypanosoma brucei reveals critical features of origin recognition complex architecture. *PLoS One* **7**: e32674.

Ulbert, S., Eide, L., Seeberg, E., and Borst, P. (2004) Base J, found in nuclear DNA of Trypanosoma brucei, is not a target for DNA glycosylases. *DNA Repair (Amst)* **3**: 145-154.

van Leeuwen, F., Dirks-Mulder, A., Dirks, R.W., Borst, P., and Gibson, W. (1998a) The modified DNA base beta-D-glucosyl-hydroxymethyluracil is not found in the tsetse fly stages of Trypanosoma brucei. *Mol Biochem Parasitol* **94**: 127-130.

van Leeuwen, F., Kieft, R., Cross, M., and Borst, P. (2000) Tandemly repeated DNA is a target for the partial replacement of thymine by beta-D-glucosyl-hydroxymethyluracil in Trypanosoma brucei. *Mol Biochem Parasitol* **109**: 133-145.

van Leeuwen, F., Taylor, M.C., Mondragon, A., Moreau, H., Gibson, W., Kieft, R., and Borst, P. (1998b) beta-D-glucosyl-hydroxymethyluracil is a conserved DNA modification in kinetoplastid protozoans and is abundant in their telomeres. *Proc Natl Acad Sci U S A* **95**: 2366-2371.

van Leeuwen, F., Wijsman, E.R., Kieft, R., van der Marel, G.A., van Boom, J.H., and Borst, P. (1997) Localization of the modified base J in telomeric VSG gene expression sites of Trypanosoma brucei. *Genes Dev* **11**: 3232-3241.

van Luenen, H.G., Farris, C., Jan, S., Genest, P.A., Tripathi, P., Velds, A., Kerkhoven, R.M., Nieuwland, M., Haydock, A., Ramasamy, G., Vainio, S., Heidebrecht, T., Perrakis, A., Pagie, L., van Steensel, B., Myler, P.J., and Borst, P. (2012) Glucosylated hydroxymethyluracil, DNA base J, prevents transcriptional readthrough in Leishmania. *Cell* **150**: 909-921.

van Steensel, B., and de Lange, T. (1997) Control of telomere length by the human telomeric protein TRF1. *Nature* **385**: 740-743.

van Steensel, B., Smogorzewska, A., and de Lange, T. (1998) TRF2 protects human telomeres from end-to-end fusions. *Cell* **92**: 401-413.

Vanhamme, L., Poelvoorde, P., Pays, A., Tebabi, P., Van Xong, H., and Pays, E. (2000) Differential RNA elongation controls the variant surface glycoprotein gene expression sites of Trypanosoma brucei. *Mol Microbiol* **36**: 328-340.

Wang, C.C. (1995) Molecular mechanisms and therapeutic approaches to the treatment of African trypanosomiasis. *Annu Rev Pharmacol Toxicol* **35**: 93-127.

Wang, Q.P., Kawahara, T., and Horn, D. (2010) Histone deacetylases play distinct roles in telomeric VSG expression site silencing in African trypanosomes. *Mol Microbiol* **77**: 1237-1245.

Welburn, S.C., and Maudlin, I. (2012) Priorities for the elimination of sleeping sickness. *Adv Parasitol* **79**: 299-337.

Wellinger, R.J., and Sen, D. (1997) The DNA structures at the ends of eukaryotic chromosomes. *Eur J Cancer* **33**: 735-749.

Wirtz, E., Leal, S., Ochatt, C., and Cross, G.A. (1999) A tightly regulated inducible expression system for conditional gene knock-outs and dominant-negative genetics in Trypanosoma brucei. *Mol Biochem Parasitol* **99**: 89-101.

Yang, X., Figueiredo, L.M., Espinal, A., Okubo, E., and Li, B. (2009) RAP1 is essential for silencing telomeric variant surface glycoprotein genes in Trypanosoma brucei. *Cell* **137**: 99-109.

Zhong, Z., Shiue, L., Kaplan, S., and de Lange, T. (1992) A mammalian factor that binds telomeric TTAGGG repeats in vitro. *Mol Cell Biol* **12**: 4834-4843.

APPENDIX A

EQUATION USED TO CALCULATE mRNA FOLD CHANGES IN Q-RT-PCR

mRNA fold change = (mRNAV, n/mRNAV, 0)/(mRNAT, n/mRNAT, o), where (mRNAV, n) and (mRNAV, 0) represent the mRNA level for a particular *VSG* in the n hr and 0 hr, and mRNAT, n and mRNAT, 0 represent the mRNA levels for β-tubulin at corresponding time points.

EQUATION UTILIZED TO CALCULATE B-GALACTOSIDASE ACTIVITY

Miller Units = (1000 x OD_{420}) /TxVx OD_{600}

Where T = time of the reaction in minutes.

V= Volume of culture used in the assay.

OD_{600}= Cell density in the cell suspension.

EQUATION USED FOR ChIP PERCENTAGE OF ENRICHMENT CALCULATION

Percentage of enrichment = (IP product/$33.3x10^6$)/(Input/$1.6x10^6$) x 100 %. ($33.3x10^6$ and $1.6x10^6$ are the total number of cells per sample).

Approximately 100 million cells are used per ChIP, where the 100 million cells are re-suspended in 300 μl of lysis buffer. The lysate is divided into 3 tubes, the first tube is the input, the second tube is sample to be precipitated without an antibody (No Ab sample) and the third tube is the actual pull-down experiment (Ab sample). For the actual ChIP samples, (No Ab and Ab samples), 100 μl of the lysate is used to do the pull-down experiments. Therefore, 1/3 of the sample is used for both the No Ab and the Ab

experiments. Therefore the total number of cells used for both the No Ab and the Ab sample is 100 x10^6 cells/3 = 33.3 x10^6 cells. The samples are not further diluted. For the input sample, only 25 μl of sample is taken out from the lysate, which corresponds to 1/12 of the sample. The sample is further diluted (1:5) dilution; this step is to ensure that the resulting intensity from the input is legible. Therefore the total number of cells used for the input = 100 x10^6 cells x 1/60 = 1.6 x10^6 cells. (Note: input sample is always highly enriched so either 5 μl of sample is taken out of the lysate or diluting the input sample if a large volume is taken out- in this case 25μl- either way will not change the final cell number of 1.6 x10^6 cells). Then the intensity of the signal obtained from the slot blot for the corresponding sample is divided by the total number of cells used, as detailed above. Finally, the percent of enrichment is determined by dividing the IP product result over the input.

EQUATION USED TO CALCULATE POPULATION DOUBLING FOR GROWTH ANALYSIS

Population doubling = log2 (total number of cell, n/total number cells, (n-1)) + PD (n-1), where n is hour or day time point and n-1 is the immediate time-point preceding n.

EQUATION USED TO CALCULATE G-OVERHANG SIGNAL

Raw G-overhang signal = (Native TelC4 signal)/ (Denatured TelC4 signal)

Normalized G-overhang signal = Raw G-overhang signal/ Raw G-overhang signal of WT.

APPENDEX B

PRIMERS USED IN THESE STUDIES

Primer number	Primer	Sequence
1	OIB-tbORC1-5`-UTR-FW-XhoI	GCGCTCGAGGTTCGTTGAGCAGTTGGG
2	OIB-tbORC1-5`-UTR-BW-RI	GCGGAATTCGGCACCTGCTAAAACCC
3	OIB-TbORC1-3`-UTR-FW-XbaI	GCGTCTAGATTGTAAAATACCGTCTTAGGACG
4	OIB-tbORC1-3`UTR-BW-NotI	GCGGCGGCCGCTCTCCAGTCCCCCTCATT
5	OIB-tbOrc1-star-FW-BamHI	GGATCCTGAAACGAAGGAGGGACA
6	OIB-TbOrc1-end-BW-SaII	GCGGTCGACCTATATCGAAAACAGTGGGC
7	OBL-tbORC1-end-RI	GCGGAATTCCTATATCGAAACAGTGGGC
8	OBL-tbORC1-start-RI	GCGGAATTCATGAAACGAAGGAGGGAC
9	OBL-tbORC1-end-BamHI	GCGGGATCCCTATATCGAAAACAGTGGGC
10	OBL-tbTRF-start-H3	GCGAAGCTTTACTGTCACGCTGGCG
11	OBL-tbTRF-myb-start(longFW)	AACTTTGCTAATGTGGGCG
12	OBL-tbTRF-myb-start(longBW)	CGCCCACATTAGCAAAGTT
13	OBL-tbTRF-END-SpeI	GCGACTAGTTCACTCGTTATTCTCCATATTG
14	OBL-tbTRF-2H-Start-BamHI	GCGGGATCCACTGTCACGCTGGCGTT
15	OBL-tbTRF-2H-5myb-FW-BamHI	GCGGGATCCGGACATCATCCGGCAAG
16	OBL-tbTRF-end-BW-PstI	GCGTGCAGCTCACTG TTATTCTCCATATTGG
17	OBL-BSD-FW1	CCAAGCCTTTGTCTCAAGA
18	OBL-BSD-end-BW1	TTAGCCCTCCCACACATAA
19	OBL-VSG221-FW1	GTCCTAGCCCAAGTTCTTC
20	OBL-VSG221-BW1	GCTGTTGCAGTAGCTGTTAC
21	OBL-splice leader –FW-new	GACTAGTTTCTGTACTATAT

22	OBL-VSG-common-BW-new	GACTAGTGTTAAAATATATCA
23	OIB- tbTOR1-5UTR-FW-Sal	GCGGTCGACAGCTGGGTTGTG CTCAGA
24	OIB- tbTOR1-5UTR-BW-RI	GCGGAATTCATGTCACTGCCC CCC
25	OIB-tbTOR1-NT-FW-XbaI	GCGTCTAGATGCGCCCATCCG TTAACA
26	OIB-tbTOR1-NT-BW-NotI	GCGCGCGGCCGCGCACGCAGC AACCTTATC

APPENDEX C

PLASMID GENERATED FROM THESE STUDIES

Tryp Plasmid name	Marker
pSk-hygro-ko-TbOrc1	Hyg
pSK-tbTRF-5`-UTR-Phleo-Ty1-Puro-TbTRF-3`-UTR (5)	Phleo, Puro
pSK-tbTRF-5`-UTR-Phleo-Ty1-Puro-R22K-TbTRF-3`-UTR (1)	Phleo, Puro
pSK-tbTRF-5`-UTR-Phleo-Ty1-Puro-R22E-TbTRF-3`-UTR (1)	Phleo, Puro
pSK-tbTRF-5`-UTR-Phleo-Ty1-Puro-H70R-TbTRF-3`-UTR (1)	Phleo, Puro
pSK-tbTRF-5`-UTR-Phleo-Ty1-Puro-Q44S-TbTRF-3`-UTR (1)	Phleo, Puro
pSK-tbTRF-5`-UTR-Phleo-Ty1-Puro-Q45S-TbTRF-3`-UTR (2)	Phleo, Puro
pSK-tbTRF-5`-UTR-Phleo-Ty1-Puro-R72K-TbTRF-3`-UTR (1)	Phleo, Puro
pSK-tbTRF-5`-UTR-Phleo-Ty1-Puro-R72E-TbTRF-3`-UTR (4)	Phleo, Puro
pSK-tbTRF-5`-UTR-Phleo-Ty1-Puro-R76K-TbTRF-3`-UTR (2)	Phleo, Puro
pSK-tbTRF-5`-UTR-Phleo-Ty1-Puro-R76E-TbTRF-3`-UTR (8)	Phleo, Puro
pSk-Ty1-TbTRF-R22K-Phleo clone 1	Phleo
pSk-Ty1-TbTRF-Q44S-Phleo clone 1	Phleo
pSk-Ty1-TbTRF-Q45S-Phleo clone 5	Phleo
pSk-Ty1-TbTRF-H70R-Phleo clone 1	Phleo
pSk-Ty1-TbTRF-R72K-Phleo clone 1	Phleo
pSk-Ty1-TbTRF-R76K-Phleo clone 1	Phleo
pSK-Ty1-TbTRF-Phleo Clone 17	Phleo

Yeast Plasmid name	Yeast marker
pACT-TbORC1	Leu2
pBTM116-TbORC1	TRP1
pBTM116-TbTRF-FL-R22K clone 1	TRP1
pBTM116-TbTRF-MYB-R22K clone 1	TRP1
pBTM116-TbTRF-FL-Q44S clone 1	TRP1
pBTM116-TbTRF-MYB-Q44S clone 1	TRP1
pBTM116-TbTRF-FL-Q45S clone 13	TRP1
pBTM116-TbTRF-MYB-Q45S clone 2	TRP1
pBTM116-TbTRF-FL-H70R clone 5	TRP1
pBTM116-TbTRF-MYB-H70R clone 2	TRP1

pBTM116-TbTRF-FL-R72K clone 1	TRP1
pBTM116-TbTRF-MYB-R72K clone 2	TRP1
pBTM116-TbTRF-FL-R76K clone 1	TRP1
pBTM116-TbTRF-MYB-R72K clone 5	TRP1

Note: TbTRF MYB domain mutants are labeled with their corresponding position within the MYB domain. The following table describes the original position within TbTRF.

Location of mutation in MYB domain	Location of mutation in TbTRF ORF
R22	R298
Q44	Q320
Q45	Q321
H70	H346
R72	R348
R76	R352

APPENDEX D

ANTIBODIES USED IN THESE STUDIES

Name	Usage	Vendor
Mouse-anti-LexA	Western Blot, detects lexA fused proteins.	*Santa Cruz Biotechnology*
Mouse-anti-Gal4	Western Blot, Gal4 fused proteins.	*AbCam*
Mouse-HA probe	Western Blot, detects F2H-tagged proteins	*Santa Cruz*
Mouse-anti-12CA5	Western Blot, detects F2H-tagged proteins	*MSKCC, AB core facility*
Mouse-anti-BB2	Western Blot, detects Ty1-tagged protiens.	*MSKCC, AB core facility*
Goat-anti-EF-2	Western Blot, detects EF-2 as a loading control.	*Santa Cruz Biotechnology*
Mouse-anti-H3	Western Blot, detects H3 as a loading control.	*Abcam*
Chicken-anti-protein A	Western Blot, detects protein A in PTP tag.	*Abcam*
Mouse-TAT-1	Western Blot, detects tubulin as a loading control.	Kind Gift from Keith Gull
Rabbit-anti-VSG9	Western Blot, detects VSG9.	Kind Gift from Piet Borst
Rabbit-anti-VSG13	Western Blot, detects VSG9.	Kind Gift from Piet Borst
Rabbit-anti-TbTRF (1260)	Western Blot, detects TbTRF.	Lab generated
Rabbit-anti-TbTRF (1261)	Western Blot, detects TbTRF.	Lab generated
Rabbit-anti-TbRAP1 (597)	Western Blot, detects TbRAP1.	Lab generated
Rabbit-anti-TbRAP1 (598)	Western Blot, detects TbRAP1.	Lab generated
Alexa-488-anti-VSG3	Immunofluorescence, detects VSG3.	Kind Gift from Nina Papavasiliou
Alexa-647-anti-VSG13	Immunofluorescence, detects VSG13.	Kind Gift from Nina Papavasiliou

APPENDEX E

STRAINS GENERATED FROM THESE STUDIES

Name	Selection Markers
SM-PBS-TbORC1-F2H-TbORC1	G419, Phleo, Puro
SM-PBS- F2H-TbOrc1-skohygro-ORC1	G418, Phleo, Puro, Hyg
SM-TbTRF-sko-hygro	G418, Hyg
SM-TbTRF-sko-ko-hygro-Ty1-TbTRF R22K	G418, Hyg, Phleo, Puro
SM-TbTRF-sko-ko-hygro-Ty1-TbTRF H70R B1	G418, Hyg, Phleo, Puro
SM-TbTRF-sko-ko-hygro-Ty1-TbTRF R72K B1	G418, Hyg, Phleo, Puro
SM-TbTRF-sko-ko-hygro-Ty1-TbTRF Q44S B1	G418, Hyg, Phleo, Puro
SM-TbTRF-sko-ko-hygro-Ty1-TbTRF R76K B1	G418, Hyg, Phleo, Puro
SM-TbTRF-sko-ko-hygro-Ty1-TbTRF Q45S B1	G418, Hyg, Phleo, Puro
HSTB261-TbTRF-sko-ko-hygro-Ty1-TbTRF R22K	G418, Hyg, Phleo, Puro, Bsd
HSTB261-TbTRF-sko-ko-hygro-Ty1-TbTRF H70R	G418, Hyg, Phleo, Puro, Bsd
HSTB261-TbTRF-sko-ko-hygro-Ty1-TbTRF R72K	G418, Hyg, Phleo, Puro, Bsd
HSTB261-tbTRF-sko-ko-hygro-Ty1-tbTRF Q44S	G418, Hyg, Phleo, Puro, Bsd
HSTB261-TbTRF-sko-ko-hygro-Ty1-TbTRF R76K	G418, Hyg, Phleo, Puro, Bsd
HSTB261-TbTRF-sko-ko-hygro-Ty1-TbTRF Q45S	G418, Hyg, Phleo, Puro, Bsd
SM-TbTEL2-Ri1/2	G418, Phleo
SM-TbTEL2-Ri1/2-sko-bsd	G418, Phleo, Bsd
SM-TbTEL2-Ri1/2-sko-bsd-F2H-TbTEL2	G418, Phleo, Bsd, Puro
HSTB261- TbTEL2-Ri1/2	G418, Phleo, Bsd, Puro
SM-TbTEL2-Ri1/2-sko-bsd-F2H-TbTOR1	G418, Phleo, Bsd, Puro

APPENDIX F

ABBREVEATIONS

BSD	Blastisidin
BF	Blood stream Form
ChIP	Chromatin Immunoprecipitation
CT	C-terminus
ES	Expression Site
EF-2	Elongation Factor-2
G418	Neomycin
GC	Gene Conversion
H3	Histone 3
Hyg	Hygromycin
ICs	Intermediate base Chromosomes
IF	Immunofluorescence
IP	Immunoprecipitation
ITC	Isothermal Titration Calorimetry
J-base	Beta-D-glucosyl-hydroxylmethyluracil
MBCs	Mega base Chromosomes
MCs	Mini base Chromosomes
mVSGs	Metacyclic form VSGs
NT	N-terminus
ORC	Origin Recognition Complex
Phleo	Phleomycin
PFGE	Pulse Field Gel Electrophoresis
PF	Procyclic Form
Puro	Puromycin
TEL2	Telomere length regulator protein
TOR1	Target of Rapamycin Kinase 1
TRF	TTAGGG Repeat Binding Factor protein
TPE	Telomere Position Effect
UTR	Un-translated Region
VSG	Variant Surface Glycoprotein
WT	Wild-type